NOVEL SCHIFF BASES AS OPTICAL PROBES FOR ENVIRONMENTALLY AND BIOLOGICALLY RELEVANT ANALYTES

Thesis submitted to the
University of Calicut in partial fulfillment of the
requirements for the award of the degree of

DOCTOR OF PHILOSOPHY IN CHEMISTRY

Under the faculty of Science

SOUFEENA P P

Under the guidance of

Dr. K. K. Aravindakshan
Professor (Retd.)

DEPARTMENT OF CHEMISTRY
UNIVERSITY OF CALICUT
KERALA
JULY 2020

Dr. K.K. ARAVINDAKSHAN Calicut University (PO)
Professor (Retd.) Kerala-673635
Department of Chemistry
University of Calicut

CERTIFICATE

This is to certify that the thesis entitled **"NOVEL SCHIFF BASES AS OPTICAL PROBES FOR ENVIRONMENTALLY AND BIOLOGICALLY RELEVANT ANALYTES"** is an authentic record of the research work carried out by **Miss. Soufeena P P** under my supervision in partial fulfillment of the requirement for the Degree of Doctor of Philosophy in Chemistry under the faculty of science of the University of Calicut, and further that no part thereof has been presented earlier for any other degree. The contents of the thesis have been checked for plagiarism using the software "Urkund" and the similarity index falls under the permissible limit.

Place: **Dr. K.K. Aravindakshan**
Date:

DECLARATION

I, Soufeena P P, hereby declare that this thesis entitled **NOVEL SCHIFF BASES AS OPTICAL PROBES FOR ENVIRONMENTALLY AND BIOLOGICALLY RELEVANT ANALYTES** is the report of the original research work done by me for the award of the degree of Doctor of Philosophy in Chemistry, under the supervision of Dr. K.K. Aravindakshan, Professor of Chemistry, University of Calicut.

I further declare that this thesis has not formed the basis for the award of any other degree, diploma or other similar title of any University/Institution.

University of Calicut   **Soufeena P P**
Date:

ACKNOWLEDGEMENT

First and foremost, praises and thank to the supreme power the Almighty Allah, for His showers of blessings throughout my research work.

It is a genuine pleasure to express my deep sense of gratitude to my supervising teacher Dr. K K Aravindakshan for his guidance and continuous supports to complete the research work. His patience, motivation, enthusiasm, vision and sincerity have deeply inspired me. His guidance helped me in all the time of research and writing of the thesis. Beside my advisor, I would like to express my sincere thanks to Yahya A Ismayil, Head of the Department of Chemistry, University of Calicut, and former heads Dr. P. Raveendran and Dr. K. Muraleedharan for providing me the necessary facilities. I also acknowledge the support provided by Dr. K. Mulareedharan, Director, CSIF, for my research. I take this opportunity to thank all other teachers and non-teaching staff of the department of chemistry for their valuable help. I am extremely grateful to all my teachers who taught me in my academic period, they motivated me to enter in the field of research, without their blessings I am impotent to accomplish the work.

I remembered the motivation, help and the whole -hearted support of my friends and co-researchers for the successful accomplishment of this research work. The stimulating discussions we have made during the research period have been very helpful in various phases of my research. My heartfelt gratitude is extended to all my friends without citing their name. I fondly remember the pleasant and fun

Soufeena P P

CONTENTS

PREFACE

Light is one of the vital and indispensable elements of life. Scientific studies about the various aspects of light bright up many technological innovations which has benefited the whole world. The study of optical response of organic luminogens received great attention which enlighten various technological inventions and developments. Proper tuning of the optical properties of the luminogens result in materials having desired functions. Organic luminogens have inevitable roles in light harvesting systems, optical sensors and optoelectronic devices.

The entire thesis is divided into two parts. Part I focuses on the development and application of colourimetric and fluorescent molecular probes (chemical sensors or optical probes) for the detection of various analytes. Chemical sensors offer a relatively simple and efficient method for monitoring environmentally and biologically relevant analytes like cations, anions and neutral molecules. The development of chemosensors received considerable attention because of their rapid response, convenience, non-destructive nature, easy operation, high sensitivity and selectivity offered in both quantitative and qualitative analysis. Presence of trace amounts of analytes can be monitored using very dilute solution of the chemosensor. The first chapter is an introduction to chemical sensors. Here a brief outline of the need of chemical sensors, design strategies of chemical sensors, types of sensors, signaling mechanisms and previously reported sensors derived from Schiff base chemical are discussed. The scope

and importance of this work are incorporated at the end of this chapter. Chapter 2, discusses the materials and methods adopted for the study. Chapters 3, 4, 5 and 6 deal with the chemosensing abilities of novel Schiff bases towards various analytes like cations and anions. Chapter 3 discusses colourimetric and fluorescence sensing ability of an antipyrine derived Schiff base towards various cations. The metal ion sensing ability of two coumarin Schiff bases are discussed in chapters 4 and 5. Chapter 6 deals the fluorescence response of a coumarin Schiff base towards various anions. The important aspects each chemical sensor is summarized in respective chapter. The applicability of these sensors to real samples are also discussed.

Part II of the thesis deals with the light-emitting behaviour of organic molecules in their aggregate state. The light emitting behaviour of organic luminogens is different in dilute - and concentrated solutions. Conventional fluorophores exhibit intense emission behavior in dilute solution and their emission intensity is weak in concentrated solutions. This thorny obstacle referred to as agegregation caused quenching (ACQ) limits the practical applications of luminogens. The first report on aggregation induced emission (AIE), a new photophysical phenomenon of luminogens was by Tang group in 2001. The colourful and promising features of this category of compounds attracted the scientific community and active researches found out the exciting uses of AIEgens in optoelectronic and biomedical fields. The AIE behavior allows the use of aggregate of luminogen in aqueous medium for sensing various analytes. To some extent an AIEgen is an organic version inorganic quantum dots. Here,

the first chapter outlines the developments and importances of AIE/AIEE materials and their contribution to innovative technologies. The attraction of this intriguing property and the effect of molecular motions towards light emission are incorporated in this chapter. Here, we have discussed the AIE/AIEE behavior of previously reported Schiff bases and their promising applications. Chapter 2 discusses the materials and methods adopted for the study. The AIEE behavior of a novel coumarin derived Schiff base is discussed in Chapter 3. Explanation to the effect of restriction of molecular motion towards the light emission with experimental support, morphological structure of the aggregate, effect of pH on the emission of aggregate, etc, are discussed. The fluorescence sensing ability of the aggregate on picric acid is incorporated in Chapter 4. The mechanism of this optical response has been elucidated with experimental and theoretical supports.

The references cited in the thesis are arranged in serial order at the end of each chapter.

PART I

COLOURIMETRIC- AND FLUORESCENCE PROBES FOR ENVIRONMENTALLY AND BIOLOGICALLY RELEVANT CATIONS AND ANIONS

CHAPTER 1

INTRODUCTION

Metal ions have inevitable role in human life. They involve in many biological processes such as transmission of nerve impulses, muscle contraction, regulation of cell activity, metabolism, biomineralization, etc. Metal ions are also the essential core of various metalloenzymes, each one has distinct functions in biological processes[1]. They have important role in chemical and environmental processes also[2]. Apart from these active roles in various fields, the excess exposure of some metal ions adversely affect life on earth[3]. The Environmental Protection Agency (EPA) and World Health Organization (WHO) have defined the upper limit of metal ion concentration in drinking water. Therefore, the monitoring of metal ions is crucial to control their concentration level in the biosphere.

Our daily life is directly and indirectly related to several anionic species. Like metal ions, above a particular limit, these anions are also detrimental to human health and environment. The toxic cyanide ion is widely dispersed in the environment through various human activities. Fluoride ion is another threatening anion, which leads to several health issues. The toxic gases released from various industries lead to various types of environmental pollutions. The excessive release of toxic species to the environment is a threat the life on earth[4-6]. Therefore, it is highly essential to detect and quantify the biologically relevant analytes and the environmentally threatening analytes such as cations, anions and neutral species.

Nowadays, a number of sophisticated instrumental facilities such as atomic absorption spectrometry[7], cyclic voltammetry[8], chromatography[9], neutron activation analysis[10], ion sensitive electrodes[11], inductively coupled plasma spectrometry[12], etc., are accessible for the detection of these types of analytes. However, several of these methods are time consuming and expensive[13]. These types of expensive instrumental facilities cannot be easily used for on-site and real time monitoring of environmentally and biologically important systems[14]. Thus, there is an urgent need of simple, fast and reliable methods for the detection of environmentally and biologically important analytes.

1. Need of chemical sensors

In recent years, chemical sensing offers simple and highly sensitive method for the detection of various analytes[15-18]. It is one of the rapid responsive simple analytical method, useful for the detection of countless varieties of analytes[19-26]. The process of detection of a particular analyte, which may be charged or neutral species, using chemosensor is known as chemical sensing or chemosensing. In recent years, optical sensors have significant role in monitoring of various analytes using UV-Visible or fluorescence spectroscopy. The development of chemosensors received considerable attention because of their rapid response, convenience, non-destructive nature, easy operation, high sensitivity and selectivity offered in both quantitative and qualitative analysis. The possibility of visual detection of analytes by the use of chemosensors is the prime attractive feature of this

method[27-29]. Chemosensors find applications in many disciplines. Scientific community, especially, chemists, biologist, physicist and material scientists are very interested in the design and development of novel sensors with better capability. Over the past two decades, a large number of chemosensors are reported for monitoring various analytes[3, 30-32].

Chemosensor is a synthetic chemical system which is capable of binding with an analyte in a selective and reversible manner. This is followed by a change in one or more properties of the system in the form of colour or fluorescence. A typical chemosensor contains a receptor (the recognition site) linked to a signal source, such as a fluorophore/chromophore. The analyte recognition by the receptor alters the electronic and molecular structure of the chemosensor, resulting changes in the sensor properties (absorption/emission), which allow naked eye detection of the analyte. Further quantification is feasible by spectroscopic methods. Changes in the electronic structure are responsible for the variations in the intensity or wavelength of absorption or emission. Molecular structural changes lead to alterations in the distance or orientation between fluorophore pairs[1, 33].

2. Design strategies of chemical sensors

There are two strategies used to design of chemosensors for analyte detection in solution (Fig 1). In one case, the binding site is directly attached to the signaling moiety. In such cases, the optical response is achieved by the alteration produced in the π-system of the signaling moiety due to the interaction of the analyte with the receptor

unit of the signaling moiety. In the other case, the receptor and signaling units are covalently linked by a 'spacer' group. In this case, in an aromatic system, the receptor communicates the binding events with the signaling moiety *via* electronic conjugation through the spacer. The binding interaction of the receptor with the analyte either increases or decreases the conjugation in the whole chemosensor system or produces a disturbance in its electronic conjugation[34]. Chemosensors having electronically independent receptor and signaling moiety, which are separated by a aliphatic spacer, photoinduced electron transfer is the leading mechanism behind the signal transduction[35].
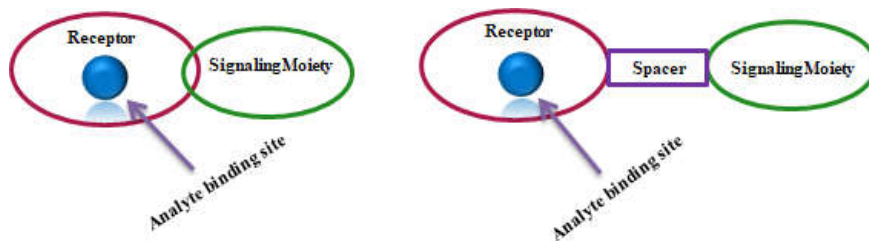
Fig 1. Schematic representation of design strategies of chemosensors

3. Role of UV-Visible- and fluorescence spectroscopy

UV-Visibe - and fluorescence spectroscopy are the prominent instrumental techniques used in chemical sensing and they permit the qualitative and quantitative estimation of analyte concentration. These spectroscopic techniques offer simple, highly sensitive and selective route for the estimation of various analytes in a cost effective manner. These enormously sensitive techniques also avoid the handling of

radioactive radiation in many biochemical measurements. These techniques do not consume analyte and detection is possible without reference. UV-Visible spectroscopy is employed in the case of colourimetric sensors for the quantification of analyte. Here, electronic properties of the sensor are changed upon interaction with the guest molecule. Thus, variations are produced in absorbance, i.e. here absorbance of the probe will be measured before and after the interaction with the analyte using UV-Visible spectroscopy. From the nature of variation of the absorbance obtained from the UV-Visible spectrum, primary information about the binding interaction between the probe molecule and the analyte is obtained. Colourimetric sensors have an additional attraction as the detection is possible with naked eye under day light[36].

In fluorescense based sensors, fluorescence spectroscopy is used for the estimation of analyte concentration. Fluorescence spectroscopy is one of the favorite instrumental methods among the scientific community and it has a decisive role in medical diagnostic, forensic analysis, DNA sequencing, genetic analysis, etc. Fluorescence is the emission of light by a substance that has absorbed light or other electromagnetic radiation which is a form of luminescence. When light of sufficient energy falls on a material, it is absorbed by the molecules and electronic excitation occurs. From the excited state, ie, from the higher energy state, the excited electrons return back to the ground state by emitting the energy in the form of light. In most cases, the emitted radiation has higher wavelength or lower in energy than that of the absorbed radiation. The difference in emission maxima and absorption maxima is called Stokes shift[37].
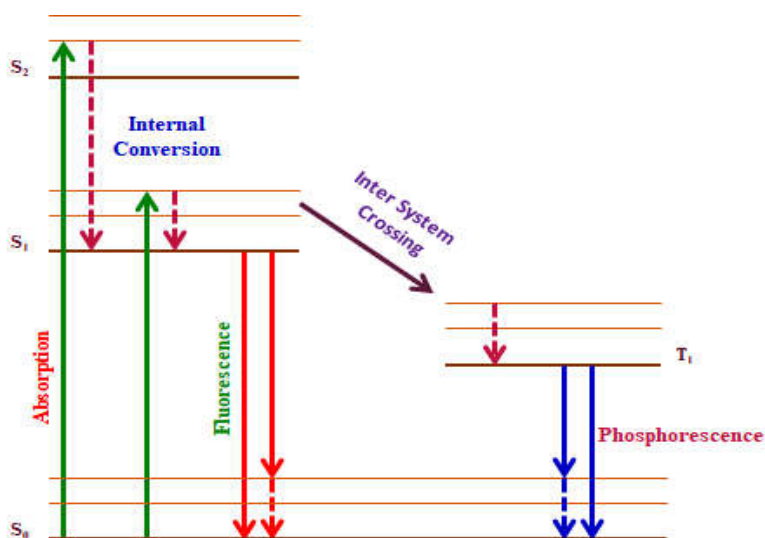
Fig 2. Jablonsky Daigram

The fluorescence phenomenon was first observed in a solution by Nicolas Monardes (Spanish physician and botanist) and he observed a blue tinge of the infusion of a wood, which is used for many medicinal purposes in Mexico[38]. Many scientists were interested in this unusual optical property and active research accompanied the discovery of a few fluorescent compounds like fluorite, chlorophyll and quinine solution. Later in 1852, George Gabriel Stokes introduced the term "fluorescence" for the first time in his report and identified that it was an emission phenomenon[39-41]. In 1935, Alexander Jablonski introduced a theoretical explanation for the novel fluorescence process with the help of a diagram known as Jablonski diagram depicted in Fig. 2. After this explanation, fluorescence received much more attention among the scientific community and now fluorescence spectroscopy is one of the most explored sophisticated instrumental techniques in various fields. Because of this valuable and great

theoretical foundation about the absorption and emission processes, Alexander Jablonski is regarded as the father of fluorescence spectroscopy[42].

4. "Turn-on" and "Turn – Off" fluorescence sensors

The idea of chemical sensing using fluorescence signal was first demonstrated in 1980 by Tsien during the synthesis of first fluorescent calcium indicator[43, 44]. In fluorescence sensors, the analyte binding responsible to change the fluorescence behavior of the sensor in the form a distinct fluorescence signal, such as by enhancing ("Turn-on"), quenching ("Turn-off") or shifting of the original signal. Most reported fluorescence sensors are either "turn-on" type or "turn-off" type. Fig. 3 represents the pictorial view of "turn-on" type and "turn-off" type fluorescence sensors. Fluorescence sensors are also designed based on the concept of fluorescence life time and fluorescence anisotropy [1] .
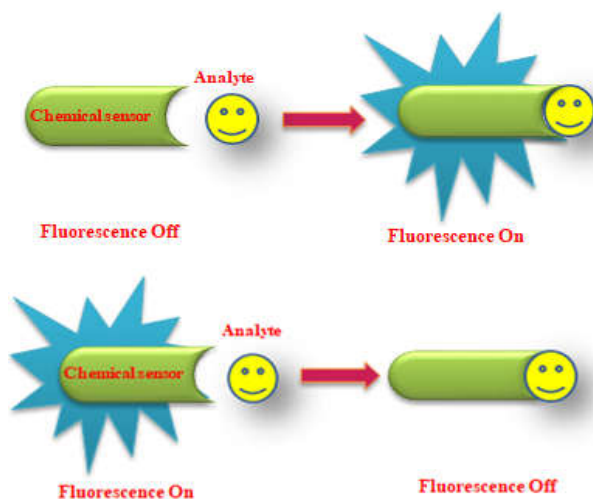
Fig 3. Pictorial representation of "Turn-On" and "Turn-Off" sensors

5. Signaling mechanisms

Several mechanisms have been put forward for exploiting the analyte sensing by optically responsible probes. They include photoinduced electron/energy transfer (PET), charge-transfer both Ligand to metal- and metal to ligand (LMCT and MLCT), intramolecular charge-transfer (ICT), excimer or exciple formation, excited-state intra-/intermolecular proton-transfer (ESIPT), and Fluorescence resonance energy transfer (FRET)[45-47]. The –C=N isomerization[48] is another mechanism responsible for cationic sensing. The electronic- and geometric environments of both the receptor and the analyte have great influence on the selectivity of a probe. The nature of the solvent also has a valuable role in the selectivity shown by a probe. Therefore, as per our need, the designing and developing appropriate molecular systems with suitable functionalities are challenging.

5.1. Photoinduced electron transfer (PET)

A typical PET molecule has an electron donating and an electron accepting group which are connected by a spacer. Upon photo excitation of the molecule, an electron from the highest occupied molecular orbital (HOMO) of the fluorophore is excited to the lowest unoccupied molecular orbital (LUMO) of it, followed by an electron transfer from the donor group of the molecule to the HOMO of the fluorophore, i.e., photo induced electron transfer (PET) occurs. This donor electron transfer blocks the radiative emission of the excited electron of the fluorophore to the ground state. Thus, this type of

molecule is non-emissive in their free state. Upon binding with a guest molecule, the redox potential of the donor group is raised so that the relevant HOMO has lower energy than the HOMO of the fluorophore. Thus, PET is not possible under this condition and leads to a radiative emission. Therefore, the analyte binding enhances the fluorescence intensity. The pictorial representation of PET is given in Fig.4. As per literature, the working mechanism behind most of the molecular systems is PET. A few of them with transition metal as guest are working based on the redox potential and electron transfer behavior of the transition metal ions.
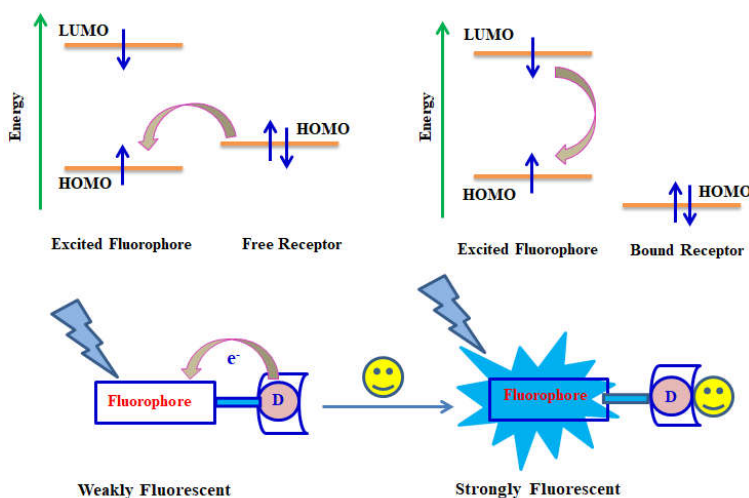
Fig.4. Pictorial representation of PET

5.2. Intramolecular charge transfer

Intramolecular charge transfer (ICT) mechanism is observed in molecular sensors having donor and acceptor group linked by a

conjugated π-system, designated as D-π-A. The π-system linker plays the role of a charge transfer channel, which means, upon photo excitation intramolecular charge transfer occurs from the donor part to the acceptor part of the fluorophore through the π-system. The need of a π-conjugated system is essential for ICT but a spacer is not must. Thus, a sensor working on this mechanism possesses different dipole moment in their ground state and electronically excited state. Upon interaction of an analyte with the donor moiety or acceptor moiety, a change in the photophysical property of the fluorophore occurs. This leads to a change in the ICT process. The interaction of an analyte with the donor moiety of the fluorophore decreases the electron donation capability of the donor toward the acceptor. This reduces the π-electron conjugation and a blue shift is observed in the spectral profile. At the same time, the π-electron conjugation is increased when an analyte binds through the receptor moiety of the fluorophore. Under this condition, a red shift is observed in the spectral profile.

5.3. Fluorescence resonance energy transfer (FRET)

A German physical chemist, Theodor Forster discovered the FRET and to acknowledge him, this process is also known as Forster Resonance Energy Transfer[49]. It is an electrodynamic process in which an excited state donor (usually fluorophore) transfers energy to the proximal ground state acceptor through dipole-dipole interaction. FRET requires spectral overlap between emission spectrum of the donor and absorption spectrum of the acceptor and it is sensitive to the distance between the donor and acceptor. Efficient FRET is observed

when the donor and acceptor are in close proximity, at angstrom distance ranges (10-100 Å). Large number of molecular sensors based on the FRET signaling mechanism are reported[50, 51].

5.4. Ligand to metal – and metal to ligand charge transfer

Ligand to metal- and metal to ligand charge transfer (LMCT and MLCT) are common signaling mechanisms observed in colourimetric sensors for metal ions. In this case, a fraction of the electronic charge is transferred between the molecular orbitals of the probe and the target. If the transfer of electronic charge occurs from molecular orbitals of the probe (ligand) to that of the target (metal), it is referred to as LMCT and in the opposite case i.e. the transfer of electronic charge from target (metal) to the molecular probe (ligand) is referred to as MLCT. Thus, *via* this electronic transfer, a weak charge transfer complex is formed. If the excitation energy of this transition occurs in the visible region of electromagnetic spectrum, it results in and observable colour change under day light. Thus molecular probes working in this mechanism produce a colour change upon the addition of target under day light.

5.5. Excited state intramolecular proton transfer (ESIPT)

Excited state intramolecular proton transfer (ESIPT) is another signaling mechanism employed in the development of molecular sensors. ESIPT arises when a molecule contains both proton donor and proton acceptor in close proximity. Upon photo excitation, a proton transfer occurs from the donor to the acceptor through a six membered

ring. This proton transfer suppresses the fluorescence intensity of the probe. Thus, the interaction of a guest molecule through either proton donor or proton acceptor or both inhibits the proton transfer and the ESIPT process, which leads to radiative emission.

5.6. Excimer formation

Formation of excimers or exciplex is another strategy exploited in the designing of chemical sensors. Excimers are the complexes formed by the interaction of the fluorophore in the exited state with the fluorophore of same structure in the ground state. If the fluorophore in the exited state has a different structure from that in the ground state, the resulting complex is called exciplex. When excimers and exciplex are formed, the emission spectral profile has a red shift when compared with that of the monomer. Thus, emission from the monomer and the complex are observed in a single spectral profile. The analyte recognition leads to the formation and deformation of excimers/ exciplex and this modification in the structure can be monitored with the help of UV-Visible - or fluorescence spectroscopic method.

5.7. C=N isomerization

A relatively new sensing mechanism, -C=N isomerization, was first introduced in 2007 and number of such type of molecular sensors are reported. Molecules bearing bridging and non-bridging –C=N double bond exhibit different fluorescence properties. Molecules possessing non-bridging –C=N double bond undergo isomerization

between their E and Z isomers. In this type of molecules, the excited state energy is used for the isomerization process and hence non-radiative emission occurs. Molecules having bridged –C=N double bond prevent the isomerization and radiative emission is possible. Fig. 5 depicts the molecular structures of bridged and unabridged -C=N compounds. From the above fact, the interaction of an analyte with the unbridged –C=N double bond of a molecule prevents the E and Z isomerization process and results in radiative emission. Thus, blocking of –C=N double isomerization by analyte recognition through imine bond is a useful signaling mechanism of chemical sensors. A number of fluorescent "turn-on" chemical sensors have been developed. A coumarin derived Schiff's base was the first fluorescent probe based on this mechanism [52].
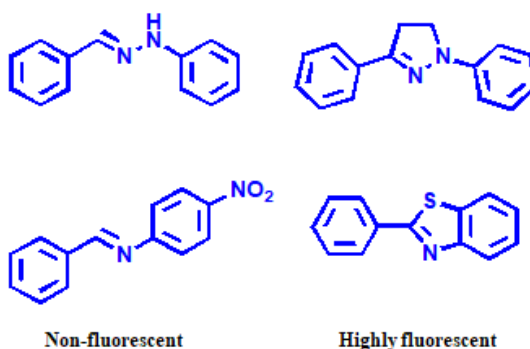
Fig. 5. Molecular structures of bridged and unabridged C=N compounds

6. Schiff bases as chemical sensors

The selective sensing response of different classes of compound towards a particular analyte is widely studied[47, 53, 54]. Schiff

bases are one of the important class of compounds displaying interesting sensing behaviour with various analytes. In 1864, Hugo Schiff introduced this new type of compound obtained by the condensation reaction between primary amines with an aldehydes or ketones[55]. Structurally, Schiff bases are nitrogen analogues of aldehydes or ketones in which the oxygen atom is replaced by nitrogen atom, i.e. carbonyl group of aldehyde or ketone is replaced by an imine or azomethine group. The basic structure of Schiff base is shown in Fig. 6. The lone pair of electron present on the *sp²* hybridized nitrogen atom of the azomethine group imparts high chelating ability to Schiff base.

Schiff bases are considered as "Privileged ligands" because of their relative ease of preparation and versatile structural features which are beneficial in various scientific areas including biological, pharmacological, clinical and analytical fields[56]. A large number of Schiff bases have been explored as chemical sensors for the detection of various species[57, 58]. The high chelating ability of the Schiff base is accountable to the selective optical response with a variety of metal ions. Supra molecular interactions have a vital role in the development of chemosensors. Based on this strategy, a large number of Schiff bases have been reported for the detection of various analytes, especially, anions like CN^-, F^-, which are real threat to human life and the environment[58-60]. The H-bond donors and acceptors present in the Schiff base skeleton is interact with the anions. In several cases, these secondary interactions function as an efficient signaling mechanism for the detection of various analytes. The selectivity of a receptor towards

a particular target depends on the electronic structures of both the receptor and target, size of the target, nature of the solvent, etc.

R1 & R2 = H or Alkyl or Aryl

R3 = Alkyl or Aryl
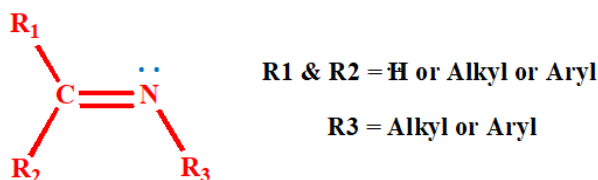
Fig. 6. General structure of Schiff base (Imine compound)

6.1. Schiff base derived chemical sensors for Fe^{3+}

Among the transition metal ions, iron is one of the most abundant metal ions on the earth crust and it exists most predominantly in the ferrous and ferric forms. In living organisms, iron plays important roles in electron transport, oxygen uptake, oxygen metabolism, etc. However, the level of iron present in human body should be fixed to a particular limit. Its excess intake as well as deficiency lead to several health problems[61, 62]. The selective detection of iron(III) has considerable importance because of its active involvement in various biological processes. In addition to the biological field, clinical, environmental and industrial areas require a selective optical probe for the qualitative and quantitative determination of iron.

Various types of chemical sensors based on colourimetric and fluorescence response (optical response) have been reported for the detection of iron. One of the major challenges in the development of

fluorescence sensors is the paramagnetic property of Fe^{3+}, which is responsible for the quenching of the fluorescence of the sensor molecule. Therefore, most of the fluorescent based sensors for Fe^{3+} are "turn-off" type[62] and only a few are of "turn-on" type[63, 64]. Fe^{3+} assisted hydrolysis is one of the strategies employed in the design of "turn-on" fluorescent sensors[36]. The colourimetric sensors, allow simple naked eye detection of the analyte. Therefore, largr numbers of colourimetric sensors have been developed based on the high complex forming ability of the Fe^{3+}. Fe^{3+} is a hard acid and therefore, form stable complexes with probes having hard donor atoms like N, O, etc. Major working mechanisms behind the colourimetric response are metal to ligand charge transfer- (MLCT), ligand to metal charge transfer- (LMCT) and intramolecualar charge transfer (ICT) transitions.

The reported chemosensors for Fe^{3+} are based on salicylaldehyde or 5-nitrosalicylaldehyde and o-aminophenol[65]; 8-formyl-7-hydroxy-4-methylcoumarine and 2-aminopyridine[66]; rhodamine-B-derivative and m-phthaloyl chloride[67]; rhodamine-B-hydrazine and 2-(N-methylpiperazinylimino)acetaldehyde[68]; 2-hydroxy-1-naphthaldehyde and 2-aminopyridine[69]; 8-hydroxyjulolidine-9-carboxaldehyde and 1-(3-Aminopropyl) imidazole[70]; rhodamine derivative and pyrazolone[71]; rhodamine hydrazide 2-tetrabutyldimethylsiloxybenzaldehyde[72]; aromatic aldehyde or substituted aromatic aldehyde andethylene diamine or *trans*-1,2-diaminocyclohexane[73]; rhodamine 6G hydrazine and 2-formylimidazole; rhodamine 6G ethylelediamine and imidazole-

2-carboxaldehyde[74]; pyrole-2-carboxaldehyde and 2-nitro-1-phenylene diamine or 1,4-phenylenediamine[75]. Several chemosensors based on LMCT mechanism are also reported. A series of five Schiff base derived colourimetric sensors were reported by Anthony and coworkers. Their chemosensing property was tuned by altering the structural motif of the sensor[33]; 2-(2'-cyanophenoxy)nitrobenzene with salicylaldehyde or substituted salicylaldehyde[15]; 2-(2'-aminophenoxy)benzene carboxylicacid and 4-methoxysalicylaldehyde or 2-hydroxynaphthaldehyde[76]; rhodamine derivative and 8-hydroxy quinolone[77]; 6-amino-3,4-benzocoumarine and 8-hydroxyquinoline-2-carbaldehyde[78].

Metal catalyzed hydrolysis of imine bond (-C=N) is another reaction used successfully for developing chemical sensors for metal ions. Wang *et al.*[79]reported a diketopyrrol Schiff base as a chemodosimeter for the detection of Fe^{3+} based on the hydrolytic cleavage of the imine bond. A chemical sensor, *bis*(coumarinyl) Schiff base developed by Lin *et al.*[80], was based on the Fe^{3+} catalyzed hydrolysis of imine bond. Kang and coworkers[81] reported a rhodamine 6G Schiff base for the detection of Fe^{3+}.

6.2. Schiff base derived chemical sensors for Cu^{2+}

Copper is the third most abundant transition metal present in the human body, actively involved in various physiological processes. Copper plays important roles in various metalloenzymes such as superoxide dismutase, cytochrome-c-oxidase, tyrosinase, etc. It plays vital roles in   bone - and tissue formation, cellular respiration, brain

functions, etc. Copper and its alloys are extensively used for industrial, pharmaceutical- and agricultural purposes. However, the high level exposure of copper leads to harmful effects in living organism. The accumulation of higher concentration of copper in human body leads to Alzheimer's-, Menkes- and Wilson's diseases. An excessive release of copper to the environment causes pollutions, which adversely affects plants and living organisms[82-87]. The Environmental Protection Agency (EPA) set a limit of copper in drinking water as 1.3 ppm (15 – 30 μM)[82]. Therefore, it is highly essential to develop suitable method to detect copper. Chemical sensors offer remarkable sensing features to detect copper ion. Different classes of organic compounds were reported as colourimetric or fluorescent sensors with outstanding detection limits.

Several Schiff base derived chemosensors based on diaminomaleonitrile and 1-pyrenealdehyde[88]; 1-aminopyrene and 2-hydroxy-1-naphthaldehyde[89]; rhodamine B hydrazide and indole-3-carboxaldehyde[90]; 2,6-diformyl-4-methylphenol and phenyl carbohydrazide[91]; 4-chloro-2-aminophenol and 4-dimethylamino cinnamaldehyde[92]; rhodamine B hydrazide and an aldehyde derived from sesamol[93]; 3, 5-di-tertbutyl-2-hydroxybenzaldehyde and 1, 4-diaminebenzene[94]; rhodamine hydrazide and 2-formylphenyl boronic acid[95]; N-aminophthalimide and 8-hydroxyjulolidine-9-carboxaldehyde[96]; 4-chloro-2-oxo-2H-chromene-3-carbaldehyde and p-nitrophenylhydrazine[97] were reported. Apart from these, a large number of Cu sensors other than those derived from Schiff base are also reported[3, 21, 98-101].

6.3.Schiff base derived chemical sensors for Al^{3+}

Aluminium is the third most abundant element on the earth crust after oxygen and silicon. The use of aluminium foil, vessels and kitchen utensils leads to its contamination in food. Once Al^{3+} ions are absorbed by the body, they are distributed in all cell and will remain there for a long time. The accumulation of aluminum in human body affects the functioning of central nervous system and leads to neurodegenerative diseases like Alzheimer's and Parkinson's syndrome[102, 103]. Due to acid rain and human activities, a large quantity of aluminum ions are released to the soil and water bodies, which adversely affect plants and aquatic species. According to a WHO report, the average daily human intake of aluminium is approximately 3–10 mg[36]. Therefore, it is highly essential to develop effective methods to detect the Al^{3+} ions.

Recently, a number of Schiff bases are reported as "off-on" fluorescent sensors for Al^{3+} with good specificity and selectivity. They are derived from - 2-hydroxyaniline and 2-hydroxyl-benzaldehyde[102]; 2-hydroxy-1-naphthaldehyde and 2-amino-3-hydroxypyridine[104]; 6-aminocoumarin and salicylaldehyde[105]; acetyl pyrazine and benzoic acid hydrazide[106]; 8-hydroxyjulolidine-9-carboxaldehyde and benzhydrazide[19]; 8-hydroxyjulolidine-9-carboxaldehyde and 3-(1Himidazol-1-yl) propan-1-amine[70]; 8-formyl-7-hydroxyl-4-methyl coumarin and 2-methyl quinoline-4-carboxylic hydrazide[107]; 2-amino-4-phenylthiazole and salicylaldehyde and 2-hydroxynaphthalene-1-carbaldehyde[108]; 4-aminoantipyrine and salicylaldehyde and

2-hydroxy-1-naphthal-dehyde[109]; 8-formyl-7-hydroxy-coumarin and o-aminophenol[110]; 2-hydroxy-1-naphthaldehyde and nicotinohydrazide[111]; 2-(quinolin-8-yloxy) acetohydrazide and acetyl pyrazine[112]; rhodamine 6G hydrazide and 1-H-pyrrole-2-carboxaldehyde[113]; 8-hydroxyquinoline-2-carbaldehyde and anisidine[114]; 1-naphthylamine and benzaldehyde[115]; antipyrine and 2,6-diformylpyridine[29]; fluorescein and 2-(aminomethyl) pyridine[116]; 1-phenyl-3-methyl-4-acetyl-pyrazolone-5 and isonicotinohydrazide[117]; benzaldehyde derivatives and 2-furoic hydrazine[14]; 4-aminoantipyrine and benzil or 1,3-diphenylpropane-1,3-dione[118]; 3-amino-4-hydroxycoumarin and salicylaldehyde[119]; 6-hydroxy-3-formylchromone and 2-furan formylhydrazine[120]; 5-chloro-7-formyl-8-hydroxyquinoline and aniline[121]; 2-hydroxy-1- naphthaldehyde and 2-quioline carboxaldehyde[103]; 2-hydroxy-1-naphthaldehyde and 5,6-diamino-2-mercaptopyrimidin-4-ol[122]. In addition to Schiff bases, a number of other class of compounds with photo responsive skeletons, like rhodamine, fluorescene, naphthalene, boron-dipyrromethene (BODIPY), coumaines and naphthalalimide have been reported for Al^{3+} detection with attractive sensing response.

6.4. Schiff base derived chemical sensors for CN^-

The monitoring of anions is highly essential because of their vital roles in many biological, environmental and chemical processes. Beyond a particular level, they too are harmful to life on earth[123]. Cyanide ions, even in trace amounts, lead to sudden death because of their strong ligating capability with the active sites of hemoglobin and

cytochrome c-oxidase. The wide spread use of cyanide and its derivatives in the industrial processes causes their contamination in the environment. Therefore, it is highly necessary to develop effective method to monitor the level of cyanide ion[4, 124-126]. Optical sensors are simple, convenient and cost effective to detect cyanide contamination *via* producing measurable changes in photophysical parameters. Three common approaches are followed to design cyanide sensors. In the most popular approach, the binding site and signaling unit of the sensors are linked by covalent bond. The cyanide recognition *via* binding cites, alters the colour or the fluorescence of the signaling unit. The second one is coordination complex based displacement approach, in which the introduction of cyanide ion leads to the regeneration of the free probe with its own photophysical property. Chemodosimetric approach is the third type, where the detection of cyanide is possible by specific and irreversible chemical reaction[127-129]. Here, the unique nucleophilicity of the cyanide ion is utilized for sensing. Schiff bases exhibit remarkable colourimetric and fluorescence response with cyanide ions and a large number such reports are available in literature.

The following Schiff base derived sensors based on 3,5-diamino-1,2,4-triazole and 2-hydroxy-1-naphthalehyde[130]; 8-hydroxyjulolidine-9-carboxaldehyde and 1-aminonaphthalen-2-ol[131]; 7-amino-4-methyl coumarin and 2-hydroxy-1-Naphthaldehyde[127]; 4-(diethylamino)salicylaldehyde and isonicotinyl hydrazide[132]; 2-hydroxyl-1-naphthaldehyde and N-(1-naphthyl) ethylenediamine dihydrochloride[133]; fluorene-2-aldehyde and

diaminomaleonitrile[134]; salicylaldehyde hydrazine and 3, 5-dibromosalicylaldehyde[135]; benzil and 2,4-(dinitrophenyl)hydrazine[136]; 2-amino-3-[(2-pyridylmethyl)amino]-2(Z)-butene-1,4-dinitrile and 2-hydroxy-1-naphthaldehyde[137] are reported. Beside Schiff bases a numbers of other class of compounds are reported as chemosensor for cyanide ions[138-143]. Most of these probes operate in organic or organic/aqueous mixture having higher organic fraction (volume).

7. Pyrazolones and their importance
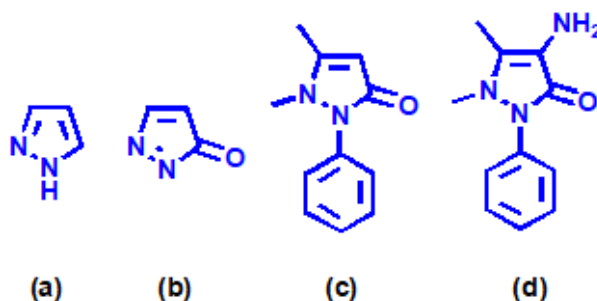
Fig. 7. Molecular structures of (a) pyrazole, (b) pyrazolone, (c) 1-phenyl-2,3-dimethylpyrazole-5-one, (d) 4-amino-1- phenyl-2,3-dimethylpyrazole-5-one

Pyrazolones are important class of heterocyclic compounds, which offer diverse pharmacological activities, including antibacterial, antifungal, antioxidant, antitumor, analgesics, antipyretic, antiinflamatory activities[144, 145]. Pyrazolones are five membered nitrogen containing heterocyclic compounds with lactum structure, which are widely used in the preparation of dyes and pigments. Among the various derivatives of pyrazolones, antipyrine is one with methyl

groups at C-2 and C-3 and with a phenyl group at N-1. Antipyrine with substitution at C-4 position by an amino group is known as 4-aminoantipyrine and hence its IUPAC name is 4-amino-2,3-dimethyl-1-phenyl-3-pyrazol-5-one. The structure of pyrazoline, pyrazolone, antipyrine and 4-aminoantipyrine are given in Fig. 7. The carbonyl group of 4-aminoantipyrine possess large dipole moment of about 5.48 D and hence it is potential donor and also have a strong basic character[146]. 4-aminoantipyrine forms a variety of Schiff's bases with aldehydes/ketones and they have many pharmacological, photovoltaic, optoelectronic and analytical applications[147-149]. Coordination chemists widely exploited the Schiff's bases of 4-aminoantipyrine as good ligands. Focusing on the coordinating ability of the carbonyl group of antipyrine, analytical chemists used their Schiff's bases for the detection of biologically - and environmentally relevant analytes. Up to now, only a few reports are available in literature on antipyrine derived Schiff's bases as chemical sensor for various analytes.

Gupta *et al.*[109] reported two antipyrine derived Schiff bases as fluorescent "turn-on" sensors for the detection of Al^{3+} with relatively good selectivity and sensitivity. A Fe^{3+} selective fluorescent probe of antipyrine was reported by Zhou and coworkers[150] and the fluorescent turn-on response of the probe with Fe^{3+} was reported in water. Chan *et al.*[151] synthesized a quinolinyl antipyrine based fluorescence sensor which selectively binds Zn^{2+}. Chelation enhanced fluorescence (CHEF) is its operating mechanism. Another antipyrine derived fluorescent probe for Al^{3+} was introduced by Zhou *et al.*[152] in 2013. A

turn-on fluorescent chemosensor was reported by Gupta *et al.*[153] which selectively binds Zn^{2+} in methanol. A 55-fold emission enhancement was observed for the probe in the presence of Zn^{2+} *via* stable chelation.

8. Coumarins and their features

Coumarins, 2H-chromen-2-ones, are benzo-2-pyrone derivatives which are widely distributed in natural samples and are used as traditional medicine. Their structures consist of fused benzene and pyrone rings with the pyrone carbonyl group at 2nd position[154, 155]. The basic skelton of coumarin is depicted in Fig.8. It is one of the most attractive class of compounds and its derivatives exhibit different biological and pharmacological activities like antibacterial, antifungal, anticancer, anti-HIV, antiinflammatory, antioxidant and antiviral activities etc[156-159]. Coumarins received considerable attention from researchers because of their attractive electronic and photonic properties. Their derivatives plays amazing role in optoelectronic application, such as, photosensitizers, chemical sensors, fluorescent dyes and pigments. They are also employed as insecticides, herbicides, fluorescent brightening agents, food additives, perfumes and cosmetics[160-164].

The incorporation of various substituents into the coumarin skeleton endues the molecule with promising properties, which encouraged the scientific community to synthesis new coumarine scaffolds. The photophysical properties of coumarin can be tuned by proper substitution. They also exhibit large Stocks shift, high fluorescence quantum yields and excellent photostabilities[165].

Compounds of coumarin are one of the most extensively studied fluorescent organic compounds. Numerous chemical sensors have been developed based on the florescence response of the coumarins for the detection of various analytes[20, 105, 142, 166].

Benzo-2-pyrone
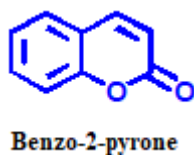
Fig. 8. Basic skelton of coumarine

9. Conclusions

Various metal ions and anions are closely related to life on earth. Up to a particular limit, most of them play an inevitable role in our day to day life. However, they are threaten to the human life and ecological balance when their contamination exceeds a particular limit. Therefore, it is highly essential to develop appropriate method for the monitoring these ions in most sensitive and selective manner. Development of optical sensors received much attention in current scenario because of their advantage of visual detection. Among the various organic probes, Schiff bases are one of the most widely studied class of compound and they exhibit exciting optical responses towards various environmentally and biologically relevant analytes with remarkable selectivity. Pyrazolones and coumarins are important class of heterocyclic compounds which show attractive optical properties. Optical probes of pyrazolones are rare in literature. Numbers of coumarin derived optical probes are reported. However, small

alteration in the structural motif of coumarin largely affects the optical response of the probe. Therefore researchers are always attracted by the intriguing optical behavior of coumarins. Number of optical probes both colourimetric- and fluorescence ones with attractive features for the detection of various cations and anions are reported by various research groups. However, the developments of new probes with significant features are still challenging.

10. Significance and scope of the present investigation

The selective and sensitive detection of biologically and environmentally significant analytes such as cations, anions and neutral species are highly essential. Many of them have a pivotal role in our life and some others are threat to life on earth and ecological balance. Thus, monitoring these analytes is highly essential and it is highly desirable to develop suitable method to monitor the concentration level of these ions. Out of the various currently available methods, detection of analytes by optical probes is attractive by means of their remarkable advantages. The simplicity in detection, that is detection is possible by naked eye is the prime attraction of this method. It also offers rapid response, convenience, non-destructive nature, easy operation, high sensitivity and selectivity both in quantitative and qualitative analysis. Thus, the design and development of optical probes or chemical sensors is an effective method for monitoring relevant anions and cations. Hence it was intend to develop optical probes for biologically and environmentally relevant analytes.

Here, we have synthesized four different Schiff bases of coumarin and antipyrine derivatives and their sensing knack towards various environmentally and biologically significant species were studied. These molecular probes and their chemo sensing responses are briefly outlined below.

1. 1,5-dimethyl-4-(2-hydroxy-1,2-diphenylethylideneamino)-2-phenylpyrazol-3-one: A Colurimetric Sensor for Fe(III) and "Turn-On" Fluorescence Sensor for Al(III).

2. 1-(8-methanylylidene-7-hydroxy-4-methyl-2H-chromen-2-one)-2-(2,4-dihydroxybenzylidene) hydrazine: A colorimetric sensor for Cu^{2+}.

3. 8-(1-(4-pyridinehydrazide)methylene-)-7-hydroxy-4-methylvoumain-2-one: A fluorescence "turn-on" sensor for Al^{3+}.

4. 8-(3-methyleneamino-2H-chromen-2-one)-7-hydroxy-4-methyl-2H-chromen-2-one: A fluorescence "turn-on" sensor for cyanide ion.

These probes exhibited remarkable colourimetric or fluorescence sensing responses with noticeable selectivity and sensitivity in dilute solution. The synthesis, characterization and sensing behaviours of each molecule with experimental support are discussed in following chapters of Part 1.

References

1. K. P. Carter, A. M. Young and A. E. Palmer, *Chemical reviews*, 2014, **114**, 4564-4601.

2. R. Bergonzi, L. Fabbrizzi, M. Licchelli and C. Mangano, *Coordination chemistry reviews*, 1998, **170**, 31-46.

3. L. D. Chebrolu, S. Thurakkal, H. S. Balaraman and R. Danaboyina, *Sensors and Actuators B: Chemical*, 2014, **204**, 480-488.

4. Z. Xu, X. Chen, H. N. Kim and J. Yoon, *Chemical Society Reviews*, 2010, **39**, 127-137.

5. V. Thiagarajan, P. Ramamurthy, D. Thirumalai and V. T. Ramakrishnan, *Organic letters*, 2005, **7**, 657-660.

6. C. Caltagirone and P. A. Gale, *Chemical Society Reviews*, 2009, **38**, 520-563.

7. M. H. Mashhadizadeh, M. Pesteh, M. Talakesh, I. Sheikhshoaie, M. M. Ardakani and M. A. Karimi, *Spectrochimica Acta Part B: Atomic Spectroscopy*, 2008, **63**, 885-888.

8. J. Di, S. Bi, T. Yang and M. Zhang, *Sensors and Actuators B: Chemical*, 2004, **99**, 468-473.

9. D. Harvey, *Modern analytical chemistry*, Boston: McGraw-Hill Companies, Inc., 2000.

10. J. Yu, J. Lo and C. Wai, *Analytica Chimica Acta*, 1983, **154**, 307-312.

11. V. Gupta, A. Singh and B. Gupta, *Analytica chimica acta*, 2007, **583**, 340-348.

12. S. L. Ferreira, W. N. Dos Santos, C. M. Quintella, B. c. B. Neto and J. M. Bosque-Sendra, *Talanta*, 2004, **63**, 1061-1067.

13. L. Wang, W. Qin, X. Tang, W. Dou and W. Liu, *The Journal of Physical Chemistry A*, 2011, **115**, 1609-1616.

14. K. Boonkitpatarakul, J. Wang, N. Niamnont, B. Liu, L. Mcdonald, Y. Pang and M. Sukwattanasinitt, *ACS Sensors*, 2015, **1**, 144-150.

15.   A. Kundu, P. Hariharan, K. Prabakaran and S. P. Anthony, *Sensors and Actuators B: Chemical*, 2015, **206**, 524-530.

16.   L. K. Kumawat and V. K. Gupta, *INTERNATIONAL JOURNAL OF ELECTROCHEMICAL SCIENCE*, 2016, **11**, 8861-8873.

17.   C.-H. Chen, D.-J. Liao, C.-F. Wan and A.-T. Wu, *Analyst*, 2013, **138**, 2527-2530.

18.   L. Wang, G. Fang and D. Cao, *Sensors and Actuators B: Chemical*, 2015, **207**, 849-857.

19.   S. A. Lee, G. R. You, Y. W. Choi, H. Y. Jo, A. R. Kim, I. Noh, S.-J. Kim, Y. Kim and C. Kim, *Dalton Transactions*, 2014, **43**, 6650-6659.

20.   J.-c. Qin, L. Fan and Z.-y. Yang, *Sensors and Actuators B: Chemical*, 2016, **228**, 156-161.

21.   T. Gunnlaugsson, J. P. Leonard and N. S. Murray, *Organic letters*, 2004, **6**, 1557-1560.

22.   Y. Zhou, J. F. Zhang and J. Yoon, *Chemical reviews*, 2014, **114**, 5511-5571.

23.   Y. Dong, J. Li, X. Jiang, F. Song, Y. Cheng and C. Zhu, *Organic letters*, 2011, **13**, 2252-2255.

24.   D. Udhayakumari, S. Suganya and S. Velmathi, *Journal of Luminescence*, 2013, **141**, 48-52.

25.   T.-Y. Gu, M. Dai, D. J. Young, Z.-G. Ren and J.-P. Lang, *Inorganic chemistry*, 2017, **56**, 4668-4678.

26.   L. Xue, C. Liu and H. Jiang, *Organic letters*, 2009, **11**, 1655-1658.

27.   S. Y. Lee, J. J. Lee, K. H. Bok, S. Y. Kim and C. Kim, *RSC Advances*, 2016, **6**, 28081-28088.

28.   A. Ghorai, J. Mondal, S. Chowdhury and G. K. Patra, *Dalton Transactions*, 2016, **45**, 11540-11553.

29.   M. Köse, S. Purtas, S. A. Güngör, G. Ceyhan, E. Akgün and V. McKee, *Spectrochimica Acta Part A: Molecular and Biomolecular Spectroscopy*, 2015, **136**, 1388-1394.

30.   J. F. Zhang, Y. Zhou, J. Yoon, Y. Kim, S. J. Kim and J. S. Kim, *Organic letters*, 2010, **12**, 3852-3855.

31.   D. Wu, A. C. Sedgwick, T. Gunnlaugsson, E. U. Akkaya, J. Yoon and T. D. James, *Chemical Society Reviews*, 2017, **46**, 7105-7123.

32.   S. B. Roy, J. Mondal, A. R. Khuda-Bukhsh and K. K. Rajak, *New Journal of Chemistry*, 2016, **40**, 9593-9608.

33.   H. Zhu, J. Fan, B. Wang and X. Peng, *Chemical Society Reviews*, 2015, **44**, 4337-4366.

34.   L. Basabe-Desmonts, D. N. Reinhoudt and M. Crego-Calama, *Chemical Society Reviews*, 2007, **36**, 993-1017.

35.   R. M. Duke, E. B. Veale, F. M. Pfeffer, P. E. Kruger and T. Gunnlaugsson, *Chemical society reviews*, 2010, **39**, 3936-3953.

36.   B. Kaur, N. Kaur and S. Kumar, *Coordination Chemistry Reviews*, 2018, **358**, 13-69.

37.   J. R. Lakowicz, *Principles of fluorescence spectroscopy*, Springer Science & Business Media, 2013.

38.   B. Valeur and M. N. Berberan-Santos, *Journal of Chemical Education*, 2011, **88**, 731-738.

39.   J. F. W. Herschel, *Philosophical Transactions of the Royal Society of London*, 1845, 143-145.

40.   G. G. Stokes, *Philosophical transactions of the Royal Society of London*, 1852, 463-562.

41.   G. G. Stokes, *Philosophical Transactions of the Royal Society of London*, 1853, 385-396.

42.   A. Jabłoński, *Zeitschrift für Physik*, 1935, **94**, 38-46.

43.   R. Y. Tsien, *Biochemistry*, 1980, **19**, 2396-2404.

44.   G. Grynkiewicz, M. Poenie and R. Y. Tsien, *Journal of biological chemistry*, 1985, **260**, 3440-3450.

45.   J. Wu, W. Liu, J. Ge, H. Zhang and P. Wang, *Chemical Society Reviews*, 2011, **40**, 3483-3495.

46. J.-S. Wu, W.-M. Liu, X.-Q. Zhuang, F. Wang, P.-F. Wang, S.-L. Tao, X.-H. Zhang, S.-K. Wu and S.-T. Lee, *Organic letters*, 2007, **9**, 33-36.

47. B. Valeur and I. Leray, *Coordination Chemistry Reviews*, 2000, **205**, 3-40.

48. O. García-Beltrán, B. Cassels, C. Pérez, N. Mena, M. Núñez, N. Martínez, P. Pavez and M. Aliaga, *Sensors*, 2014, **14**, 1358-1371.

49. S.-J. Moon, E. Baranoff, S. M. Zakeeruddin, C.-Y. Yeh, E. W.-G. Diau, M. Grätzel and K. Sivula, *Chemical Communications*, 2011, **47**, 8244-8246.

50. V. K. Praveen, S. J. George, R. Varghese, C. Vijayakumar and A. Ajayaghosh, *Journal of the American Chemical Society*, 2006, **128**, 7542-7550.

51. Y. Hu, J. Wang, L. Long and X. Xiao, *Luminescence*, 2016, **31**, 16-21.

52. J. E. Johnson, N. M. Morales, A. M. Gorczyca, D. D. Dolliver and M. A. McAllister, *The Journal of organic chemistry*, 2001, **66**, 7979-7985.

53. A. K. Das and S. Goswami, *Sensors and Actuators B: Chemical*, 2017, **245**, 1062-1125.

54. L. E. Santos-Figueroa, M. E. Moragues, E. Climent, A. Agostini, R. Martínez-Máñez and F. Sancenon, *Chemical society reviews*, 2013, **42**, 3489-3613.

55. H. Schiff, *Justus Liebigs Annalen der Chemie*, 1864, **131**, 118-119.

56. Y. Jia and J. Li, *Chemical reviews*, 2014, **115**, 1597-1621.

57. J. Cheng, K. Wei, X. Ma, X. Zhou and H. Xiang, *The Journal of Physical Chemistry C*, 2013, **117**, 16552-16563.

58. W. Y. Kim, H. Shi, H. S. Jung, D. Cho, P. Verwilst, J. Y. Lee and J. S. Kim, *Chemical Communications*, 2016, **52**, 8675-8678.

59. X. Zhang, L. Guo, F.-Y. Wu and Y.-B. Jiang, *Organic letters*, 2003, **5**, 2667-2670.

60.   S. Nandi and D. Das, *ACS Sensors*, 2015, **1**, 81-87.

61.   B.-R. Gao, H.-Y. Wang, Y.-W. Hao, L.-M. Fu, H.-H. Fang, Y. Jiang, L. Wang, Q.-D. Chen, H. Xia and L.-Y. Pan, *The Journal of Physical Chemistry B*, 2009, **114**, 128-134.

62.   L. McDonald, J. Wang, N. Alexander, H. Li, T. Liu and Y. Pang, *The Journal of Physical Chemistry B*, 2016, **120**, 766-772.

63.   Y. Xiang and A. Tong, *Organic Letters*, 2006, **8**, 1549-1552.

64.   C.-H. Chen, P.-J. Hung, C.-F. Wan and A.-T. Wu, *Inorganic Chemistry Communications*, 2013, **38**, 74-77.

65.   S. Prabhu, S. Saravanamoorthy, M. Ashok and S. Velmathi, *Journal of Luminescence*, 2012, **132**, 979-986.

66.   S. Devaraj, Y.-k. Tsui, C.-Y. Chiang and Y.-P. Yen, *Spectrochimica Acta Part A: Molecular and Biomolecular Spectroscopy*, 2012, **96**, 594-599.

67.   X. Chen, H. Hong, R. Han, D. Zhang, Y. Ye and Y.-f. Zhao, *Journal of fluorescence*, 2012, **22**, 789-794.

68.   S.-R. Liu and S.-P. Wu, *Sensors and Actuators B: Chemical*, 2012, **171**, 1110-1116.

69.   T.-B. Wei, P. Zhang, B.-B. Shi, P. Chen, Q. Lin, J. Liu and Y.-M. Zhang, *Dyes and Pigments*, 2013, **97**, 297-302.

70.   Y. W. Choi, G. J. Park, Y. J. Na, H. Y. Jo, S. A. Lee, G. R. You and C. Kim, *Sensors and Actuators B: Chemical*, 2014, **194**, 343-352.

71.   S. Parihar, V. P. Boricha and R. Jadeja, *Luminescence*, 2015, **30**, 168-174.

72.   Z.-Q. Hu, M. Du, L.-F. Zhang, F.-Y. Guo, M.-D. Liu and M. Li, *Sensors and Actuators B: Chemical*, 2014, **192**, 439-443.

73.   C. Wang, Y. Liu, J. Cheng, J. Song, Y. Zhao and Y. Ye, *Journal of Luminescence*, 2015, **157**, 143-148.

74.   X. Wan, T. Liu, H. Liu, L. Gu and Y. Yao, *RSC Advances*, 2014, **4**, 29479-29484.

75. D. Udhayakumari and S. Velmathi, *Spectrochimica Acta Part A: Molecular and Biomolecular Spectroscopy*, 2014, **122**, 428-435.

76. A. Kundu, P. Hariharan, K. Prabakaran and S. P. Anthony, *Spectrochimica Acta Part A: Molecular and Biomolecular Spectroscopy*, 2015, **151**, 426-431.

77. Z. Li, H. Li, C. Shi, M. Yu, L. Wei and Z. Ni, *Spectrochimica Acta Part A: Molecular and Biomolecular Spectroscopy*, 2016, **159**, 249-253.

78. N. Roy, A. Dutta, P. Mondal, P. C. Paul and T. S. Singh, *Sensors and Actuators B: Chemical*, 2016, **236**, 719-731.

79. L. Wang, L. Yang and D. Cao, *Sensors and Actuators B: Chemical*, 2014, **202**, 949-958.

80. W. Lin, L. Yuan, W. Tan, J. Feng and L. Long, *Chemistry–A European Journal*, 2009, **15**, 1030-1035.

81. M. H. Lee, T. Van Giap, S. H. Kim, Y. H. Lee, C. Kang and J. S. Kim, *Chemical Communications*, 2010, **46**, 1407-1409.

82. H. S. Jung, P. S. Kwon, J. W. Lee, J. I. Kim, C. S. Hong, J. W. Kim, S. Yan, J. Y. Lee, J. H. Lee and T. Joo, *Journal of the American Chemical Society*, 2009, **131**, 2008-2012.

83. J.-J. Xiong, P.-C. Huang, C.-Y. Zhang and F.-Y. Wu, *Sensors and Actuators B: Chemical*, 2016, **226**, 30-36.

84. I. Bertini, H. B. Gray, S. J. Lippard and J. S. Valentine, *Bioinorganic chemistry*, University Science Books, 1994.

85. J. Zhang, B. Zhao, C. Li, X. Zhu and R. Qiao, *Sensors and Actuators B: Chemical*, 2014, **196**, 117-122.

86. D. J. Waggoner, T. B. Bartnikas and J. D. Gitlin, *Neurobiology of disease*, 1999, **6**, 221-230.

87. J. Y. Noh, G. J. Park, Y. J. Na, H. Y. Jo, S. A. Lee and C. Kim, *Dalton transactions*, 2014, **43**, 5652-5656.

88. S.-P. Wu, T.-H. Wang and S.-R. Liu, *Tetrahedron*, 2010, **66**, 9655-9658.

89.   Y. R. Bhorge, H.-T. Tsai, K.-F. Huang, A. J. Pape, S. N. Janaki and Y.-P. Yen, *Spectrochimica Acta Part A: Molecular and Biomolecular Spectroscopy*, 2014, **130**, 7-12.

90.   Y.-A. Son, *Textile Coloration and Finishing*, 2014, **26**, 7-12.

91.   S. Anbu, R. Ravishankaran, M. F. C. Guedes da Silva, A. A. Karande and A. J. Pombeiro, *Inorganic chemistry*, 2014, **53**, 6655-6664.

92.   D. Peralta-Domínguez, M. Rodriguez, G. Ramos-Ortiz, J. Maldonado, D. Luna-Moreno, M. Ortiz-Gutierrez and V. Barba, *Sensors and Actuators B: Chemical*, 2016, **225**, 221-227.

93.   B. Zhang, Q. Diao, P. Ma, X. Liu, D. Song and X. Wang, *Sensors and Actuators B: Chemical*, 2016, **225**, 579-585.

94.   P. Torawane, S. K. Sahoo, A. Borse and A. Kuwar, *Luminescence*, 2017, **32**, 1426-1430.

95.   X. Tang, J. Han, Y. Wang, L. Ni, X. Bao, L. Wang and W. Zhang, *Spectrochimica Acta Part A: Molecular and Biomolecular Spectroscopy*, 2017, **173**, 721-726.

96.   D. H. Joo, J. S. Mok, G. H. Bae, S. E. Oh, J. H. Kang and C. Kim, *Industrial & Engineering Chemistry Research*, 2017, **56**, 8399-8407.

97.   D. Roy, A. Chakraborty and R. Ghosh, *Spectrochimica Acta Part A: Molecular and Biomolecular Spectroscopy*, 2018, **191**, 69-78.

98.   A. Kumar, V. Kumar, U. Diwan and K. Upadhyay, *Sensors and Actuators B: Chemical*, 2013, **176**, 420-427.

99.   Z. Xu, J. Pan, D. R. Spring, J. Cui and J. Yoon, *Tetrahedron*, 2010, **66**, 1678-1683.

100.   P. Kaur, D. Sareen and K. Singh, *Talanta*, 2011, **83**, 1695-1700.

101.   Y. Peng, Y.-M. Dong, M. Dong and Y.-W. Wang, *The Journal of organic chemistry*, 2012, **77**, 9072-9080.

102.   S. Kim, J. Y. Noh, K. Y. Kim, J. H. Kim, H. K. Kang, S.-W. Nam, S. H. Kim, S. Park, C. Kim and J. Kim, *Inorganic chemistry*, 2012, **51**, 3597-3602.

103.   S. B. Roy and K. K. Rajak, *Journal of Photochemistry and Photobiology A: Chemistry*, 2017, **332**, 505-514.

104.   W.-H. Ding, W. Cao, X.-J. Zheng, D.-C. Fang, W.-T. Wong and L.-P. Jin, *Inorganic chemistry*, 2013, **52**, 7320-7322.

105.   S. Guha, S. Lohar, A. Sahana, A. Banerjee, D. A. Safin, M. G. Babashkina, M. P. Mitoraj, M. Bolte, Y. Garcia and S. K. Mukhopadhyay, *Dalton Transactions*, 2013, **42**, 10198-10207.

106.   Z.-C. Liao, Z.-Y. Yang, Y. Li, B.-D. Wang and Q.-X. Zhou, *Dyes and Pigments*, 2013, **97**, 124-128.

107.   J.-c. Qin, T.-r. Li, B.-d. Wang, Z.-y. Yang and L. Fan, *Spectrochimica Acta Part A: Molecular and Biomolecular Spectroscopy*, 2014, **133**, 38-43.

108.   V. K. Gupta, A. K. Singh and L. K. Kumawat, *Sensors and Actuators B: Chemical*, 2014, **195**, 98-108.

109.   V. K. Gupta, A. K. Singh and N. Mergu, *Electrochimica Acta*, 2014, **117**, 405-412.

110.   Y.-G. Zhang, Z.-H. Shi, L.-Z. Yang, X.-L. Tang, Y.-Q. An, Z.-H. Ju and W.-S. Liu, *Inorganic Chemistry Communications*, 2014, **39**, 86-89.

111.   J.-c. Qin, Z.-y. Yang and P. Yang, *Inorganica Chimica Acta*, 2015, **432**, 136-141.

112.   C.-r. Li, J.-c. Qin, G.-q. Wang, B.-d. Wang, A.-k. Fu and Z.-y. Yang, *Inorganica Chimica Acta*, 2015, **430**, 91-95.

113.   H. Kim, B. A. Rao, J. W. Jeong, S. Mallick, S.-M. Kang, J. S. Choi, C.-S. Lee and Y.-A. Son, *Sensors and Actuators B: Chemical*, 2015, **210**, 173-182.

114.   J. Tian, X. Yan, H. Yang and F. Tian, *RSC Advances*, 2015, **5**, 107012-107019.

115.   J. Kumar, M. J. Sarma, P. Phukan and D. K. Das, *Dalton Transactions*, 2015, **44**, 4576-4581.

116.   Q. Diao, P. Ma, L. Lv, T. Li, Y. Sun, X. Wang and D. Song, *Sensors and Actuators B: Chemical*, 2016, **229**, 138-144.

117. J.-C. Qin, X.-y. Cheng, R. Fang, M.-f. Wang, Z.-y. Yang, T.-r. Li and Y. Li, *Spectrochimica Acta Part A: Molecular and Biomolecular Spectroscopy*, 2016, **152**, 352-357.

118. L. K. Kumawat, N. Mergu, M. Asif and V. K. Gupta, *Sensors and Actuators B: Chemical*, 2016, **231**, 847-859.

119. B. Sen, S. K. Sheet, R. Thounaojam, R. Jamatia, A. K. Pal, K. Aguan and S. Khatua, *Spectrochimica Acta Part A: Molecular and Biomolecular Spectroscopy*, 2017, **173**, 537-543.

120. C.-r. Li, J.-c. Qin, B.-d. Wang, L. Fan, J. Yan and Z.-y. Yang, *Journal of fluorescence*, 2016, **26**, 345-353.

121. J. Wang, Y. Li, K. Li, X. Meng and H. Hou, *Chemistry–A European Journal*, 2017, **23**, 5081-5089.

122. N. Yadav and A. K. Singh, *Materials Science and Engineering: C*, 2018, **90**, 468-475.

123. P. A. Gale and C. Caltagirone, *Chemical Society Reviews*, 2015, **44**, 4212-4227.

124. R. Badugu, J. R. Lakowicz and C. D. Geddes, *Journal of the American Chemical Society*, 2005, **127**, 3635-3641.

125. S. Kumar, P. Singh, G. Hundal, M. S. Hundal and S. Kumar, *Chemical Communications*, 2013, **49**, 2667-2669.

126. C. R. Nicoleti, L. G. Nandi and V. G. Machado, *Analytical chemistry*, 2014, **87**, 362-366.

127. Y.-L. Leng, J.-H. Zhang, Q. Li, Y.-M. Zhang, Q. Lin, H. Yao and T.-B. Wei, *New Journal of Chemistry*, 2016, **40**, 8607-8613.

128. L. Yang, X. Li, J. Yang, Y. Qu and J. Hua, *ACS applied materials & interfaces*, 2013, **5**, 1317-1326.

129. Z. Yang, Z. Liu, Y. Chen, X. Wang, W. He and Y. Lu, *Organic & biomolecular chemistry*, 2012, **10**, 5073-5076.

130. J. J. Lee, S. Y. Lee, K. H. Bok and C. Kim, *Journal of fluorescence*, 2015, **25**, 1449-1459.

131. G. J. Park, I. H. Hwang, E. J. Song, H. Kim and C. Kim, *Tetrahedron*, 2014, **70**, 2822-2828.

132. J.-H. Hu, Y. Sun, J. Qi, P.-X. Pei, Q. Lin and Y.-M. Zhang, *RSC Advances*, 2016, **6**, 100401-100406.

133. T. Wei, H. Li, Q. Wang, G. Yan, Y. Zhu, T. Lu, B. Shi, Q. Lin and Y. Zhang, *Supramolecular Chemistry*, 2016, **28**, 314-320.

134. S. Sarveswari, A. J. Beneto and A. Siva, *Sensors and Actuators B: Chemical*, 2017, **245**, 428-434.

135. B. Yu, C.-Y. Li, Y.-X. Sun, H.-R. Jia, J.-Q. Guo and J. Li, *Spectrochimica Acta Part A: Molecular and Biomolecular Spectroscopy*, 2017, **184**, 249-254.

136. J. Mondal, A. K. Manna and G. K. Patra, *Inorganica Chimica Acta*, 2018, **474**, 22-29.

137. K. Rezaeian, H. Khanmohammadi and S. G. Dogaheh, *New Journal of Chemistry*, 2018, **42**, 2158-2166.

138. N. Kumari, S. Jha and S. Bhattacharya, *Chemistry–An Asian Journal*, 2012, **7**, 2805-2812.

139. L. Tang, Y. Zou, K. Zhong and Y. Bian, *RSC Advances*, 2016, **6**, 48351-48356.

140. T.-B. Wei, W.-T. Li, Q. Li, W.-J. Qu, H. Li, G.-T. Yan, Q. Lin, H. Yao and Y.-M. Zhang, *RSC Advances*, 2016, **6**, 43832-43837.

141. K.-S. Lee, H.-J. Kim, G.-H. Kim, I. Shin and J.-I. Hong, *Organic letters*, 2008, **10**, 49-51.

142. Y. Shiraishi, M. Nakamura, N. Hayashi and T. Hirai, *Analytical chemistry*, 2016, **88**, 6805-6811.

143. Q. Lin, L. Liu, F. Zheng, P.-P. Mao, J. Liu, Y.-M. Zhang, H. Yao and T.-B. Wei, *RSC Advances*, 2017, **7**, 38458-38462.

144. A. Grieco, R. CASTELLANO, A. MATERA, S. MARCOCCIA, P. DI ROCCO, E. RAGAZZONI, F. M. VECCHIO and G. GASBARRINI, *Journal of gastroenterology and hepatology*, 1998, **13**, 460-466.

145. K. Annola, V. Karttunen, P. Keski-Rahkonen, P. Myllynen, D. Segerbäck, S. Heinonen and K. Vähäkangas, *Toxicology letters*, 2008, **182**, 50-56.

146. N. Raman, S. Johnson Raja and A. Sakthivel, *Journal of Coordination Chemistry*, 2009, **62**, 691-709.

147. H. Zeyada, M. El-Nahass, I. El-Zawawi and E. El-Menyawy, *The European Physical Journal-Applied Physics*, 2010, **49**.

148. Y. Sun, Q. Hao, W. Tang, Y. Wang, X. Yang, L. Lu and X. Wang, *Materials Chemistry and Physics*, 2011, **129**, 217-222.

149. N. El-Ghamaz, M. Diab, A. El-Bindary, A. El-Sonbati and H. Seyam, *Materials Science in Semiconductor Processing*, 2014, **27**, 521-531.

150. Y. Zhou, H. Zhou, J. Zhang, L. Zhang and J. Niu, *Spectrochimica Acta Part A: Molecular and Biomolecular Spectroscopy*, 2012, **98**, 14-17.

151. Q.-H. You, P.-S. Chan, W.-H. Chan, S. C. Hau, A. W. Lee, N. Mak, T. C. Mak and R. N. Wong, *RSC Advances*, 2012, **2**, 11078-11083.

152. Y. Zhou, J. Zhang, H. Zhou, X. Hu, L. Zhang and M. Zhang, *Spectrochimica Acta Part A: Molecular and Biomolecular Spectroscopy*, 2013, **106**, 68-72.

153. V. K. Gupta, A. K. Singh and L. K. Kumawat, *Sensors and Actuators B: Chemical*, 2014, **204**, 507-514.

154. S. S. Bahekar and D. B. Shinde, *Tetrahedron letters*, 2004, **45**, 7999-8001.

155. K. N. Venugopala, V. Rashmi and B. Odhav, *BioMed research international*, 2013, **2013**.

156. C. Gnerre, M. Catto, F. Leonetti, P. Weber, P.-A. Carrupt, C. Altomare, A. Carotti and B. Testa, *Journal of medicinal chemistry*, 2000, **43**, 4747-4758.

157. M. Matos, S. Vazquez-Rodriguez, L. Santana, E. Uriarte, C. Fuentes-Edfuf, Y. Santos and A. Muñoz-Crego, *Molecules*, 2013, **18**, 1394-1404.

158. G. Borges Bubols, D. da Rocha Vianna, A. Medina-Remon, G. von Poser, R. Maria Lamuela-Raventos, V. Lucia Eifler-Lima and S. Cristina Garcia, *Mini reviews in medicinal chemistry*, 2013, **13**, 318-334.

159. M. Joao Matos, D. Viña, S. Vazquez-Rodriguez, E. Uriarte and L. Santana, *Current topics in medicinal chemistry*, 2012, **12**, 2210-2239.

160. T. Yu, Y. Zhao and D. Fan, *Journal of molecular structure*, 2006, **791**, 18-22.

161. G. Jones, W. R. Jackson, S. Kanoktanaporn and W. R. Bergmark, *Photochemistry and photobiology*, 1985, **42**, 477-483.

162. R. M. Christie and C.-H. Lui, *Dyes and Pigments*, 1999, **42**, 85-93.

163. I. P. Kostova, I. I. MANOLOV and M. K. RADULOVA, *Acta Pharmaceutica*, 2004, **54**, 37-47.

164. B. Ren, D. Zhao, S. Liu, X. Liu and Z. Tong, *Macromolecules*, 2007, **40**, 4501-4508.

165. Y.-W. Duan, H.-Y. Tang, Y. Guo, Z.-K. Song, M.-J. Peng and Y. Yan, *Chinese Chemical Letters*, 2014, **25**, 1082-1086.

166. R. Kaushik, A. Ghosh, A. Singh, P. Gupta, A. Mittal and D. A. Jose, *Acs Sensors*, 2016, **1**, 1265-1271.

CHAPTER 2

MATERIALS AND METHODS

This chapter deals with a brief description about the materials used, analytical methods and the instrumental technique adopted for the study.

1. Chemicals and reagents

4-Aminoantipyrine, 2-hydroxy-1,2-di(phenyl)ethanone (benzoin), resorcinol, 2,4-dihydroxysalicylaldehyde, hydrazine hydrate, isonicotinylhydrazide, salicylaldehyde, N - acetylglycine, hexamine, acetic anhydride, ethylacetoacetate, anhydrous sodium acetate, sodium bicarbonate, sodium hydroxide and potassium hydroxide pellets were purchased from Sigma Aldrich, Alfa Aesar, E.Merk or Qualigen. Chloride- or nitrate salts of different metals ions like Cr^{3+}, Fe^{3+}, Co^{2+}, Ni^{2+}, Cu^{2+}, Zn^{2+}, Al^{3+}, Ca^{2+}, Mg^{2+}, Na^{+}, K^{+}, Cd^{2+}, Hg^{2+} and Pb^{2+} were used for the cation sensing studies. These metal salts were purchased from Sigma Aldrich or E.Merk. Tertiary butyl ammonium salts of different anions like F^{-}, Cl^{-}, Br^{-}, I^{-}, CN^{-}, OH^{-}, OAc^{-}, NO_3^{-}, HSO_4^{-} and $H_2PO_4^{-}$ were used for the anion sensing studies and were purchased from Sigma Aldrich.

The solvents, methanol, ethanol, acetonitrile, dimethyl sulphoxide (DMSO), dimethylformamide (DMF), acetone and ethyl acetate were received from the chemical suppliers and were used without further purification. Concentrated - sulphuric acid, hydrochloric acid, nitric acid and glacial acetic acid were also used.
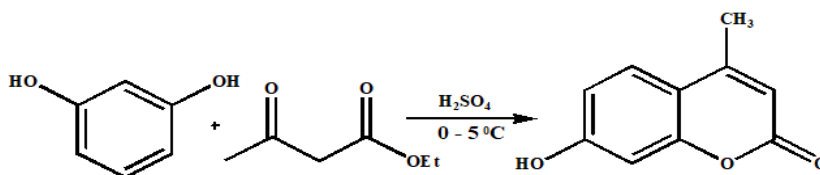
2. Synthesis of coumarins

2.1. Synthesis of 8-Formyl-7-hydroxy-4-methylcoumarin

8-Formyl-7-hydroxy-4-methylcoumarin was synthesized as per the following method[1, 2]
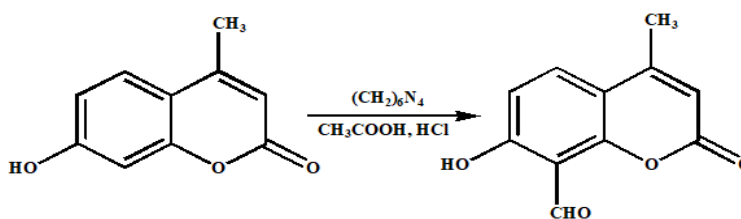
2.1.1. Synthesis of 7-Hydroxy-4-methylcoumarin

Resorcinol (11 g, 0.1 mol) was dissolved in ethyl acetoacetate (13 g, 0.1 mol) and this solution was added to 25 ml concentrated sulphuric acid under constant stirring at 0–5∘C. This mixture was stirred for about 30 min and then added to crushed ice with vigorous stirring. The precipitate obtained was filtered, washed with water and dried.

Scheme 1. Synthetic route of 7-hydroxy-4-methylcoumarin

2.1.2. Synthesis of 8-Formyl-7-hydroxy-4-methylcoumarin

Scheme 2. Synthetic route of 8-Formyl-7-hydroxy-4-methylcoumarin

7-Hydroxy-4-methylcoumarin (5 g) and hexamine (9.9 g) in glacial acetic acid (90 mL) were refluxed for 6 h. Then, 20% HCl (60 mL) was added to the mixture and further refluxed for about 1 h. After cooling, the mixture was extracted twice with ether (50 mL× 2). The combined organic layer was concentrated, keeps for 30 min and obtained light yellow coloured 8-formyl-7-hydroxy-4-methylcoumarin.

2.2. Synthesis of 3-Aminocoumarin

3 – Aminocoumarin was synthesized as per the following procedure[3].

2.2.1. Synthesis of 3-Acetamidocoumarin

A mixture of salicylaldehyde (1.2 g, 0.01 mol), N-acetylglycine (1.2 g, 0.01 mol), anhydrous sodium acetate (3.28 g, 0.04 mol) and freshly distilled acetic anhydride (30 mL) were taken in a 500 mL round-bottomed flask. This mixture was refluxed for about 6 h. The reaction mixture was cooled, diluted with 10 ml of water and further refluxed for 30 min. It solidified after cooling and the resulting solid mass was broken up into pieces with a spatula and filtered. It was washed with cold water, filtered and dried. The product was again washed with ethyl acetate, air dried and obtained an off-white precipitate.
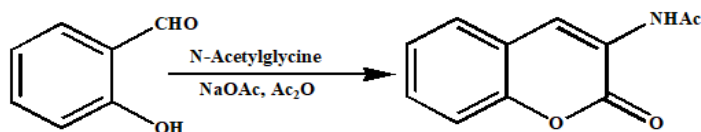
Scheme 3. Synthetic route of 3-Acetamidocoumarin

2.2.2. Hydrolysis of 3-Acetamidocoumarin
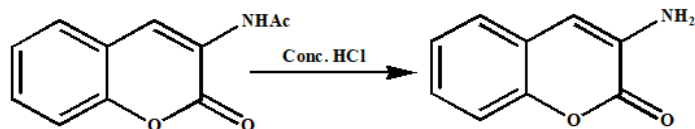
Scheme 4. Synthetic route of 3-Aminocoumarin

3-acetamidocoumarin was dissolved in hot ethanol (25 mL) and then treated with concentrated hydrochloric acid (5 mL). The resulting mixture was refluxed for 2 h, cooled, diluted with water, neutralized with aqueous saturated sodium bicarbonate and kept overnight. The resulting solid was filtered and washed with ethanol. The precipitate obtained was dried in air.

Schiff's bases used in the present investigation were synthesized by usual condensation reaction and the detailed synthetic procedures are discussed in respective chapters.

3. Methods

3.1. Jobs method of continuous variation

The stoichiometry and formula of a solid metal complex can be determined from the elemental analysis of the complex by standard procedure. But in the case of solutions, this is not a possible method. Job introduced a method to find out the formula of complex in solution and the method is known as Job's method of continuous variation.

In this method, the total molar concentration of metal plus ligand is kept constant and the ratio is varied from zero to infinity.

Initially, when the solution containins no metal ions, the absorbance or fluorescence obtained is due to the probe molecule. As the concentration of metal ions increases, absorbance or fluorescence increases (due to the formation of complex) until the metal to probe atio in the solution mixture equals to that in the complex. Under the Job conditions, i.e. total molar concentration of the two species is constant, this represents the maximum possible concentration of the complex. Further increasing metal ion concentration will decreases the absorbance or fluorescence. A plot of absorbance or fluorescence versus mole fraction of probe shows a maximum, this will be the ratio of complexation of metal with the probe[4].

3.2. Benesi – Hildebrand method

Benesi – Hildebrand method was used for the calculation of binding constant of non- bonded interactions, particularly 1 : 1 and 1 : 2 interactions . This method is based on the assumption that when one of the reactants is present in excess amount over the other reactant, the characteristic electronic absorption spectra/fluorescence spectra of the other reactant will be transparent in the collective absorption/emission range of the reaction system. Therefore, by measuring the absorption/emission spectra of the reaction before and after the formation of the product and its equilibrium, the association constant of the reaction can be determined[5]. The Benesi – Hildebrand equation for absorption and emission processes are given below

$$\frac{1}{(A - A_0)} = \frac{1}{K_a(A_{max} - A_0)} \; x \; \frac{1}{[M]^n} + \frac{1}{(A_{max} - A_0)}$$

where, A_0 and A are the absorbances of probe molecule in the absence - and presence of the analyte, A_{max} absorbance at maximum concentration of analyte, [M] is concentration of analyte and K_a is the association constant.

$$\frac{1}{(F - F_0)} = \frac{1}{K_a(F_{max} - F_0)} \; x \; \frac{1}{[M]^n} + \frac{1}{(F_{max} - F_0)}$$

where, F_0 and F are the fluorescence intensities of probe molecule in the absence - and presence of the analyte, F_{max} fluorescence intensity at maximum concentration of analyte, [M] is concentration of analyte and K_a is the association constant.

4. Instrumental techniques

Melting points of the probes were determined using standard melting point apparatus. CHN analyses were carried out on Vario EL III CHNS analyzer. The FTIR spectra (4000 - 400cm^{-1}) were recorded as KBr pellets on a Jasco FTIR 4100 spectrometer. The ^{1}H NMR and ^{13}C NMR spectra were recorded on a 400 MHz Bruker Avance III spectrometer using CDCl$_3$. The Electron-Spray Ionization Mass Spectrum (ESI-MS) was recorded on Waters **(**UPLC- TQD) mass spectrometer. The UV-Visible studies were carried out on a Jasco UV-Visible spectrophotometer of model V-550. Fluorescence measurements were carried out on an Agilent Technologies model Cary Eclipse Fluorescence spectrophotometer. Magnetic susceptibility measurements were carried out using a Sherwood Scientific magnetic susceptibility balance of model, Sherwood Scientific Cambridge employing Hg[Co(NCS)$_4$] as calibrant.

References

1.   A. Kulkarni, S. A. Patil and P. S. Badami, *European journal of medicinal chemistry*, 2009, **44**, 2904-2912.

2.   Y. Dong, X. Mao, X. Jiang, J. Hou, Y. Cheng and C. Zhu, *Chemical Communications*, 2011, **47**, 9450-9452.

3.   A. A. Kudale, J. Kendall, C. C. Warford, N. D. Wilkins and G. J. Bodwell, *Tetrahedron letters*, 2007, **48**, 5077-5080.

4.   J. S. Renny, L. L. Tomasevich, E. H. Tallmadge and D. B. Collum, *Angewandte Chemie International Edition*, 2013, **52**, 11998-12013.

5.   R. Wang and Z. Yu, *Acta Physico-Chimica Sinica*, 2007, **23**, 1353-1359.

CHAPTER 3

ANTIPYRINE DERIVED SCHIFF BASE: A COLOURIMETRIC SENSOR FOR Fe(III) AND "TURN-ON" FLUORESCENCE SENSOR FOR Al(III)

Work in Brief....

➡️ *Synthesised a new antipyrine derived Schiff base (L) for dual sensing of Fe^{3+} and Al^{3+}.*

➡️ *Observed colourimetric response towards Fe^{3+} and turn-on fluorescence behaviour towards Al^{3+} in methanol.*

➡️ *Due to the transient interaction of Fe^{3+} with L in protic solvent, methanol the study was extended in an aprotic solvent, acetonitrile.*

1. Introduction

Iron is the most abundant transition metal ion in human body. It plays crucial role in many biological and chemical processes. Under physiological condition, this essential element of life exists in two stable oxidation states, Fe^{3+} (ferric ion) and Fe^{2+} (ferrous ion). Fe^{3+} is a crucial constituent of hemoglobin and also has an inevitable role in oxygen storage and transport. The excessive intake of iron leads to several health issues including vomiting, stomach pain, diarrhea, etc. Its deficiency also adversely affects human health[1, 2]. Therefore, it is highly essential to detect these ions in an effective manner. In addition to the biological field, clinical, environmental and industrial areas require a selective optical probe for the qualitative and quantitative determination of iron[3].

Al^{3+}, the third most abundant element on the earth crust, finds a variety of applications in our day to day life. The excess exposure to Al^{3+} adversely affects human health[4]. Due to the poor coordinating ability of Al^{3+} compared to transition metal ions, it is difficult to develop a selective optical probe for its detection[5-8]. Fe^{3+} and Al^{3+} have same charge, similar ionic radius and Lewis acid character and therefore it is difficult to discriminate them by means of one and the same optical probe. Wang *et al.*[9] reported a diketopyrrolopyrrol based Schiff base for the detection of Fe^{3+} and Al^{3+} based on the metal catalysed imine hydrolysis. Thus, the development of single probe molecule that has different sensing ability towards these metal ions is still challenging.

Colourimetric and fluorescence sensors offer simple and highly sensitive sensing method for the detection of various analytes[10-12]. Naked-eye detection is the prime attraction of the optical sensors and the analyte can be quantified by spectroscopic methods. Antipyrine, a pyrazolone derivative, exhibits a variety of biological properties. A number of antipyrine Schiff bases are found in literature and their applicability in several areas, including optoelectronic field are well established[13, 14].

Here, we report a new Schiff base, 1,5-dimethyl-4-(2-hydroxy-1,2-diphenylethylideneamino)-2-phenylpyrazol-3-one (L) obtained by the condensation of 4-amino-2, 3-dimethyl-1-phenyl-3-pyrazolin-5-one (4-aminoantipyrine) with 2-hydroxy-1,2-di(phenyl)ethanone (benzoin). The probe molecule exhibited a naked-eye colourimetric response toward Fe^{3+} and turn-on fluorescence behaviour towards Al^{3+} ion in methanol. Here, the nature of solvent affects the structural rigidity of the complex formed. Hence, we have also studied the nature of recognition of Fe^{3+} by our sensing system in an aprotic solvent, acetonitrile.

2. Experimental methods

2.1. Materials and methods

4-Amino-2,3-dimethyl-1-phenyl-3-pyrazolin-5-one (4-aminoantipyrine) and 2-hydroxy-1,2-di(phenyl)ethanone (benzoin) were purchased from Sigma Aldrich. The solvents were received from the chemical suppliers and were used without further purification.

Chloride- or nitrate salts of different metals were used for the sensing studies.

CHN analyses were carried out on Vario EL III CHNS analyzer. The FTIR spectra (4000 – 400 cm^{-1}) of the Schiff base and the Fe(III) complex were recorded as KBr pellets on a Jasco FTIR 4100 spectrometer. The ^{1}H NMR and ^{13}C NMR spectra were recorded on a 400MHz Bruker Avance III spectrometer using CDCl$_3$. The Electron-Spray Ionization Mass Spectrum (ESI-MS) was recorded on Waters (UPLC- TQD) mass spectrometer. The UV-Visible studies were carried out on a Jasco UV-Visible spectrophotometer of model V-550. Fluorescence measurements were carried out on an Agilent Technologies model Cary Eclipse Fluorescence spectrophotometer. Magnetic susceptibility measurements were carried out using a Sherwood Scientific magnetic susceptibility balance.

2.2. Synthesis of Schiff base and its Fe(III) complex

2.2.1. Synthesis of Schiff base

An ethanol solution of 2-hydroxy-1,2-di(phenyl)ethanone (1mmol, 0.212g) was added drop wise to an ethanol solution of |4-amino- 2, 3-dimethyl-1-phenyl-3-pyrazolin-5-one (1mmol, 0.203g) under constant stirring .The mixture was refluxed for 3 h. The resulting yellow coloured clear solution was allowed to crystallize at room temperature. The yellow precipitate formed was washed with acetone and recrystallized from ethanol. Yield

70%. Mp 173-178^{0}C. ^{1}H NMR (CDCl$_3$) δ (ppm): 3 (s, 1H, C-H); 2.9 (s,3H, N-CH$_3$), 2.4(s,3H, O-H); 2.1 (s,1H, C-CH$_3$), 7.2-8 (aromatic protons). ^{13}C NMR (CDCl$_3$) δ (ppm): 194.46, 162.22, 158.70, 149.91, 137.12, 136.73, 134.73, 134.90, 132.88, 132.32, 129.42, 129.00, 128.35, 127.93,126.76, 124.53, 36.11, 10.99. IR (KBr disk, cm^{-1}) 3432 υ(O-H), 1650 υ(C=O), 1590 υ(C=N). ESI-MS m/z: calcd. C$_{25}$H$_{23}$N$_3$O$_2$, 397.18; found, 396.19 [M-1]. CHN for C$_{25}$H$_{23}$N$_3$O$_2$ Anal.Calcd C, 78.5; H, 5.7; N, 10.5; O, 8.06. Found: C, 78; H, 5.3; N, 10.66; O, 8.4.

2.2.2. Synthesis of Fe(III) complex

Hot aqueous solution of FeCl$_3$ (0.162 g, 1 mmol) was added in drops to a hot ethanol solution of L (0.198 g, 0.5 mmol) taken in a round bottom flask. The mixture was allowed to reflux for about 2 - 3 h and kept aside for 3 - 4 days for evaporation. The solid product obtained was filtered, washed with petroleum benzene and dried. Yield 60%. Mp 93-96^{0}C, CHN for Fe$_2$C$_{25}$H$_{29}$N$_3$O$_6$Cl$_5$ Anal.Calcd C, 39.8; H, 3.8; N, 5.5; Found: C, 39.3; H, 3.5; N 5.3, Fe (III), Anal.Calcd, 14.6; Found: Fe, 14.1. IR (KBr disk, cm^{-1}) 3413 cm^{-1} υ(O-H), 1630 cm^{-1} υ(C=O), 1548 cm^{-1} υ(C=N), 473 cm^{-1} υ(M-N) and 438 cm^{-1} υ(M-O). UV-Visible (CH$_3$CN) 568, 362 and 241 nm. μ$_{eff}$ 3.72 BM.

2.3. Sample preparation for sensing studies

Fe^{3+}: Stock solutions of different metal ions in 5 mM concentration were prepared in methanol. From the above stock solutions, 1 equivalent (0.8 ml) of each of the different metal ions

such as Fe^{3+}, Co^{2+}, Ni^{2+}, Cu^{2+}, Zn^{2+}, Al^{3+}, Mg^{2+}, Ca^{2+}, Ba^{2+}, Pb^{2+}, Cd^{2+} and Hg^{2+} was added to 4 ml of 1 mM methanol solution of L in different vials. After mixing, UV-Visible spectra were recorded at room temperature. UV-Visible titration was carried out by adding 0 - 10 equivalent of Fe^{3+} (1 mM) to 0.1 mM solution of L (4 ml) in acetonitrile, shaking for a few seconds and measuring the absorbance using UV-Visible spectrophotometer at room temperature.

Job's plot analysis was carried out by keeping the total concentration of L and Fe^{3+} as 0.1 mM and total volume as 5 ml. The mole fraction of Fe^{3+} was varied from 0.1 to 0.9. Limit of detection was calculated from the UV-Visible titration profile using an equation, $3\sigma/slope$, where σ is the standard deviation and K is the slope of the calibration curve. The association constant was calculated by Benesi – Hildebrand method using the equation:

$$\frac{1}{(A - A_0)} = \frac{1}{K_a(A_{max} - A_0)} \; x \; \frac{1}{[M]^n} + \frac{1}{(A_{max} - A_0)}$$

where, A_0 and A are the absorbances of probe molecule in the absence - and presence of the analyte, A_{max} is absorbance at maximum concentration of analyte, [M] is concentration of analyte and K_a is the association constant.

Al^{3+} ions: L (3.97 mg, 0.01 mM) was dissolved in 1 ml methanol (10 mM). 20 µL of this was added to 3.98 ml of methanol to obtain a solution of L in 50 µM concentration. 1 equivalent of each of the different metal ions such as Fe^{3+}, Co^{2+}, Ni^{2+}, Cu^{2+}, Zn^{2+}, Al^{3+}, Mg^{2+}, Ca^{2+}, Ba^{2+}, Pb^{2+}, Cd^{2+} and Hg^{2+} was added to 4 ml of 50 µM solution

of L in different vials. After half an hour, its fluorescence response was recorded at room temperature. Fluorescence titration was carried out as follows, 50 µM solution of L and 0 - 4 equivalents of Al^{3+}, were mixed well and after half an hour fluorescence spectrum was recorded.

Job's method of continuous variation was used for the determination of stoichiometry of the complex formed. Limit of detection was calculated from the fluorescence titration profile based on the equation, 3σ/slope. The association constant was calculated by Benesi-Hildebrand equation given below.

$$\frac{1}{(F - F_0)} = \frac{1}{K_a(F_{max} - F_0)} \; x \; \frac{1}{[M]^n} + \frac{1}{(F_{max} - F_0)}$$

where, F_0 and F are the fluorescence intensities of probe molecule in the absence - and presence of the analyte, F_{max} is fluorescence intensity at maximum concentration of analyte, $[M]$ is concentration of analyte and K_a is the association constant.

Competition with other metal ions was checked by adding 1 equivalent of solution of different metal ions into 3 ml 50 µM solution of L. ^{1}HNMR titration of L with Al^{3+} was carried out by dissolving L (3.98 mg. 0.01 mmol) in methanol in three different NMR tubes. Of the three different equivalents (0.1, 0.5 and 1 equivalent) of $Al(NO_3)_3.6H_2O$ dissolved in methanol, one each was added to each L solution. Shaken well for one minute and ^{1}HNMR spectra were recorded. After mixing well, 1 equivalent of Al^{3+} solution was added, kept half an hour and fluorescence response was recorded

at room temperature. The reversibility of the complex formed was checked using disodium salt of EDTA.

2.4. Estimation of Fe(III)

Fe(III) was estimated colourimetrically by thiocyanate method[15]. For this, the Fe(III) complex was digested with a mixture of con HNO_3 and perchloric acid. Finally, excess of nitric acid was decomposed by digesting with con. HCl. The residue was then dissolved in water. Colour was developed using hydrochloric acid and potassium thiocyanate solution as reagent. Measured the absorbance of the resulting solution at 490 nm using a UV-Visible spectrophotometer.

2.5. Computational study

All the DFT calculations were performed using Guassian 05 package[16]. The geometry optimizations of L and its Al^{3+} complex were carried out by DFT/B3LYP/3-21G method[17, 18] and TDDFT calculations[19, 20] were done both in gas phase and in methanol using conductor-like polarizable continuum model (CPCM)[21, 22] to find out the most probable electronic transitions.

3. Results and discussion

3.1. Structural characterization

A common method was adopted for the synthesis of the Schiff base, 1,5-dimethyl-4-(2-hydroxy-1,2-diphenylethylideneamino)-2-phenylpyrazol-3-one (L) (Scheme 1). The compound was yellow in

colour and melted in the range of 173 - 178^{0}C. It was soluble in almost all organic solvents. L was structurally characterized by elemental analysis, IR- and ^{1}H- and ^{13}C NMR spectroscopic techniques. The elemental analysis data were close to the theoretically calculated ones.
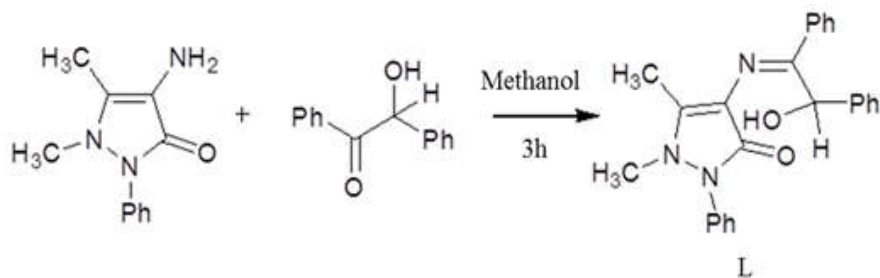
Scheme 1. Synthetic route of 1,5-dimethyl-4-

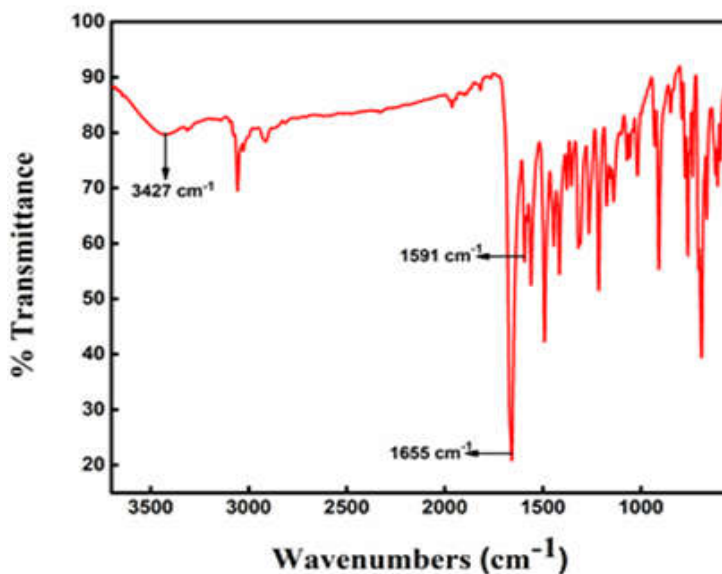(2-hydroxy-1,2-diphenylethylideneamino)-2-phenylpyrazol-3-one (L)

Fig. 1. IR spectrum of L

In the IR spectrum of the L, the characteristic stretching frequency of –C=O of antipyrine moiety appeared at 1655 cm^{-1}. The spectrum also displayed a sharp band at 1591cm^{-1} [due to ν(-C=N)] indicating the formation of the Schiff base. The –O-H stretching frequency appeared at 3432 cm^{-1} (Fig. 1). In ^{1}HNMR spectrum of L, appeared four singlets at 3 ppm (s, 1H, C-H); 2.9 ppm (s, 3H, N-CH$_3$), 2.4 ppm (s, 3H, O-H), and 2.1 ppm (s,1H, C-CH$_3$). A series of multiplets appeared in the range 7.2-8 ppm correspond to aromatic protons (Fig. 2). The formation of Schiff base was again conformed from ^{13}C NMR spectrum (Fig. 3) and by mass spectrometric analysis (Fig. 4).
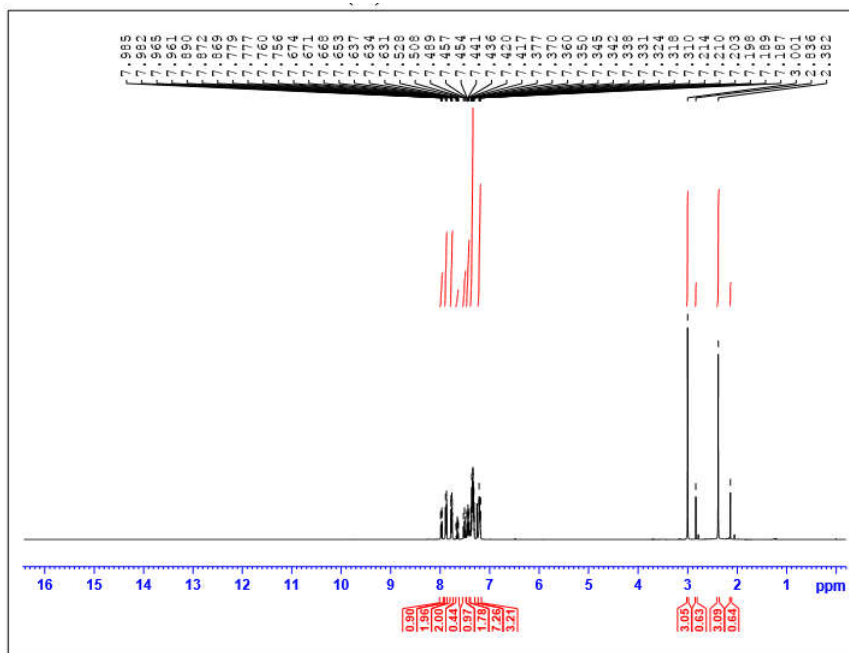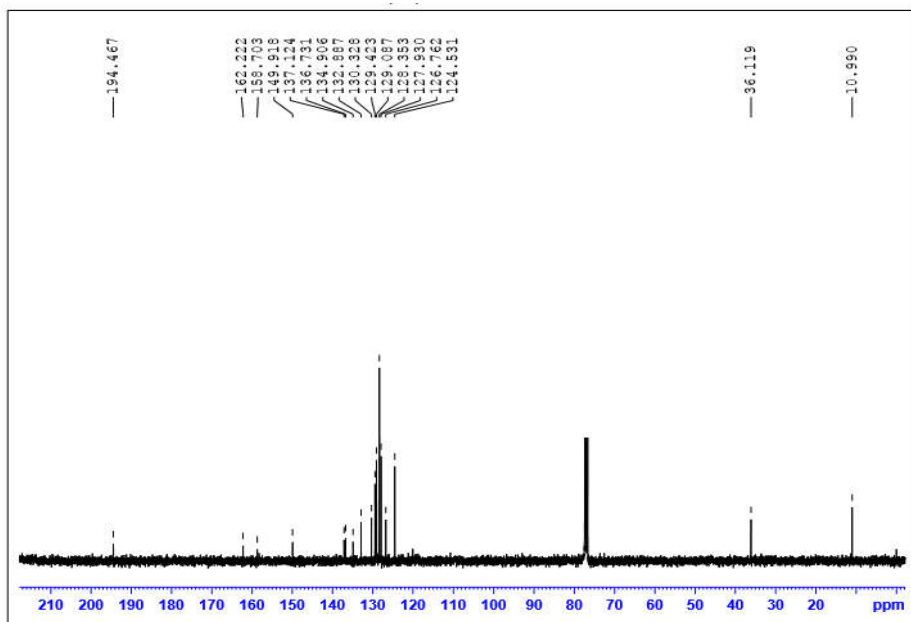

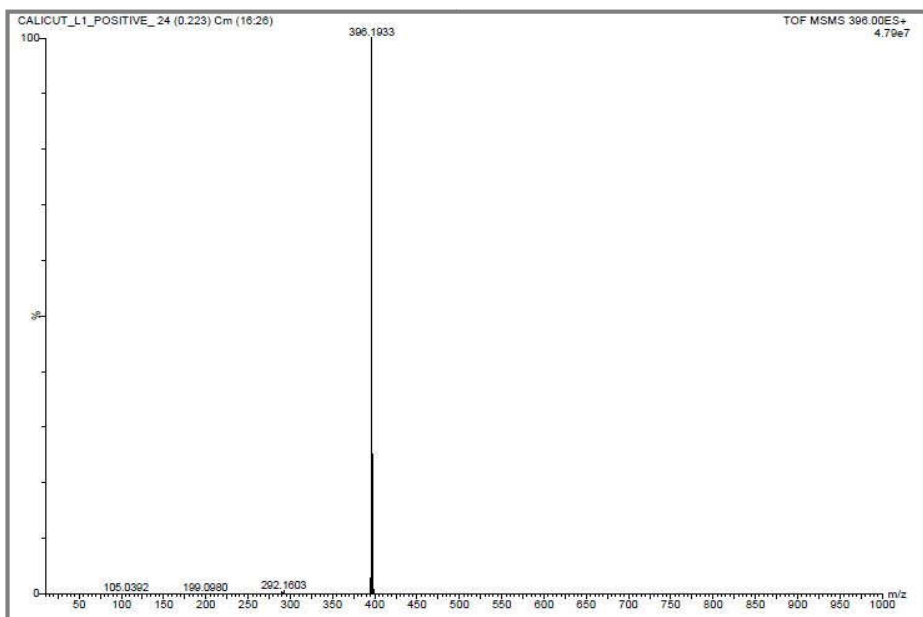Fig. 2. ^{1}HNMR spectrum of L

Fig. 3. ^{13}C NMR spectrum of L

Fig. 4. ESI-MS of L
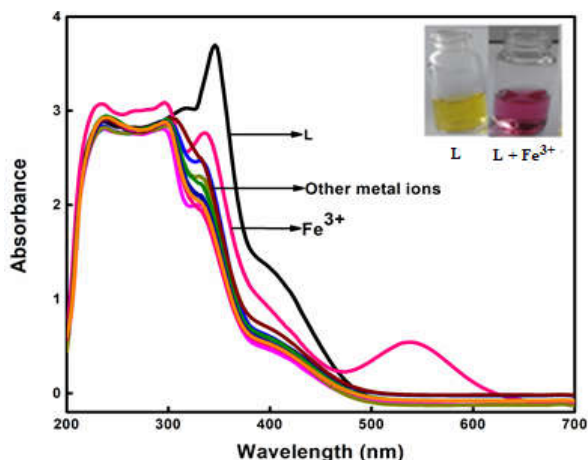
3.2. Photophysical investigations

Fig 5. UV-Visible spectral changes of L (1mM) on the addition of different metal ions (1mM). (Inset: The colour of L and L+Fe^{3+} under day light)

The colourimetric sensing ability of the L was studied with different metal ions such as Fe^{3+}, Co^{2+}, Ni^{2+}, Cu^{2+}, Zn^{2+}, Al^{3+}, Mg^{2+}, Ca^{2+}, Ba^{2+}, Pb^{2+}, Cd^{2+} and Hg^{2+} in methanol. The UV-Visible spectrum of the free ligand (L) exhibited three absorption bands at 236, 346 and 414 nm as shown in Fig 5. Addition of aqueous solutions of the metal ions mentioned above to a methanol solution of L did not show any change in its spectrum. Upon the addition of methanol solution of different metal ions, only in the case of Fe^{3+} there was a distinct change in UV-Visible spectrum. This type of spectral changes did not observe with the other metal ions under similar condition. In the case of Fe(III), a new peak observed in the region, 500-550 nm. This may be due to ligand to metal charge-transfer (LMCT) transition. The spectral changes observed with various metal ions are shown in

Fig 5. In accordance with the spectral data, there was an observable colour change of L from yellow to purple on adding Fe^{3+} ion solution. This indicates the formation of a complex. The above observation divulges that the Schiff base, L can be used to detect Fe^{3+} ions by "naked-eye" in methanol solution.

It was also observed that the intensity of the UV-Visible spectral peak in the region 500 - 550 nm decreased with time and within 10 min the peak disappeared completely. Due to this reason, we recorded the UV-Visible spectrum at higher concentration. When we conducted the same experiment at low concentration, the absorbance at 539 nm was very low. We believe that the reason for this observation is the transient nature of the complex formed, i.e. the formed complex decomposes within 5 min, so the spectroscopic detection will be difficult at low concentration. At the same time, the visual detection was possible at very low concentration. The variation of absorbance of the formed complex with time is shown in Fig 6. In consistent with the spectral change, the solution became colourless from purple. The above observation revealed that the complex formed was not stable in the protic solvent, methanol, for a long time. This may be due to the hydrolytic cleavage of the imine bond in presence of Fe^{3+} ions in a protic solvent, methanol. The strong Lewis acidic nature of Fe^{3+} ions also influences the hydrolytic cleavage of >C=N bond of the Schiff base. According to literature, the presence of any specific electrophilic catalyst, including acids and metal ions, initiate the hydrolysis of Schiff bases and its mechanisms are well reported[23, 24]. Based on this strategy, a few optical probes have been developed for the selective detection of metal ions and the details are available in literature[25, 26].

From the above observations, it can be seen that the nature of the solvent affects the complex formation and the structural rigidity of the formed complex.
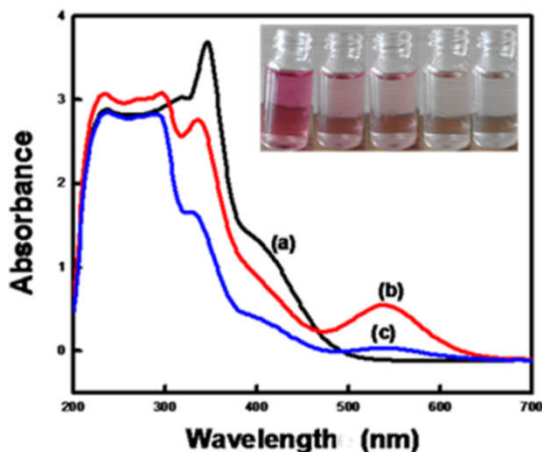

Fig. 6. Variation of absorption spectra of free L (a), with Fe (III) at the time of addition
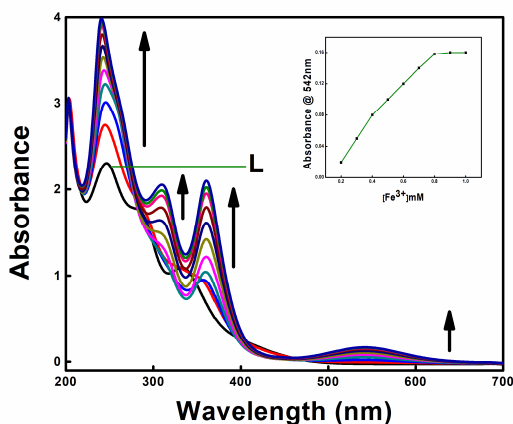(b) and after 5minute(c). Inset: Colour variation of Fe + L with time

Fig. 7. UV-Visible absorption spectal change of L (0.1 mM) upon the addition of Fe^{3+}
(0-10 equivalent) in acetonitrile at room temperature
(Inset: Absorbance at 542 nm versus concentration of Fe^{3+} added)

Due to the transient nature of the complex formed in methanol, we tested the sensing ability of L towards Fe^{3+} in an aprotic solvent, acetonitrile. 0.1 mM solutions of $FeCl_3$ and L were prepared in acetonitrile. Upon the addition of Fe^{3+} to a solution of L, the yellow colour slowly changed to purple indicating the formation of a complex. Thus, the Schiff base has an ability to bind Fe^{3+} in acetonitrile also and the complex formed was stable. In protic solvent, methanol, a sudden colour change from yellow to purple occurred by the addition of Fe^{3+} and it disappeared slowly and finally it became colourless. But upon the addition of Fe^{3+} in an aprotic solvent, acetonitrile, the development of purple colouration was slow and the intensity of the colour attained maximum after 5 min. From the above observations, it is clear that the complex formation is a slow process in acetonitrile and the solvent has a significant role in the complex formation.
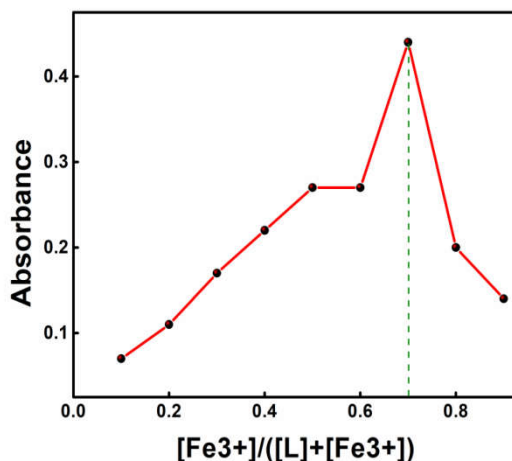

Fig. 8. Job's plot of L with Fe^{3+} in acetonitrile.

The UV-Visible titration of L with Fe^{3+} was monitored in acetonitrile as shown in Fig. 7. Upon the addition of 0 to 10

equivalents of Fe^{3+} to an acetonitrile solution of L, three new peaks emerged at 311, 361 and 542 nm. It was observed that the intensities of the absorption peaks increased with increasing the concentration of Fe^{3+} from 0 to 10 equivalents. There was a noticeable colour change from yellow to purple. The complex formation behavior was also different in protic- and aprotic solvents. The stoichiometry of the complex was determined by Job's method by keeping the total concentration as 0.1 mM and the total volume as 5 ml of L and Fe^{3+} (Fig. 8).

The Job's plot indicated that the complex formation was in the ratio of 1: 2 (L: $2Fe^{3+}$). The 1: 2 complex formation between L and Fe^{3+} was also confirmed by the appearance of a peak at m/z 752.9 (calculated 753) in ESI -MS profile (Fig. 9).

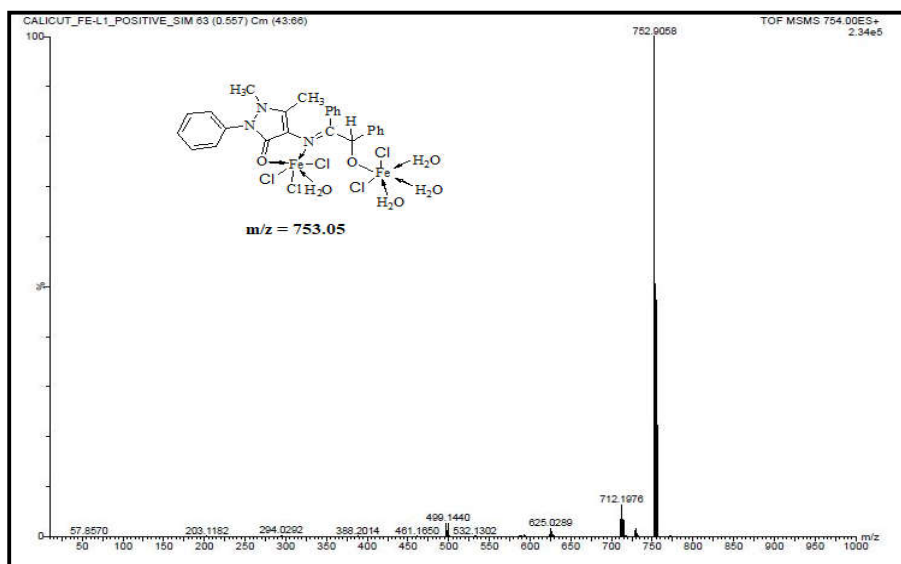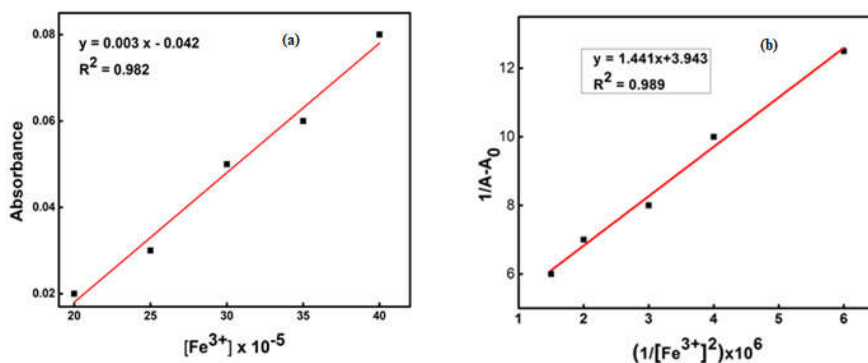Fig. 9. ESI-mass spectrum of L with Fe^{3+}

Fig. 10. (a) Calibration curve of Fig. L-Fe^{3+} for LOD calculation,

(b) Benesi-Hildebrand plot of the complex formed between Fe^{3+} and L

From the UV-Visible titration profile of L with Fe^{3+}, the limit of detection of Fe^{3+} was calculated as 2.38 x 10^{-4} M based on the equation, $3\sigma/K$ [Fig. 10 (a)]. Using the Benesi-Hildbrand equation, the association constant of the complex formed was calculated as 4.34×10^{6} M^{-1} [Fig. 10 (b)]. The high value of association constant indicated the strong affinity of L towards Fe^{3+}.
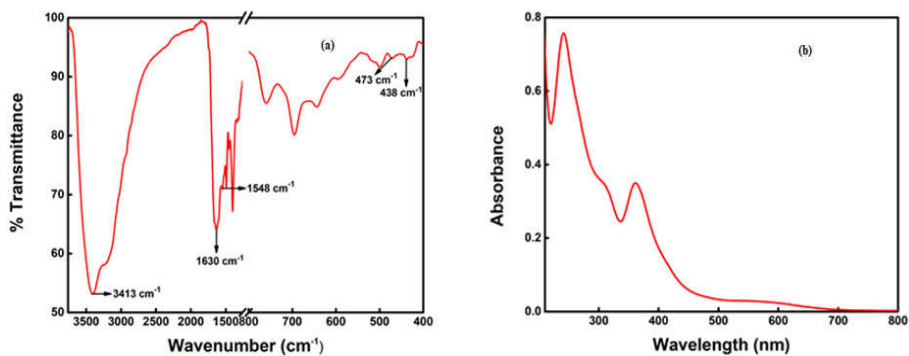

Fig. 11. (a) Infrered spectrum of Fe(III) complex,

(b) UV-Visible spectrum of the Fe (III) complex in acetonitrile

To get more information about the interaction of L with Fe^{3+}, we have synthesized the solid complex and characterized it. The results confirmed the formation of a 2 : 1 complex between Fe^{3+} and L. The elemental analysis data of the metal complex were in good agreement with the calculated values. In the IR spectrum [Fig. 11 (a)], the characteristic stretching frequencies of –C=O and–C=N of L appeared at 1655 and 1591 cm^{-1}, respectively. In the spectrum of the complex, they were found to be shifted to 1630 and 1548 cm^{-1}, respectively, indicating the coordination of –C=O and –C=N to Fe(III)[27]. A broad band at 3413 cm^{-1} is due to the O-H stretching of coordinated water in the complex. The appearance of new bands with very low intensities at 473 and 438 cm^{-1} are due to the formation of M-N and M-O bonds, confirming the formation of the complex[28]. The UV-Visible spectrum of the complex in acetonitrile [Fig. 11 (b)] resembled to the spectrum obtained during UV-Visible titration. Experimental μ_{eff} value of the complex was found to be 3.7 BM. It is somewhat lower than the μ_{eff} value expected for five unpaired electrons in high-spin Fe(III) complex. The lower magnetic moment value may be due to spin exchange interactions present in the dinuclear complex[29, 30].

The fluorescence responses of the Schiff base, L with the above mentioned metal ions were also studied in methanol solution. Upon excitation at 331 nm at room temperature, free L exhibited a weak emission at 378 nm. Schiff bases are feebly emissive because of the isomerization of unbridged –C=N which exhausts the excited state energy. Upon the addition of Al^{3+} ions, the intensity of the emission at

367 nm increased and a new emission was observed at 463 nm with very high intensity (Fig. 12). However, the other metal ions didn't induce this type of emission under the similar condition. This fluorescence turn-on behavior of L in the presence of Al^{3+} is due to the formation of a stable chelate which rigidifies the molecule and thereby suppresses the isomerization of –C=N leading to a radiative emission [4].
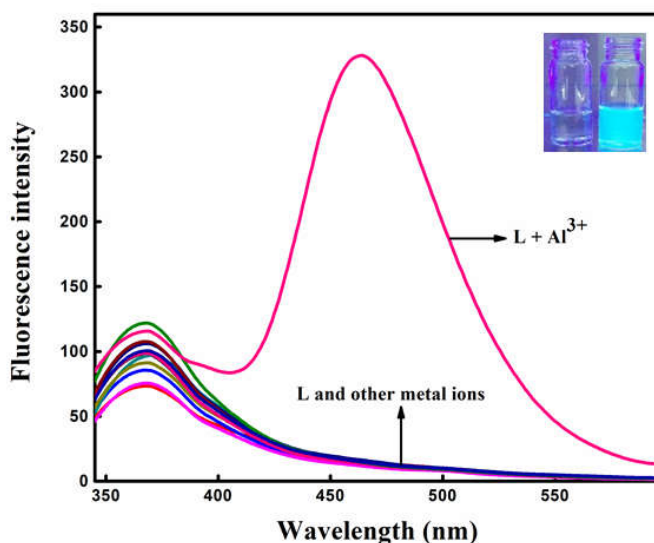

Fig. 12. Fluorescence emission spectra of L (50μM) in methanol before and after the addition different metal ions such as (1 eq) Fe^{3+}, Co^{2+}, $Ni2^{+}$, Cu^{2+}, Zn^{2+}, Al^{3+}, Mg^{2+}, Ca^{2+}, Ba^{2+}, Pb^{2+}, Cd^{2+} and Hg^{2+}, λ_{ex} = 331 nm (Inset : The colour of L and L+Al^{3+} under UV lamp)

To get a quantitative idea about the complexation, we carried out fluorescence titration experiment by the gradual addition of Al^{3+} solution in methanol from 0 to 4 equivalents to 50 μM methanol solution of L. As depicted in Fig. 13, on increasing the concentration

of Al^{3+}, the emission intensity gradually increased up to 3.5 equivalents of Al^{3+} and thereafter, the emission intensity decreased. The stoichiometry of the complex formed between L and Al^{3+} was determined from the plot of the intensity of emission at 468 nm versus mole fraction of L by keeping the total volume and total concentration as constant (Fig. 14). From the plot, it can be seen that the maximum intensity of emission is obtained at 0.5 mole fraction of L. This suggested the formation of 1: 1 complex of L with Al^{3+} and which was further confirmed from ESI-MS analysis. The positive ion ESI-mass spectrum, shown in Fig. 15, exhibited a peak at m/z 579.5 (calculated m/z 579.6) corresponding to a 1: 1 binding stoichiometry. The proposed mechanism of the formation of Al^{3+} complex is depicted in Scheme 2.
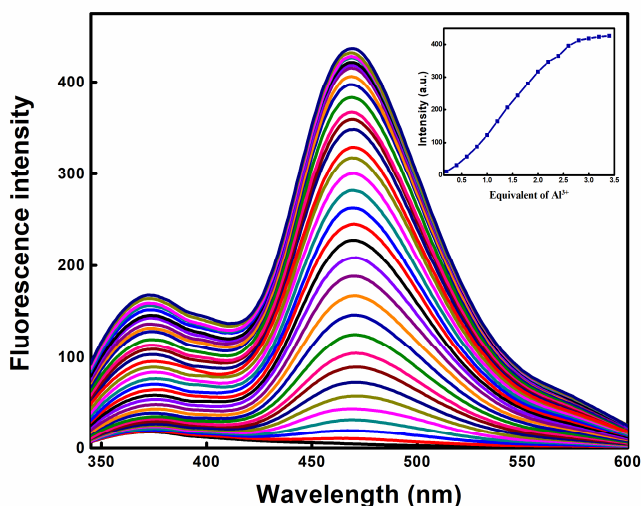
Fig. 13. Fluorescence titration of L (50μM) with Al^{3+} (0- 3.5equivalent) in methanolic solution λ_{ex} = 331nm (Inset : Emission intensity at 463 nm versus number of equivalents of Al^{3+})
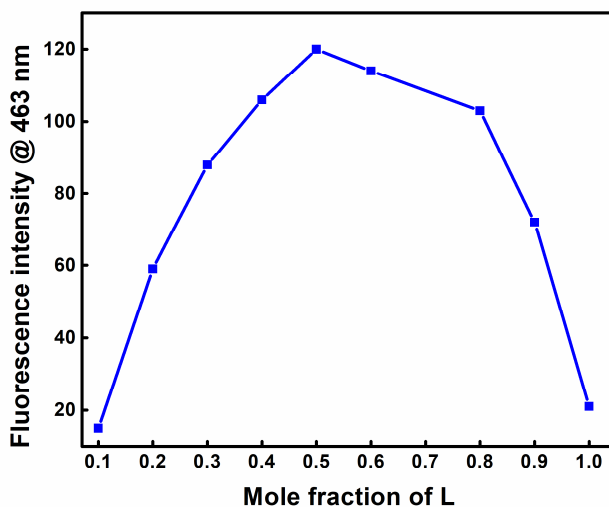
Fig. 14. Job's plot of L upon the addition of Al^{3+} in methanol
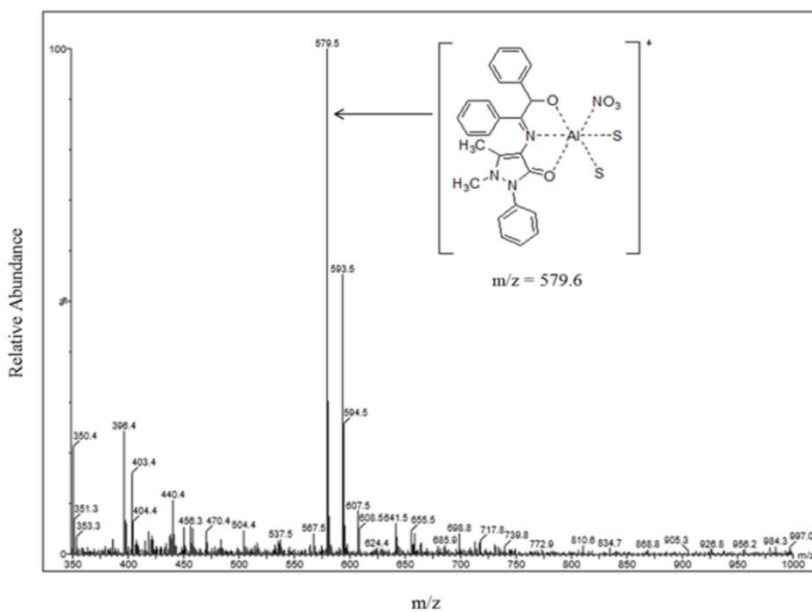
Fig. 15. Positive ion ESI-mass spectrum of L with Al^{3+}
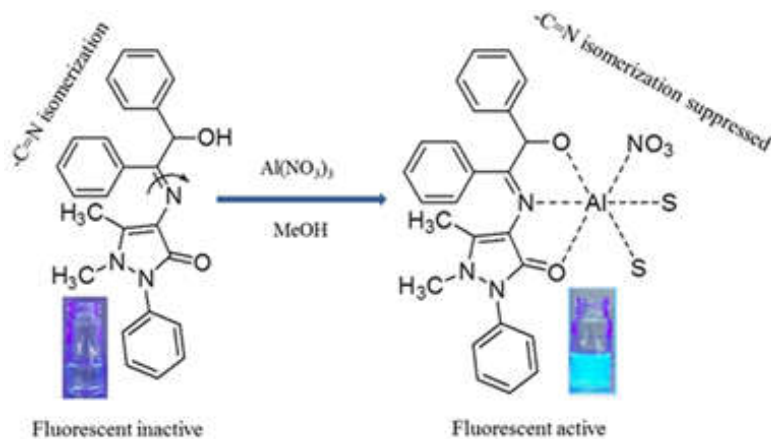
Scheme 2. Proposed mechanism for fluorescent emission of
L with Al^{3+} (S = Solvent).
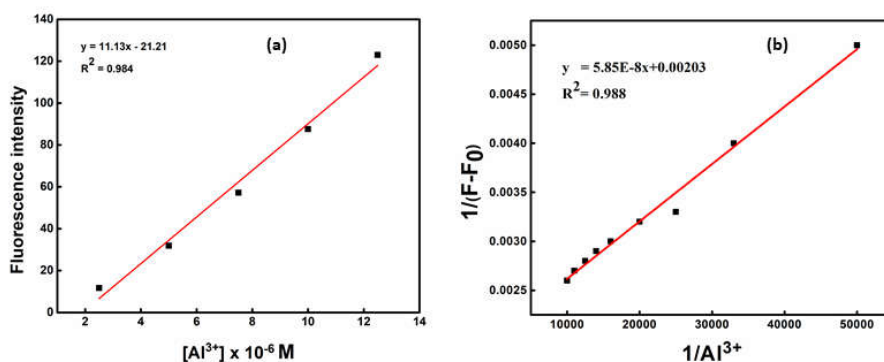
Fig. 16. (a) Calibration curve of L-Al^{3+} for LOD calculation, (b) Benesi-Hildebrand plot of complex formed between Al^{3+} and L

From the fluorescence titration data, the limit of detection (LOD) of Al^{3+} and binding constant of the complex formed were determined. The LOD was calculated by using the equation, $3\sigma/K$,

which was found to be 11.9 μM [(Fig. 16 (a)]. For binding constant calculation, Benesi-Hildebrand equation was used assuming a 1:1 binding stoichiometry and it was found to be 4.53×10^4 M^{-1} [Fig 16 (b)]. The interaction of L with Al^{3+} was further checked by ^{1}HNMR titration experiment at room temperature. The hydroxyl proton (-O-H) which appeared at 4.61 ppm in free L, completely disappeared even on the addition of 0.1 equivalent of Al^{3+} , indicating the deprotonation of the hydroxyl group and coordination of O^- to Al^{3+} (Fig. 17). We have calculated the quantum yield of L before and after the interaction with Al^{3+} using quinine sulphate as standard. The quantum yield of L after interaction with Al^{3+} was 13.6 times higher than that of the free L.
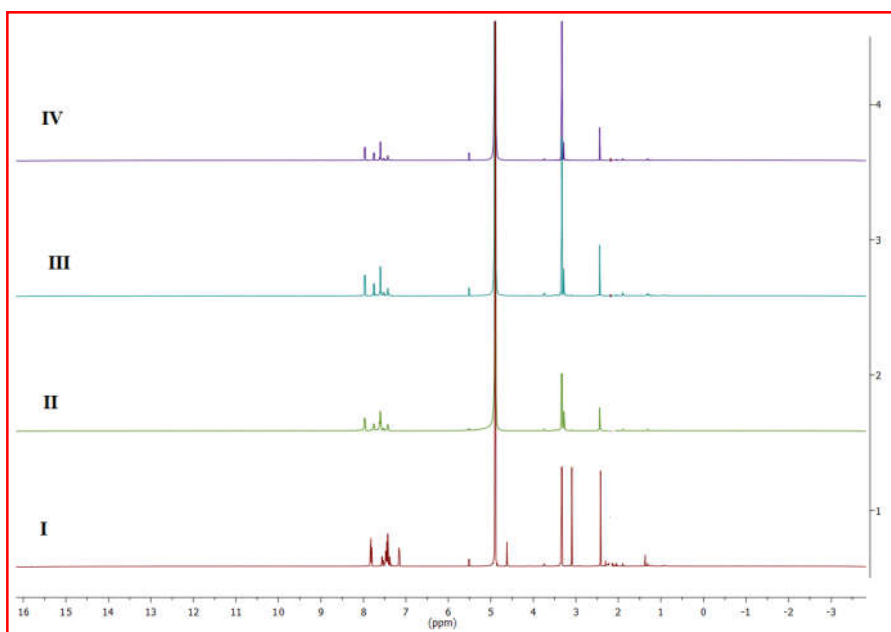
Fig. 17. ^{1}H NMR titration of L (I) with 0.1 (II), 0.5 (III) and (IV) equivalents of Al^{3+}

One of the important aspects of metal ion sensors is their ability to selectively detect a particular metal ion in the presence of other metal ions. Therefore, we carried out a competition study to determine the selectivity of L towards Al^{3+} in the presence of other metal ions. L was treated with 1 equivalent of Al^{3+} and 1 equivalent of other metal ions having same concentration (Fig. 18). The result indicated that the other metal ions, except Fe^{3+} and Cu^{2+} have relatively lower interference in the detection of Al^{3+} using L. Comparatively higher interferences of Fe^{3+} and Cu^{2+} are due to their paramagnetic nature which quenches the fluorescent emission intensity of the Al^{3+} complex formed.
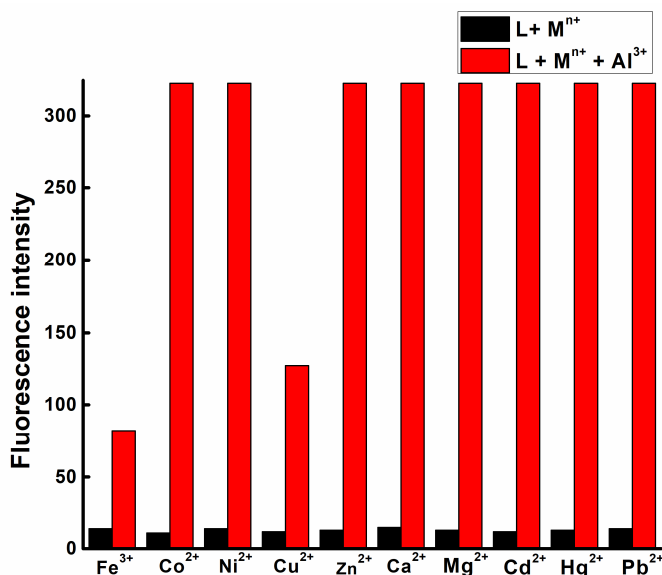
Fig. 18. Competition study of L (50 μM) toward Al^{3+} (1 equivalent) in the presence of other metal ions (1 equivalent) with emission at 463 nm.
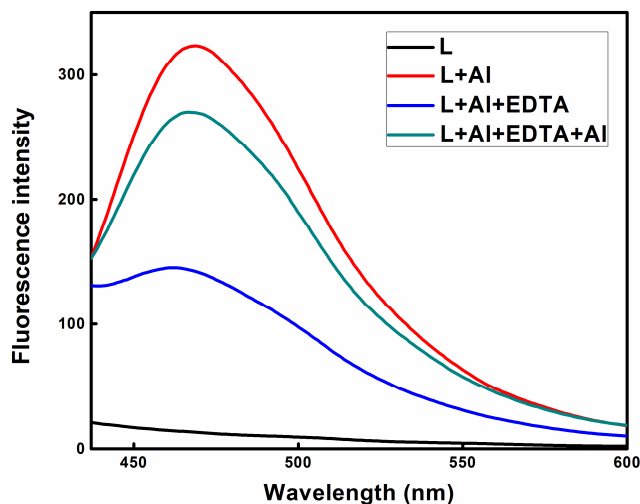
Fig. 19. Fluorescent emission changes of L (50 μM) upon alternate addition of Al^{3+} and EDTA (1 equivalent each) (λ_{ex} = 331 nm)

The reversibility of the probe is another important criterion of metal sensors. To ensure the reversibility of the complex formed, we performed an analysis using disodium salt of EDTA and the changes in the emission behaviour are shown in Fig. 19. The addition of 1equivalent of EDTA to a solution containing 1 equivalent each of L and Al^{3+} resulted a fluorescence quenching at 463 nm. It revealed the regeneration of the probe. The addition of a strong chelating agent, EDTA leads to the formation of an aluminium-EDTA chelate and thereby liberates L, resulting in the quenching of fluorescence. Again, on the addition of 1 equivalent of Al^{3+} to the above solution, the fluorescent emission intensity returned almost to the original level. This observation suggests the reversible coordinating nature of L with

Al^{3+}. On comparing with the previously reported colourimetric Fe^{3+} - and "turn on" Al^{3+} sensors, L shows a comparable response toward Fe^{3+} and Al^{3+}. The comparison was made based on the association constant and limit of detection. The details are shown in the Table 1.

3.3. Computational studies

To get more idea about the electronic structure and electronic transitions, theoretical studies of L and its Al^{3+} complex have been performed by DFT/B3LYP/3-21G method and TDDFT calculations. The calculation of the complex was done based on the 1:1 stoichiometry obtained from Job's plot, ^{1}H NMR and ESI-MS analysis. The optimized geometry of the Al^{3+} complex indicated the tridentate coordination (N,O,O) behaviour of L towards Al^{3+} (Fig. 20).

Table 1

Comparison of sensing of L with the previously reported sensors

Probe	Association constant	LOD	Sensing response
Ref [4]	3.3×10^4	6.8×10^{-6}	Fe^{3+} (colourimetric)
Ref [31]	2.8×10^4	0.27×10^{-6}	Fe^{3+} (colourimetric)
Ref [32]	4.3×10^4	2.9×10^{-3}	Fe^{3+} (colourimetric)
Ref [33]	0.4×10^6	5×10^{-5}	Al^{3+} (fluorescence)
Ref [34]	4.58×10^4	7.94×10^{-5}	Al^{3+} (fluorescence)
Ref [35]	5.1×10^3	$1.5 \times 10\text{-}6$	Al^{3+} (fluorescence)
Ref [36]	1×10^4	8.12×10^{-6}	Al^{3+} (fluorescence)
Ref [37]	5.23×10^5	8.87×10^{-7}	Al^{3+} (fluorescence)
Ref [38]	8.84×10^3	5×10^{-7}	Al^{3+} (fluorescence)
L	$\mathbf{4.34 \times 10^6}$	$\mathbf{2.38 \times 10^{-4}}$	$\mathbf{Fe^{3+}}$ **(colourimetric)**
	$\mathbf{4.53 \times 10^4}$	$\mathbf{11.9 \times 10^{-6}}$	$\mathbf{Al^{3+}}$ **(fluorescence)**

The HOMO - LUMO energy difference is 4.357 eV for free L. This decreases to 3.582 eV after interacting with Al^{3+}. This decrease in the energy gap indicates the formation of complex (Fig. 21). The TDDFT calculations were carried out both in gas phase and in methanol using conductor-like polarizable continuum model (CPCM) and the UV spectral data in methanol fit well to the experimental results. The results indicated that mainly two transitions are observed in the free L. The first one from HOMO to LUMO at 310 nm with oscillator strength, $f = 0.1017$ corresponding to the experimental value of 346 nm and the second transition occurs from HOMO-1 to LUMO at 244 nm with oscillator strength, $f = 0.1915$ corresponding to the absorption band at 246 nm obtained experimentally. The HOMO - LUMO transition of L-Al^{3+} is obtained at 327 nm with oscillator strength, $f = 0.3134$ corresponding to the experimentally observed absorption at 331 nm. The other peak of L-Al^{3+} appeared at 248 nm ($f = 0.0379$) due to the HOMO-6 to LUMO transition which corresponds with the experimentally observed absorption band at 238 nm.
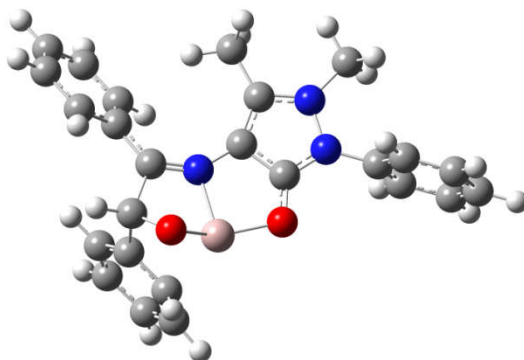
Fig. 20. The optimized geometry of L-Al^{3+} complex
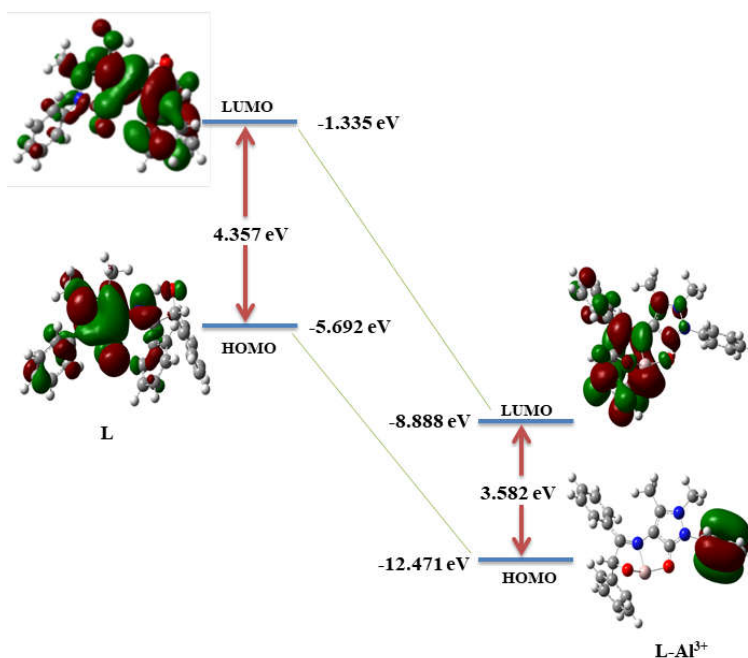
Fig. 21. HOMO, LUMO and HOMO-LUMO gap between L and L-Al^{3+}

4. Conclusions

We synthesized a new Schiff base, 1,5-dimethyl-4-(2-hydroxy-1,2-diphenylethylideneamino)-2-phenylpyrazol-3-one (L) by refluxing ethanol solution of 4-aminoantipyrine and benzoin. The synthesized compound, L was characterized by CHN analysis, IR-, ^{1}H NMR- and mass spectral techniques. The colourimetric and fluorescence metal sensing abilities of the synthesized compound were studied. The addition of aqueous solutions of different metal ions to a methanol solution of L did not produce any observable spectral change. Upon the addition of different metal ions in methanol, only in the presence of Fe^{3+} and

Al^{3+} distinct changes were observed. The yellow coloured solution of L changed to purple in the presence Fe^{3+} and exhibited a rapid fluorescence turn-on response towards Al^{3+} in methanol. Because of the transient nature of the complex formed between Fe^{3+} and L in methanol, the recognising ability of Fe^{3+} with L in an aprotic solvent, acetonitrile was also studied. The binding stoichiometries of L with Fe^{3+} and Al^{3+} were investigated based on the Job's plot and ESI-MS analysis. In the case of Al^{3+}, ^1H NMR titration was also carried out. These studies suggested a 1 : 2 stoichiometry of L towards Fe^{3+} and   1 : 1 stoichiometry with Al^{3+}. Thus, the synthesized Schiff base exhibited a solvent dependent binding ability towards Fe^{3+} and Al^{3+}. We compared the sensing abilities of L towards Fe^{3+} and Al^{3+} with the previously reported Fe^{3+} and Al^{3+} sensors and got comparable results. These results divulge that the new Schiff base, L is useful for the naked eye detection of Fe^{3+} and Al^{3+}.

References

1. B.-R. Gao, H.-Y. Wang, Y.-W. Hao, L.-M. Fu, H.-H. Fang, Y. Jiang, L. Wang, Q.-D. Chen, H. Xia and L.-Y. Pan, *The Journal of Physical Chemistry B*, 2009, **114**, 128-134.

2. L. McDonald, J. Wang, N. Alexander, H. Li, T. Liu and Y. Pang, *The Journal of Physical Chemistry B*, 2016, **120**, 766-772.

3. D. Harvey, *Modern analytical chemistry*, Boston: McGraw-Hill Companies, Inc., 2000.

4. Y. W. Choi, G. J. Park, Y. J. Na, H. Y. Jo, S. A. Lee, G. R. You and C. Kim, *Sensors and Actuators B: Chemical*, 2014, **194**, 343-352.

5. C.-r. Li, J.-c. Qin, G.-q. Wang, B.-d. Wang, A.-k. Fu and Z.-y. Yang, *Inorganica Chimica Acta*, 2015, **430**, 91-95.

6. D. Prabhu and N. Laxmeshwar, *Asian Journal of Chemistry*, 1997, **9**, 70-74.

7. W.-H. Ding, W. Cao, X.-J. Zheng, D.-C. Fang, W.-T. Wong and L.-P. Jin, *Inorganic chemistry*, 2013, **52**, 7320-7322.

8. S. M. Hossain, A. Lakma, R. N. Pradhan, A. Chakraborty, A. Biswas and A. K. Singh, *RSC Advances*, 2015, **5**, 63338-63344.

9. L. Wang, L. Yang and D. Cao, *Sensors and Actuators B: Chemical*, 2014, **202**, 949-958.

10. S. Y. Lee, J. J. Lee, K. H. Bok, S. Y. Kim and C. Kim, *RSC Advances*, 2016, **6**, 28081-28088.

11. A. Ghorai, J. Mondal, S. Chowdhury and G. K. Patra, *Dalton Transactions*, 2016, **45**, 11540-11553.

12. M. Köse, S. Purtas, S. A. Güngör, G. Ceyhan, E. Akgün and V. McKee, *Spectrochimica Acta Part A: Molecular and Biomolecular Spectroscopy*, 2015, **136**, 1388-1394.

13. V. K. Gupta, A. K. Singh and L. K. Kumawat, *Sensors and Actuators B: Chemical*, 2014, **204**, 507-514.

14. V. K. Gupta, A. K. Singh and N. Mergu, *Electrochimica Acta*, 2014, **117**, 405-412.

15. A. I. Vogel, *Quantitative inorganic analysis*, Longmans, 1961.

16. R. A. Gaussian09, *Inc., Wallingford CT*, 2009, **121**, 150-166.

17. C. Lee, W. Yang and R. Parr, *Phys. Rev, vol. B*, 1988, **37**, 785-789.

18. A. D. Becke, *J. Chem. Phys*, 1993, **98**, 5648-5652.

19. M. E. Casida, C. Jamorski, K. C. Casida and D. R. Salahub, *The Journal of chemical physics*, 1998, **108**, 4439-4449.

20. C. J. Cramer, *Journal*, 2004.

21. M. Cossi, N. Rega, G. Scalmani and V. Barone, *Journal of computational chemistry*, 2003, **24**, 669-681.

22. D. C. Young, 1999.

23. V. G. Machado, M. Nascimento and M. Rezende, *J Braz Chem Soc*, 1993, **4**, 76-79.

24. T. Okuyama, H. Nagamatsu, M. Kitano and T. Fueno, *The Journal of Organic Chemistry*, 1986, **51**, 1516-1521.

25. J.-S. Wu, W.-M. Liu, X.-Q. Zhuang, F. Wang, P.-F. Wang, S.-L. Tao, X.-H. Zhang, S.-K. Wu and S.-T. Lee, *Organic letters*, 2007, **9**, 33-36.

26. H. T. Tsai, Y. R. Bhorge, A. J. Pape, S. N. Janaki and Y. P. Yen, *Journal of the Chinese Chemical Society*, 2015, **62**, 316-320.

27. K. Nakamoto, *Inc, New York*, 1986.

28. P. Sreeja and M. P. Kurup, *Spectrochimica Acta Part A: Molecular and Biomolecular Spectroscopy*, 2005, **61**, 331-336.

29. B. N. Figgis and J. Lewis, *Progress in inorganic chemistry*, 1964, **6**, 37-239.

30. F. A. Cotton, L. M. Daniels, E. A. Hillard and C. A. Murillo, *Inorganic chemistry*, 2002, **41**, 2466-2470.

31. T. G. Jo, K. H. Bok, J. Han, M. H. Lim and C. Kim, *Dyes and Pigments*, 2017, **139**, 136-147.

32. S. Hou, Z. Qu, K. Zhong, Y. Bian and L. Tang, *Tetrahedron Letters*, 2016, **57**, 2616-2619.

33. J. Kumar, M. J. Sarma, P. Phukan and D. K. Das, *Dalton Transactions*, 2015, **44**, 4576-4581.

34. P. Saluja, H. Sharma, N. Kaur, N. Singh and D. O. Jang, *Tetrahedron*, 2012, **68**, 2289-2293.

35. K. Kaur, V. K. Bhardwaj, N. Kaur and N. Singh, *Inorganic Chemistry Communications*, 2012, **18**, 79-82.

36. X. Leng, W. Xu, C. Qiao, X. Jia, Y. Long and B. Yang, *RSC advances*, 2019, **9**, 6027-6034.

37. C.-H. Chen, D.-J. Liao, C.-F. Wan and A.-T. Wu, *Analyst*, 2013, **138**, 2527-2530.

38. Y. Lu, S. Huang, Y. Liu, S. He, L. Zhao and X. Zeng, *Organic letters*, 2011, **13**, 5274-5277.

CHAPTER 4

COUMARIN DERIVED SCHIFF BASE AS A COLOURIMETRIC SENSOR FOR Cu^{2+}
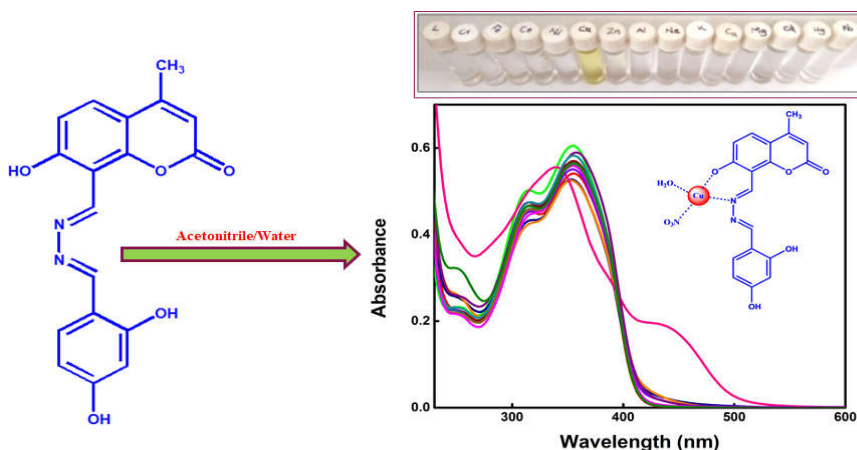
Work in Brief….

◆ *Synthesized and characterized a new Schiff base, 1-(8-methanylylidene-7-hydroxy-4-methyl-2H-chromen-2-one)-2-(2, 4-dihydroxybenzylidene)hydrazine, L.*

◆ *Observed a colourimetric response towards Cu^{2+} with relatively a little or no interference of other common metal ions.*

◆ *The observed detection limit was below 30 μM for Cu^{2+} which is lower than that proposed by WHO.*

◆ *The probe showed good response for the detection of Cu^{2+} of samples prepared in tap water and canal water.*

1. Introduction

Monitoring of environmental pollutants and biological important metal ions is highly essential in present scenario. Among the transition metal ions, Cu^{2+}, an essential trace metal, is closely related to human life[1-3]. Because of the redox nature of Cu^{2+}, its enzymes involve in electron transfer, oxygen binding and oxidation catalysis[4-6]. It also has inevitable roles in bone and tissue formation, cellular respiration, immune and brain functions, and gene transcription[7-9]. Copper is also essential to the growth of plants and microorganisms[10]. Contrary to these active physiological roles of Cu^{2+}, its excessive intake adversely affects human health and leads to neurodegenerative diseases likes Menkes-, Wilson's-, Parkinson's-, Alzheimer's- and Prion disease[11-15]. The effluents from industries and the agricultural waste contribute copper contamination in water, air and soil. Therefore, on account of health and environmental issues, it is essential to monitor Cu^{2+} in a cost effective manner.

For monitoring various metal ions, researchers are interested in methods based on chemical sensors. The simplicity in detection is the prime attraction of these methods. Their advantages are rapid response, high sensitivity and selectivity and inexpensive instrumental facility[16-18]. The changing photophysical properties of chemical sensors before and after interaction with metal ions can be monitored and quantified using UV-Visible- or fluorescence spectroscopic method. Among these optical sensing methods, colourimetric sensing is attractive because of the advantages of naked eye detection under

day light. A challenge of this chemical sensor based method for copper ion is the interference of other metal ions like Fe^{3+}, Zn^{2+}, Hg^{2+} and Pb^{2+} [19]. Even though, a number of chemical probes are available for monitoring Cu^{2+} [20-25], the development of new one with better capability is still challenging.

Here we discussed the synthesis and characterization of a new Schiff base, 1(8-methanylylidene-7-hydroxy-4-methyl-2H-chromen-2-one)-2-(2,4-dihydroxybenzylidene) hydrazine, L by condensing 8-formyl-7-hydroxy-4-methylcoumarine and 2,4-dihydroxy salicylaldehyde with hydrazine. L exhibited a colourimetric response towards Cu^{2+} ion by changing from colourless to yellow with relatively a little or no interference of other common metal ions. The probe also showed good response for the detection of Cu^{2+} of samples prepared in tap water and canal water.

2. Experimental

2.1. Materials and methods

All the chemicals used for the study were purchased from Sigma Aldrich or Alfa Aesar. The solvents were received from the chemical suppliers and were used without further purification. The sensing study was carried out using nitrate salts of different metals.

Elemental analyses were carried out on VarioEL III CHNS analyzer. A Jasco FTIR 4100 spectrometer was used to record the FTIR spectrum (4000-400 cm^{-1}) of the compound. The ^{1}H NMR- and ^{13}C NMR spectra were recorded on a 400 MHz Bruker Avance III

spectrometer using DMSO-d6. The Electron-Spray Ionization Mass Spectrum (ESI-MS) was recorded on Waters (UPLC- TQD) mass spectrometer. The UV-Visible spectrum was recorded on a Jasco UV-Visible spectrophotometer, model V-550.

2.2. Synthesis of Schiff base

The procedures for the synthesis of 8-formyl-7-hydroxy-4-methylcoumarin was adopted from the literature[26, 27].

1 mmol of 8-formyl-7-hydroxy-4-methylcoumarin (0.204 g) was refluxed with excess of hydrazine hydrate (1.5 mmol, 75 µL) in 30 ml ethanol for about 6 h. On concentrating the above mixture, obtained a pale yellow solid product. It was filtered and washed with acetone. In the next step, 1 mmol of the product obtained in the first step was dissolved in 15 ml methanol by stirring. To this solution, 1 mmol of 2, 4-dihydroxybenzaldehyde dissolved in 15 ml methanol was added in drops and the mixture was refluxed about 4 h. The bright yellow solid product obtained was, filtered, washed with ethanol, dried and kept in a desiccator. Yield: 78%. Anal. Calcd for $C_{18}H_{14}N_2O_5$: C, 63.90; H, 4.17%; N, 8.28%; Found: C, 71.12; H, 5.17%; N, 8.63%. IR (cm⁻¹, KBr): ν(C=N) 1625 cm⁻¹. ¹H NMR (400 MHz, DMSO d_6, δ (ppm)) δ: 12.62 (1H, s), 11.11 (1H, s), 10.43 (1H, s), 9.20 (1H, s), 8.92 (s, 1H), 7.79 (d, 1H), 7.51 (d, 1H), 6.99(d, 1H), 6.43 (d, 1H), 6.41 (s,1H), 6.31 (s,1H), 2.41(s, 3H); ¹³C NMR (400 MHz, DMSO d_6, δ (ppm)) δ 163.72, 159.08, 156.36, 153.81, 153.23, 129.59, 113.33, 110.84, 105.31, 79.05, 18.29; ESI MS (m/z): [M + H]⁺: Calculated: 339.3, Found: 339.2

2.3. Sample preparation for colourimetric studies

Stock solutions of different metal ions like Cr^{3+}, Fe^{3+}, Co^{2+}, Ni^{2+}, Cu^{2+}, Zn^{2+}, Al^{3+}, Ca^{2+}, Mg^{2+}, Na^+, K^+, Cd^{2+}, Hg^{2+} and Pb^{2+} in 1 mM concentration were prepared in deionized water. 1 mM stock solution of L was prepared in acetonitrile. Colourimetric sensing studies were carried out by recording the UV-Visible spectrum of the solution mixture of 1 equivalent of the stock solution of one of the metal ions and 3 ml of 20 μM solution of L, at room temperature. In UV-Visible titration, 0 to 4 equivalents of Cu^{2+} solution was added gradually to 3 ml of 20 μM solution of L and the spectral change after each addition was monitored spectroscopically. To find out the mode of interaction between L and Cu^{2+}, conducted Job's plot analysis by keeping the total concentration of L and Cu^{2+} as 0.1 mM and total volume as 3 ml. Limit of detection (LOD) was calculated from the UV-Visible titration profile based on the equation, 3σ/slope, where σ is the standard deviation and K is the slope of the calibration curve. The association constant was calculated using Benesi-Hildebrand equation by assuming a 1:1 binding stoichiometry. Competition studies were conducted by adding appropriate amount of cations to 20 μM solution of L.

Benesi-Hildebrand equation is

$$\frac{1}{(A - A_0)} = \frac{1}{K_a(A_{max} - A_0)} \; x \; \frac{1}{[M]^n} + \frac{1}{(A_{max} - A_0)}$$

where, A_0 and A are the absorbances of probe molecule in the absence and presence of the analyte, A_{max} is absorbance at maximum concentration of analyte, [M] is concentration of analyte and K_a is the association constant.

3. Results and discussion

3.1. Structural characterization

The compound, 1-(8-methanylylidene-7-hydroxy-4-methyl-2H-chromen-2-one)-2-(2, 4-dihydroxybenzylidene) hydrazine, L was synthesized in a two-step procedure (Scheme 1). L was readily soluble in acetonitrile, DMF and DMSO. The formation of the target compound was confirmed by elemental analysis, IR (Fig. 1), ^{1}H NMR (Fig. 2), ^{13}C NMR (Fig. 3) and mass spectrometric (Fig. 4) studies.

The elemental analysis data were close to the theoretically calculated ones. In the IR spectrum of L, the characteristic stretching frequency of –O-H appeared at 3425 cm^{-1} and that of –C=O appeared at 1730 cm^{-1}. Formation of imine bond was confirmed by the characteristic band appeared at 1621 cm^{-1}. In the mass spectrum, peak at (m/z) 339.2 (Calculated: 339.3) confirmed the formation of L. The formation L was again confirmed by ^{1}H NMR and ^{13}C NMR spectra.
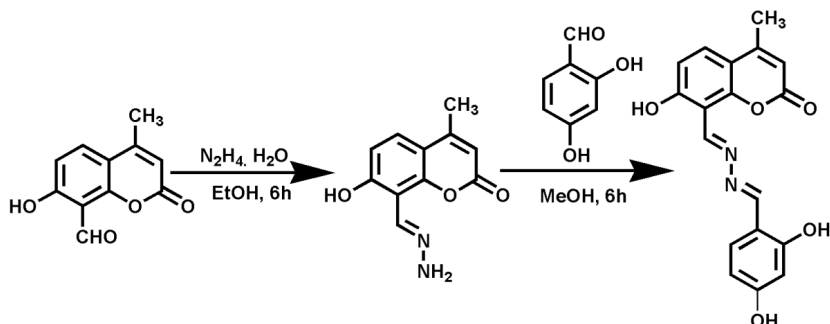
Scheme 1. Synthetic route of 1(8-methanylylidene-7-hydroxy-4-methyl-2H-chromen-2-one)-2-(2, 4-dihydroxybenzylidene) hydrazine, L
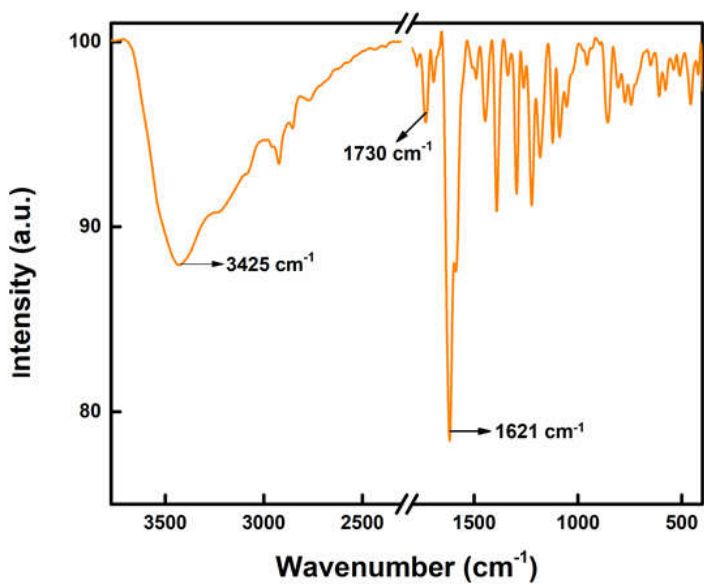
Fig. 1. Infrared spectrum of L
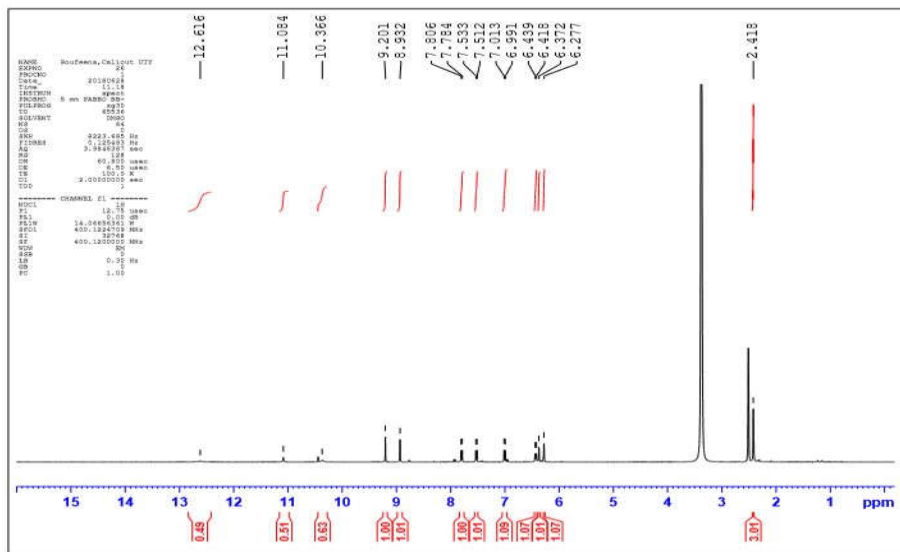
Fig. 2. ¹H NMR spectrum of L
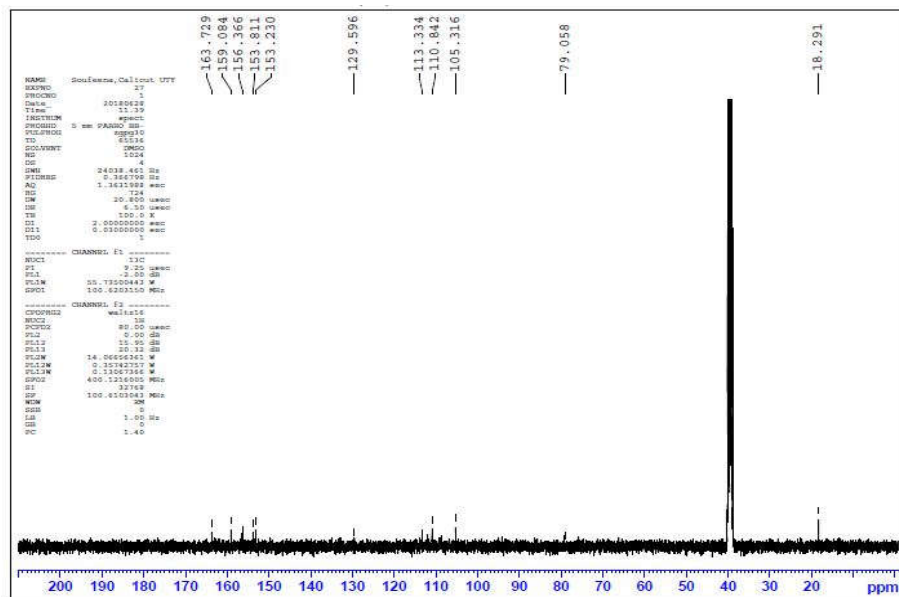
Fig. 3. ¹³C NMR of L in DMSO
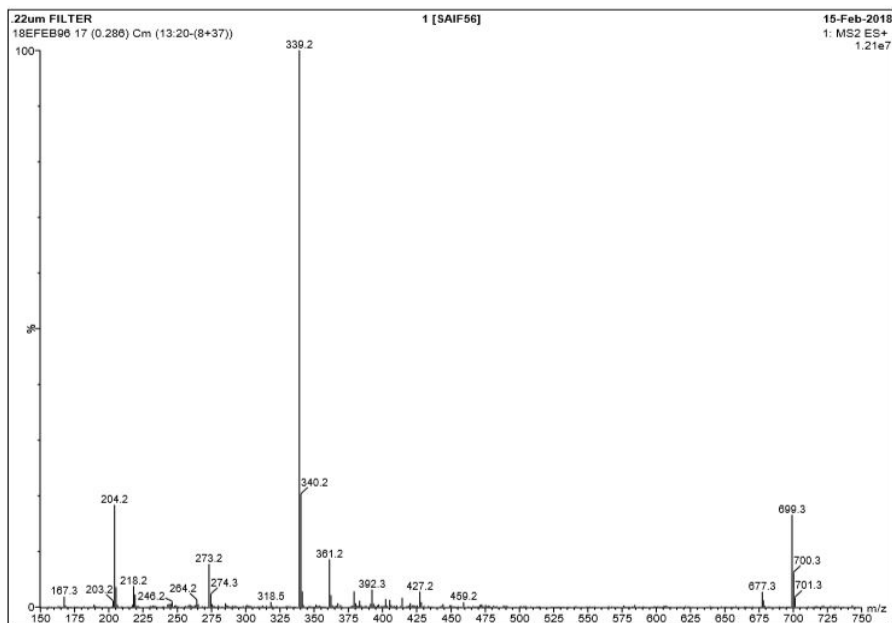
Fig. 4. Positive ion ESI-MS of L

3.2. Photophysical investigations

The colourimetric sensing ability of L with various metal ions like, Cr^{3+}, Fe^{3+}, Co^{2+}, Ni^{2+}, Cu^{2+}, Zn^{2+}, Al^{3+}, Ca^{2+}, Mg^{2+}, Na^+, K^+, Cd^{2+}, Hg^{2+} and Pb^{2+} was monitored in acetonitrile by UV-Visible spectroscopy. The UV-Visible spectrum of L showed two distinct peaks at 314 and 356 nm. The addition of metal ions, except Cu^{2+}, did induce slight or no spectral change, while the addition of Cu^{2+} produced a distinct change in the spectral behavior of L. In the presence of Cu^{2+}, the absorption peak of L at 354 nm was blue shifted to 340 nm and a new peak appeared at 436 nm (Fig 5a). In consistent with the spectral changes, the colourless solution of L changed to yellow with the addition of Cu^{2+} ion. Thus, L can act as a "naked-eye"

colourimetric sensor for Cu^{2+} ion (Fig 5b). Calculation of electron distribution in frontier molecular orbitals (HOMO and LUMO) of the L by DFT analysis indicated the possibility of strong intramolecular charge- transfer (ICT) (Fig. 6). The phenolic unit together with imine bond act as electron donors and coumarin unit acts as electron acceptor and generates a "push-pull" interaction in L. The interaction of L with Cu^{2+} (complex formation), restricted the ICT process, resulting a remarkable spectral change.
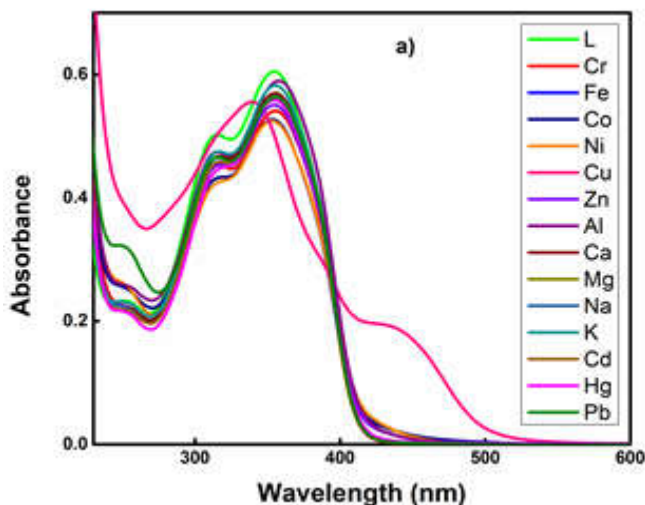
Fig.5 (a) Absorption spectral change of L (20μM) with
1 equivalent of various metal ions in acetonitrile- water mixture
(b) The colour change of L(20μM) with 1 equivalent ofvarious metal ions.

UV-Visible titration was carried out to get a quantitative idea about the interaction between L and Cu^{2+}. Upon the addition of Cu^{2+} to a solution of L, appeared a new absorption peak at 436 nm and the absorbance of this band increased gradually on increasing the concentration of Cu^{2+} up to 3.6 equivalents (Fig. 7). Besides this change, the absorbances at 356 and 314 nm decreased. The appearance of a clear isosbestic point at 397 nm divulged the formation of a single species. The Job's plot of L-Cu^{2+} (Fig. 8) revealed a 1:1 stoichiometry, which was further confirmed from the positive ion ESI-MS analysis. In the mass spectrum of L, upon the addition of 1 equivalent of Cu^{2+} appeared a peak at m/z 483.7 corresponding to $L + Cu^{2+} + NO_3^- + H_2O + 3H^+$ (calculated 483. 8) revealing the 1 : 1 binding stoichiometry between L and Cu^{2+}(Fig. 9).

HOMO   LUMO
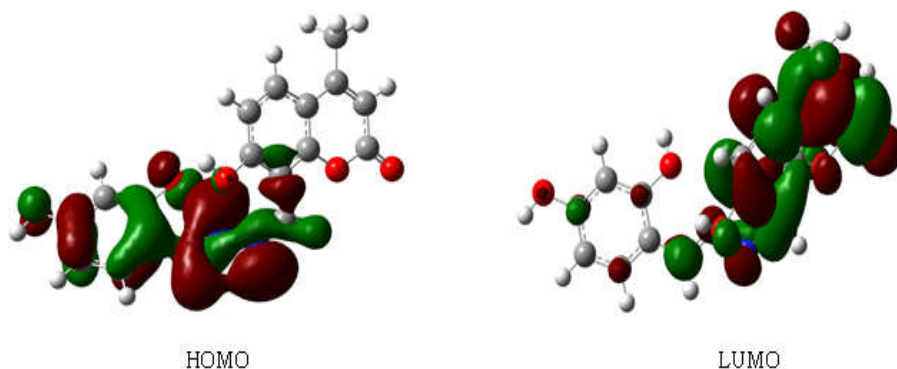
Fig. 6 Frontier molecular orbitals (HOMO and LUMO) of L
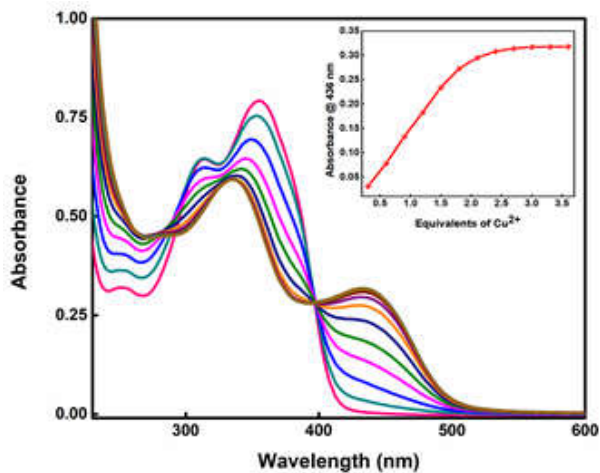
Fig. 7. Absorption spectra of L (20 μM) upon the addition of Cu²⁺ from 0 to 3.6 equivalents. Inset: Absorbance at 436 nm versus the number of equivalents of Cu²⁺ added.
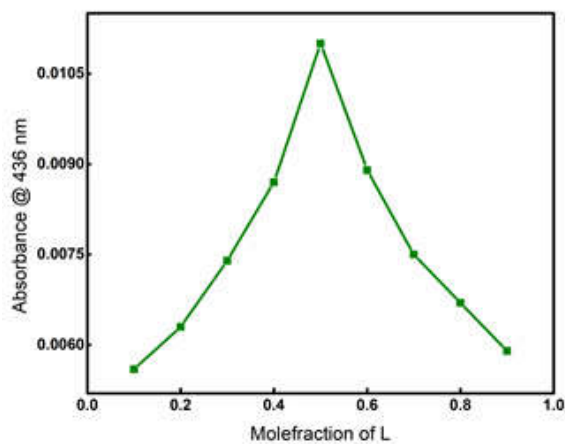
Fig. 8. Job's plot of L with Cu²⁺ in acetonitrile
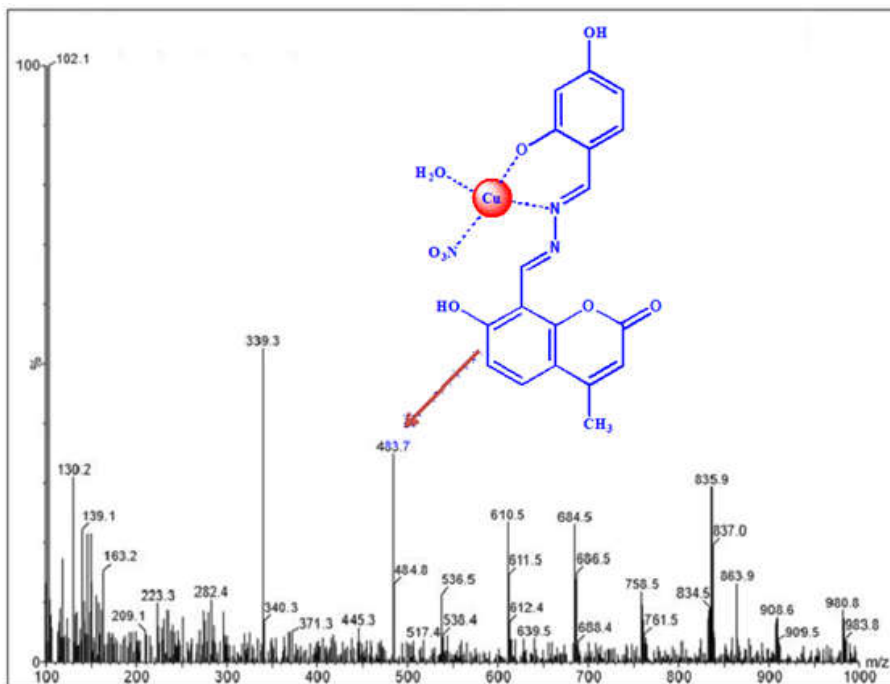
Fig. 9. Positive ESI-MS of CuL
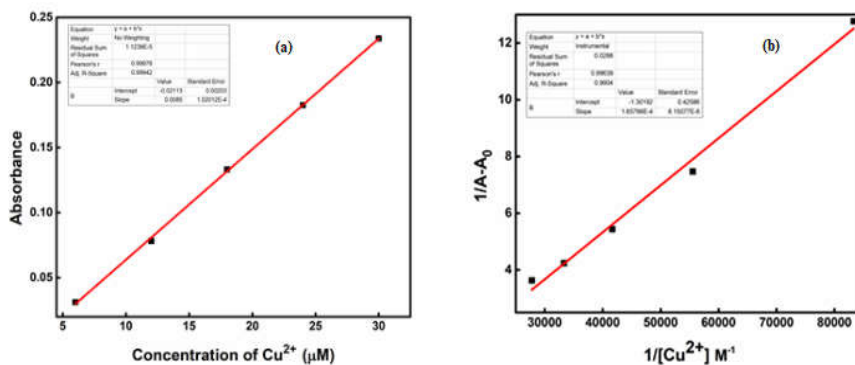
Fig. 10 (a) Calibration curve of L-Cu²⁺ for LOD calculation,
(b) Benesi-Hildebrand plot of complex formed between Cu²⁺ and L

The limit of detection was calculated from the slope of the calibration curve by using the equation, $3\sigma/K$, where σ is the standard deviation and K is the slope of the calibration curve. It was found to be 28 µM at this concentration range [Fig 10(a)]. The calculated value was lower than the LOD permitted by WHO (30 µM)[28]. Based on the UV-Visible titration, calculated the binding constant of L with Cu^{2+} using the Benesi-Hilderbrand equation [Fig 10(b)]. The calculated binding constant, 1.87×10^4 M^{-1}, was comparable with the previously reported binding constant values of copper sensors.

One of the important factors of chemical sensors is their ability to selectively detect a particular metal ion in the presence of other metal ions. Therefore, we conducted the competition experiment to check the selectivity of L towards Cu^{2+} in presence of other metal ions like Cr^{3+}, Fe^{3+}, Co^{2+}, Ni^{2+}, Zn^{2+}, Al^{3+}, Ca^{2+}, Mg^{2+}, Na$^+$, K$^+$, Cd^{2+}, Hg^{2+} and Pb^{2+}. The experiment was carried out by adding 1 equivalent of Cu^{2+} to a solution containing L and 1equivalent one of the following metal ions Cr^{3+}, Fe^{3+}, Co^{2+}, Ni^{2+}, Zn^{2+}, Al^{3+}, Ca^{2+}, Mg^{2+}, Na$^+$, K$^+$, Cd^{2+}, Hg^{2+} and Pb^{2+} at one time. The Fig. 11 depicts that the presence of other metal ions mentioned above have no or relatively a little interference in the detection of Cu^{2+} by L. The result accredited that the probe, L has high selectivity and sensitivity for the detection of Cu^{2+}. Comparing with the previously reported Cu^{2+} sensors, L shows a comparable response toward Cu^{2+}. The comparison was made based on the association constants and limits of detection. The details are shown in the Table 1.
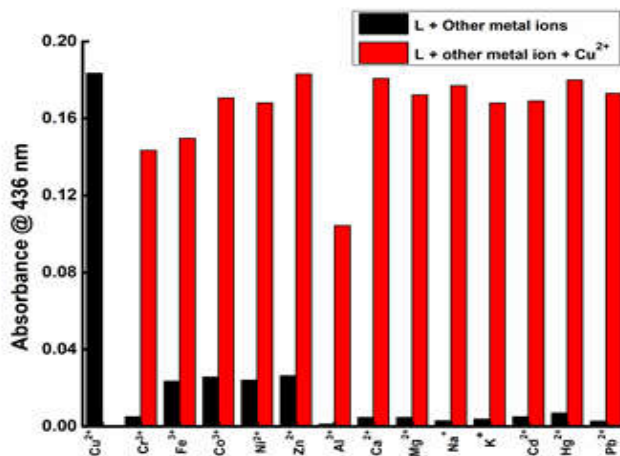
Fig. 11. The selectivity ol L (20 μM) toward Cu^{2+} (1 equivalent)
in the presence of other metal ions (1 equivalent)
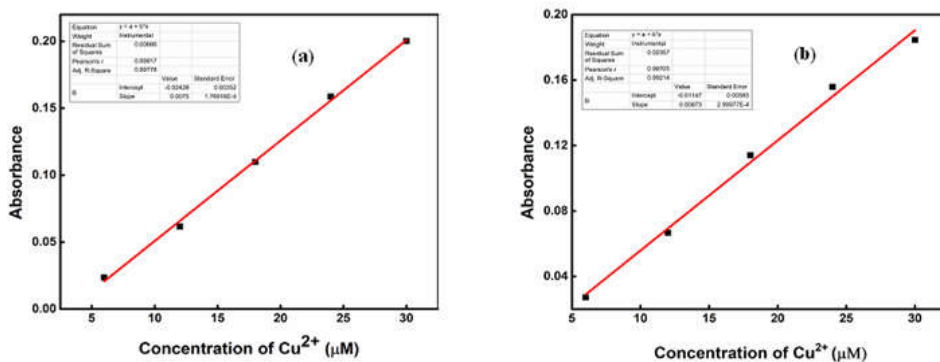
Fig. 12. Calibration curve of L-Cu^{2+} for LOD calculation in
(a) tap water and (b) canal water

To investigate the practical applicability of the probe L , we carried out the detection of Cu^{2+} in two different water samples. For this, 1 mM solution of copper salt was prepared in tap water and canal water and their UV-Visible titrations were carried out. The result divulged that the detection of Cu^{2+} with the same detection limit of

28.4 µM was possible with the probe L if the sample were prepared in either tap water or canal water [Fig. 12]

Table 1. Comparison of sensing of L with the previously reported sensors

Probe	Association constant	LOD	Sensing response
Ref[29]	1.26×10^6 M^{-1}	1×10^{-5} M	Colourimetric
	1.44×10^6 M^{-1}	1×10^{-6} M	Colourimetric
Ref[30]	2.23×10^4 M^{-1}	20×10^{-6} M	Fluorescence
Ref[31]	NA	3.43×10^{-7} M	Colourimetric
Ref[32]	6.3×10^3 M^{-1}	NA	Ratiometric
	1.4×10^5 M^{-1}	NA	Fluorescence
Ref[33]	NA	1.36×10^{-5} M	Colourimetric
L	$\mathbf{1.87 \times 10^4}$ **M^{-1}**	$\mathbf{2.84 \times 10^{-5}}$ **M**	**Colourimetric**

4. Conclusions

A new hydrazine based Schiff base, 1-(8-methanylylidene-7-hydroxy-4-methyl-2H-chromen-2-one)-2-(2,4-dihydroxybenzylidene) hydrazine, L was synthesized and characterized. The colourimetric sensing ability of L towards various metal ions was checked. The selective fast response of L with Cu^{2+} was quantified by using UV-Visible titration. The observed detection limit was below 30 µM for Cu^{2+} which was lower than that proposed by WHO. The competition study revealed that the other common metal ions have a little or no interference in the detection of copper ion using the probe, L. Meanwhile, L showed good practical applicability for the detection of Cu^{2+} samples prepared in tap water and canal water.

References

1.   H. S. Jung, P. S. Kwon, J. W. Lee, J. I. Kim, C. S. Hong, J. W. Kim, S. Yan, J. Y. Lee, J. H. Lee and T. Joo, *Journal of the American Chemical Society*, 2009, **131**, 2008-2012.

2.   J.-J. Xiong, P.-C. Huang, C.-Y. Zhang and F.-Y. Wu, *Sensors and Actuators B: Chemical*, 2016, **226**, 30-36.

3.   R. F. Viguier and A. N. Hulme, *Journal of the American Chemical Society*, 2006, **128**, 11370-11371.

4.   I. Bertini, H. B. Gray, S. J. Lippard and J. S. Valentine, *Bioinorganic chemistry*, University Science Books, 1994.

5.   P. Torawane, S. K. Sahoo, A. Borse and A. Kuwar, *Luminescence*, 2017, **32**, 1426-1430.

6.   V. Kumar, U. Diwan, I. Sanskriti, R. K. Mishra and K. Upadhyay, *ChemistrySelect*, 2017, **2**, 11358-11363.

7.   D. Peralta-Domínguez, M. Rodriguez, G. Ramos-Ortiz, J. Maldonado, D. Luna-Moreno, M. Ortiz-Gutierrez and V. Barba, *Sensors and Actuators B: Chemical*, 2016, **225**, 221-227.

8.   J. Zhang, B. Zhao, C. Li, X. Zhu and R. Qiao, *Sensors and Actuators B: Chemical*, 2014, **196**, 117-122.

9.   P. Verwilst, K. Sunwoo and J. S. Kim, *Chemical Communications*, 2015, **51**, 5556-5571.

10.   R. A. Festa and D. J. Thiele, *Current Biology*, 2011, **21**, R877-R883.

11.   D. J. Waggoner, T. B. Bartnikas and J. D. Gitlin, *Neurobiology of disease*, 1999, **6**, 221-230.

12.   D. R. Brown, *Brain research bulletin*, 2001, **55**, 165-173.

13.   J. Y. Noh, G. J. Park, Y. J. Na, H. Y. Jo, S. A. Lee and C. Kim, *Dalton transactions*, 2014, **43**, 5652-5656.

14.   G. J. Park, D. Y. Park, K.-M. Park, Y. Kim, S.-J. Kim, P.-S. Chang and C. Kim, *Tetrahedron*, 2014, **70**, 7429-7438.

15.   K. Mariappan, M. Alaparthi, G. Caple, V. Balasubramanian, M. M. Hoffman, M. Hudspeth and A. G. Sykes, *Inorganic chemistry*, 2014, **53**, 2953-2962.

16.   A. Ghorai, J. Mondal, S. Chowdhury and G. K. Patra, *Dalton Transactions*, 2016, **45**, 11540-11553.

17.   J. R. Askim, M. Mahmoudi and K. S. Suslick, *Chemical Society Reviews*, 2013, **42**, 8649-8682.

18.   H. Zhu, J. Fan, B. Wang and X. Peng, *Chemical Society Reviews*, 2015, **44**, 4337-4366.

19.   M. Shellaiah, Y.-H. Wu, A. Singh, M. V. R. Raju and H.-C. Lin, *Journal of Materials Chemistry A*, 2013, **1**, 1310-1318.

20.   T. G. Jo, Y. J. Na, J. J. Lee, M. M. Lee, S. Y. Lee and C. Kim, *New Journal of Chemistry*, 2015, **39**, 2580-2587.

21.   M. Saleem and K.-H. Lee, *Journal of Luminescence*, 2014, **145**, 843-848.

22.   Y. J. Na, Y. W. Choi, J. Y. Yun, K.-M. Park, P.-S. Chang and C. Kim, *Spectrochimica Acta Part A: Molecular and Biomolecular Spectroscopy*, 2015, **136**, 1649-1657.

23.   S. S. Razi, P. Srivastava, R. Ali, R. C. Gupta, S. K. Dwivedi and A. Misra, *Sensors and Actuators B: Chemical*, 2015, **209**, 162-171.

24.   J.-T. Yeh, W.-C. Chen, S.-R. Liu and S.-P. Wu, *New Journal of Chemistry*, 2014, **38**, 4434-4439.

25.   G.-K. Li, Z.-X. Xu, C.-F. Chen and Z.-T. Huang, *Chemical Communications*, 2008, 1774-1776.

26.   A. Kulkarni, S. A. Patil and P. S. Badami, *European journal of medicinal chemistry*, 2009, **44**, 2904-2912.

27.   Y. Dong, X. Mao, X. Jiang, J. Hou, Y. Cheng and C. Zhu, *Chemical Communications*, 2011, **47**, 9450-9452.

28.   W. H. Organization, *Guidelines for Drinking-Water Quality. 3rd ed. Geneva*, 2008.

29.   V. K. Gupta, A. Singh, M. Ganjali, P. Norouzi, F. Faridbod and N. Mergu, *Sensors and Actuators B: Chemical*, 2013, **182**, 642-651.

30.   R. V. Rathod, S. Bera, M. Singh and D. Mondal, *RSC advances*, 2016, **6**, 34608-34615.

31.   A. Kumar, V. Kumar, U. Diwan and K. Upadhyay, *Sensors and Actuators B: Chemical*, 2013, **176**, 420-427.

32.   Z. Xu, J. Pan, D. R. Spring, J. Cui and J. Yoon, *Tetrahedron*, 2010, **66**, 1678-1683.

33.   P. Kaur, D. Sareen and K. Singh, *Talanta*, 2011, **83**, 1695-1700.

A FLUORESCENCE "TURN-ON" SENSOR BASED ON THE RESTRICTION OF –C=N ISOMERISATION FOR Al³⁺ IN ORGANIC/AQUEOUS MIXTURE
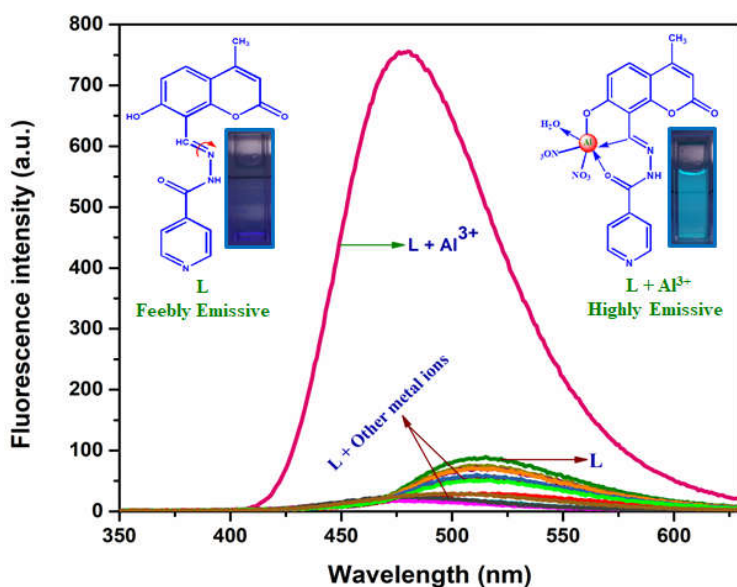
Work in brief……………

- *Synthesized and characterized a coumarin based "turn-on" fluorescence sensor for Al³⁺.*
- *The probe functioned well in organic - aqueous mixture of 1:1 volume fraction.*
- *The observed limit of detection was lower than that proposed by WHO.*
- *The probe exhibited good response with Al³⁺ present in the real water samples.*

1. Introduction

The topic of selective detection of biologically- and environmentally relevant chemical species are of immense importance in the present scenario because of their inevitable roles in our day to day life. Various types of cations, anions and neutral species have different roles in our life. Among the various metal ions, aluminum, third most abundant element on the earth crust and its compounds are widely associated with human life[1]. Compounds of aluminium are employed in various industries including paper industry, textile industry, water treatment plants, aluminum cook wares, food additives, production of alloys, etc. Quite contrary to the vital roles of aluminium compounds in human life, their excessive releases to the environment threaten the life on earth. Aluminum ions released to the earth and water bodies adversely affect the plant and aquatic species[2]. Excessive absorption of aluminum by human body leads to serious health issues such as Alzheimer's and Parkinson's diseases[3-6]. According to WHO reported, the average daily human intake of aluminum should be only around 3-10 mg[7]. Therefore, it is highly desirable to develop a suitable method to estimate the concentration of Al^{3+}.

Fluorescence sensors offer simple analytical procedure for the detection of various analytes with amazing sensitivity and selectivity[8-10]. The attraction of fluorescence sensing over the other methods employed for the detection of analytes, like atomic absorption spectrometry[11], cyclic voltammetry[12], chromatography[13], inductively

coupled plasma spectrometry[14] etc. is its non-destructive nature, rapid response and relatively inexpensive instrumentation required. The poor coordinating ability of the Al^{3+} compared to the other relevant metal ions is problematic [15-17]. However, a number of fluorescence sensors are reported for Al^{3+} by various groups. But most of them function in organic solvents alone [18-21].

Here, we have developed a coumarin based Schiff base, 8-(1-(4-pyridinehydrazide)methylene-)-7-hydroxy-4-methylvoumain-2-one, L *via* condensing 8-formyl-7-hydroxy-4-mthylcoumarine and isonicotinylhydrazide. It exhibited a highly selective and sensitive fluorescence response towards Al^{3+} in DMF/water (1:1) mixture. It has a very low detection limit towards Al^{3+} in organic/aqueous mixture. The sensing ability of L was checked at different pH. The study was extended for the detection of Al^{3+} in real water samples also.

2. Experimental
2.1. Materials and methods

All the chemicals used for the study were purchased from Sigma Aldrich or Alfa Aesar. The solvents were received from the chemical suppliers and were used without further purification. The sensing study was carried out using nitrate salts of different metals.

Elemental analyses were carried out on Vario EL III CHNS analyzer. A Jasco FTIR 4100 spectrometer was used to record the FTIR spectrum (4000 - 400 cm⁻¹) of the compound. The ¹H NMR- and

^{13}C NMR spectra were recorded on a 400 MHz Bruker Avance III spectrometer using DMSO-d6. The Electron-Spray Ionization Mass Spectrum (ESI-MS) was recorded on Waters (UPLC- TQD) mass spectrometer. Fluorescence spectrum was recorded on an Agilent Technologies model Cary Eclipse Fluorescence Spectrophotometer.

2.2. Synthesis of Schiff base

The procedures for the synthesis 8-formyl-7-hydroxy-4-methylcoumarin was adopted from the literature[22, 23].

Hot ethanol solution of isonicotinylhyadrazide (1mmol, 0.137g) was added in drops to hot ethanol solution of 8-formyl-7-hydroxy-4-methylcoumarine with constant stirring. The resulting mixture was refluxed for about 4 h and concentrated to half its volume. The yellow coloured solution was allowed to crystallize at room temperature and the solid obtained was washed with acetone for several times and recrystallized from ethanol, dried and kept in a desiccator. Yield: 85 %. Anal. Calcd for $C_{17}H_{13}N_3O_4$: C, 63.16; H, 4.05%; N, 13.00%; Found: C, 68.12%; H, 4.87%; N, 12.63%. IR (cm^{-1}, KBr): ν(O-H) 3427 cm^{-1}, ν(N-H) 3262 cm^{-1}, ν(-C=O of coumarin) 1712 cm^{-1}, ν(-C=O of isonicotinylhydrazide) 1678 cm^{-1}, ν(C=N) 1625 cm^{-1}. ^{1}H NMR (400 MHz, DMSO d$_6$, δ (ppm)) δ: 12.63 (1H, s), 9.11 (1H, s), 8.83 (1H, s), 2.50 (s, 3H); 7.87, 7.86, 7.72, 7.70, 6.96, 6.94, 6.24 (aromatic protons),^{13}C NMR (400 MHz, DMSO d$_6$, δ (ppm)) δ 161.5, 161.4, 159.5, 154.2, 153, 150.9, 145.1, 139.5, 128.8, 121.8, 114, 113.9, 112.2, 111.2, 105.7, 18.7. ESI MS (m/z): $[L + H]^+$:

Calculated: 324.09, Found: 324, m/z [L + Na]$^+$: Calculated: 346.07, Found: 346.

2.3. Sample preparation for fluorescence studies

Stock solutions of different metal ions like, Cr^{3+}, Fe^{3+}, Co^{2+}, Ni^{2+}, Cu^{2+}, Zn^{2+}, Al^{3+}, Ca^{2+}, Mg^{2+}, Na^+, K^+, Cd^{2+}, Hg^{2+} and Pb^{2+} in 1 mM concentration were prepared in deionized water. 1 mM stock solution of L was prepared in DMF. From the above stock solution of L, 20 µM solution was prepared in DMF/water (1:1) mixture.

Fluorescence sensing studies were carried out by recording the fluorescence spectrum of the solution mixture of 1 equivalent of the stock solution of one of the metal ions and 3 ml of 20 µM solution of L, at room temperature. In fluorescence titration, 0 to 6 equivalents of 0.1 mM Al^{3+} solution were added gradually to 3 ml of 10 µM solution of L and the spectral change after each addition was monitored spectroscopically. To find out the mode of interaction between L and Al^{3+}, conducted Job's plot analysis by keeping the total concentration of L and Al^{3+} as 0.1 mM and total volume as 3 ml. Fluorescence titration was carried out by using a 50 µM solution of Al^{3+} and 3 ml of 5 µM solution of L. From the titration profile, LOD was calculated based on the equation, 3σ/slope. The association constant was calculated using Benesi-Hildebrand equation by assuming a 1:1 binding stoichiometry. The effect of pH was also checked using HEPES buffer. Competition studies were conducted by adding appropriate amount of cations in 0.1 mM concentration to 3 ml of 10

μM solution of L. The practical applicability of the probe was checked by recording the spectra in different water samples. In all cases, fluorescence spectra were recorded at a 560 V pmt voltage.

$$\frac{1}{(F - F_0)} = \frac{1}{K_a(F_{max} - F_0)} \; x \; \frac{1}{[M]^n} + \frac{1}{(F_{max} - F_0)}$$

where, F_0 and F are the fluorescence intensities of the probe molecule in the absence- and presence of the analyte, F_{max} is fluorescence intensity at maximum concentration of the analyte, [M] is the concentration of the analyte and K_a is the association constant.

3. Results and discussion

3.1. Structural characterization
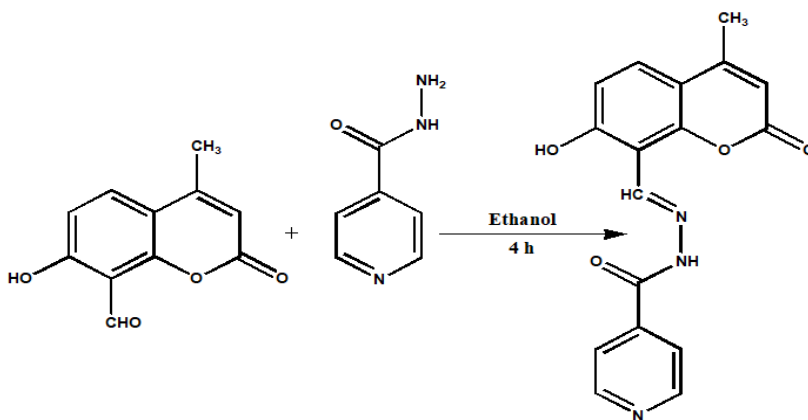
Scheme 1. Synthetic route of 8-(1-(4-pyridinehydrazide)methylene-
)-7-hydroxy-4-methylvoumain-2-one, L

Fig. 1. IR spectrum of L

Fig 2. ¹H NMR spectrum of L

Fig 3. ¹³C NMR spectrum of L

Fig. 4. ESI-MS of L

L was synthesized by the condensation reaction of 8-hydroxy-4-methylcoumarine and nicotinicacid hydrazide in ethanol. The compound was characterized by elemental analysis, IR-, ^{1}HNMR and ^{13}CNMR spectroscopic and mass spectrometric analyses. The compound was soluble in almost all organic solvents.

The elemental analysis data were close to the theoretically calculated ones. In the IR spectrum of L (Fig. 1), characteristic stretching of O-H group appeared at 3427 cm^{-1} and a sharp band due to N-H stretching appeared at 3262 cm^{-1}. The formation of Schiff base was confirmed by the appearance of a band at 1604 cm^{-1}. The characteristic stretching frequency of –C=O group of coumarin moiety appeared at 1712 cm^{-1} and that of isonicotinylhydrazide appeared at 1678 cm^{-1}. The ^{1}HNMR- and ^{13}CNMR data again supported the formation of Schiff base. In the mass spectrum of L (Fig. 4), peak at m/z 324 (calculated 323.09) also supported the formation of Schiff base.

3.2. Photophysical investigation

The fluorescence sensing ability of L with various metal ions like, Cr^{3+}, Fe^{3+}, Co^{2+}, Ni^{2+}, Cu^{2+}, Zn^{2+}, Al^{3+}, Ca^{2+}, Mg^{2+}, Na^+, K^+, Cd^{2+}, Hg^{2+} and Pb^{2+} was monitored in DMF/Water mixture by fluorescence spectroscopic studies at room temperature (Fig. 5). On excitation at 320 nm, free L exhibited a weak emission at 514 nm. Generally, Schiff bases are feebly emissive because the excited state energy will be

utilized for the isomerization of −C=N and hence non- radiative emission occurs. Upon the addition of various metal ions, only in the presence of Al^{3+}, L exhibited a fluorescence "turn-on" response at 479 nm on excitation at 320 nm. Any of the other metal ions did not show this behavior under same experimental condition. The fluorescence responses of L in DMF/water system towards various metal ions are shown in Fig. 5. From the above observation, it is clear that, Al^{3+} arrest the −C=N isomerization *via* stable interaction with the imine bond[18, 24].
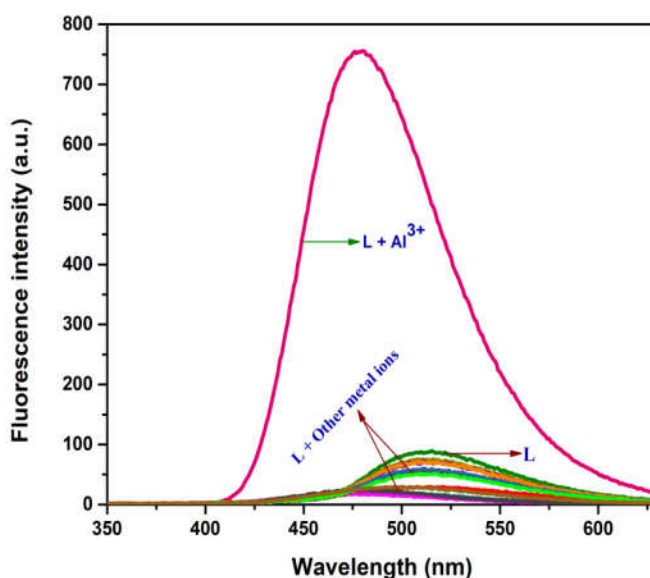
Fig. 5. Fluorescent spectral changes of L (20 μM) in the presence of 1 equivalent various metal ions (Fe^{3+}, Co^{2+}, $Ni2^{+}$, Cu^{2+}, Zn^{2+}, Al^{3+}, Na^{+}, K^{+}, Mg^{2+}, Ca^{2+}, Ba^{2+},Pb^{2+},Cd^{2+} and Hg^{2+},) in DMF/water mixture λ_{ex} = 320 nm
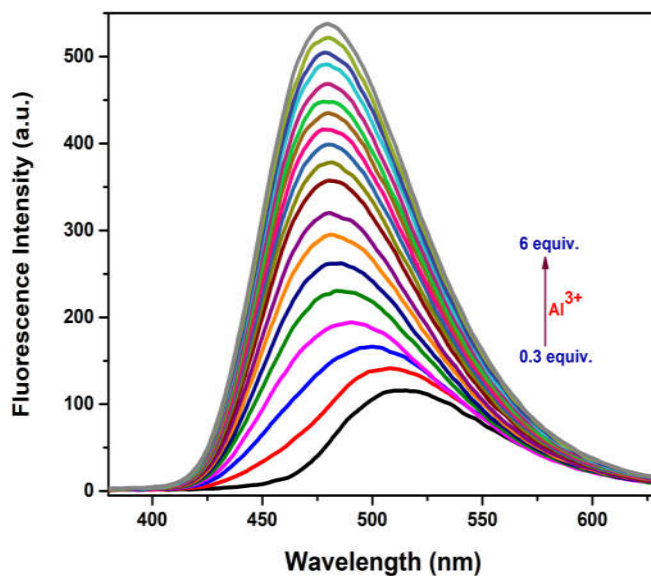
Fig 6. Fluorescence titration profile of L (10 μM) with Al^{3+}
(0 to 6 equivalents) in DMF/water mixture on exciting at 320 nm.
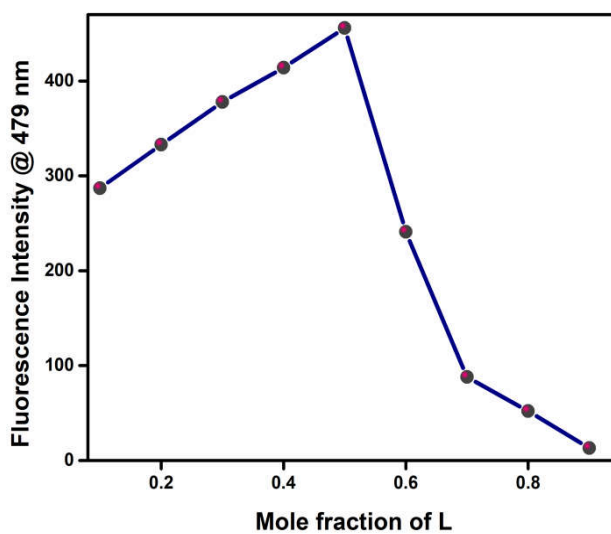
Fig.7. Job's plot of countinuous variation

The fluorescence titration was carried out by the gradual addition of a solution of Al^{3+} in water (0 - 6 equivalents) to 10 μM solution of L in DMF/water mixture. As depicted in Fig. 6, upon the gradual addition of Al^{3+} up to 6 equivalents to a solution of L, the intensity of emission increased gradually with a blue shift observed in the emission maxima. The spectral profile of L was shifted from 514 nm to 479 nm (a 35 nm blue shift) in the presence of Al^{3+}. However, above 6 equivalents of Al^{3+}, no further changes were observed in the spectral profile.
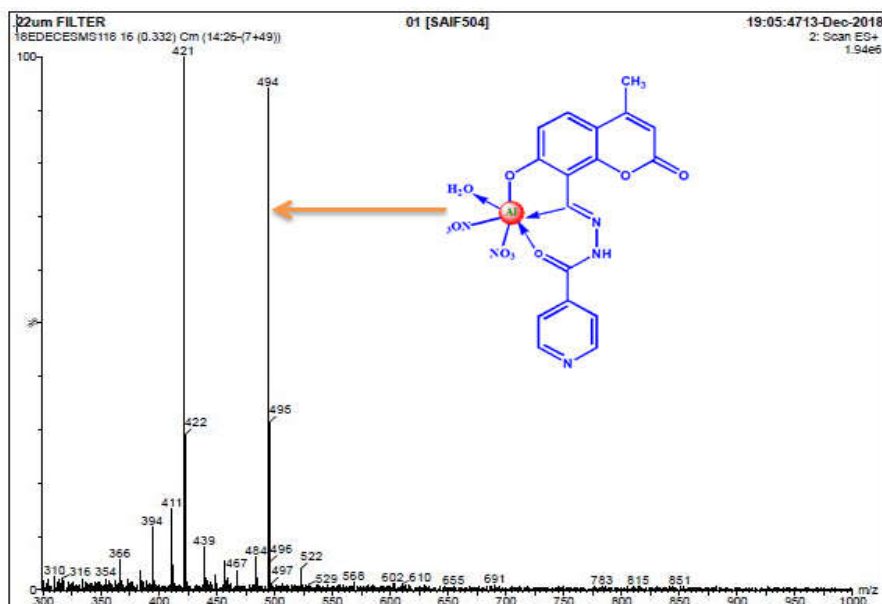
Fig 8. ESI-MS spectrum of L with Al^{3+}

Job's method of continuous variation was used to find out the stoichiometry of interaction between L and Al^{3+}. From the plot of mole

fraction *versus* intensity of fluorescence (Job's plot), it was clear that the binding between the L and Al^{3+} was in the ratio of 1:1 (Fig. 7). 1: 1 binding stoichiometry was again confirmed by ESI-MS analysis. As depicted in Fig. 8, positive ESI-MS spectrum exhibited a peak at m/z 494 (calculated m/z 494.15) due to the formation of an adduct, ($L + Al^{3+} + 2NO_3^- + H_2O + 4H^+$) supporting 1:1 binding stoichiometry.
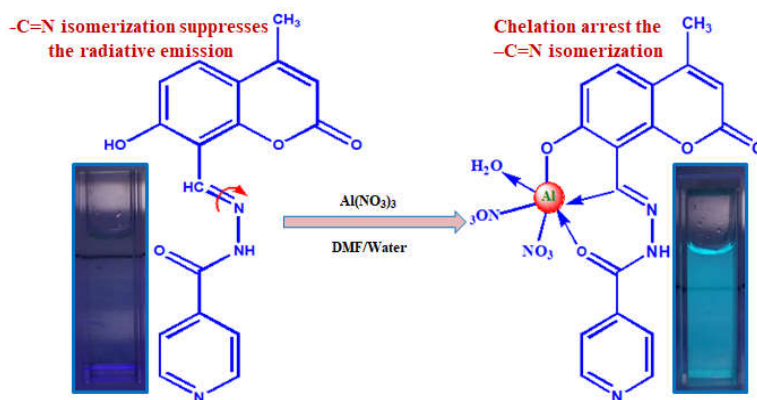
Fig. 9. Proposed mechanism of sensing of Al^{3+} with L
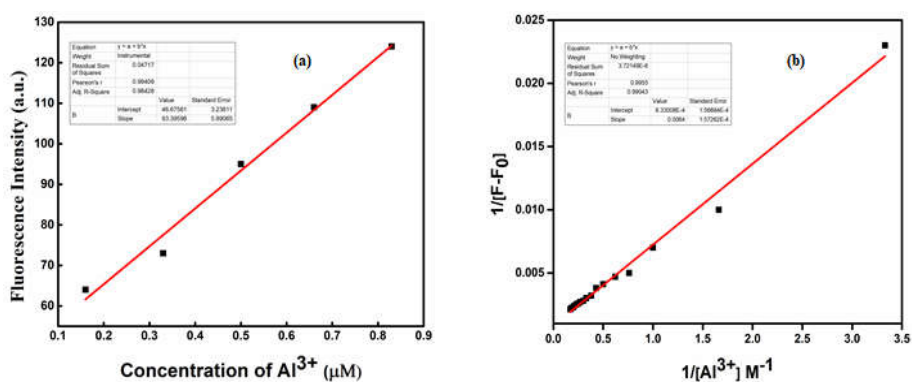
Fig. 10. (a) Calibration curve of L with Al^{3+} for LOD calculation, (b) Benesi-Hildebrand plot of L with Al^{3+}

Schiff bases are generally feeble emissive because of the −C=N isomerization process[25]. This class of compounds, on exciting with a radiation of specific wavelength, the excited state energy is used for the isomerization process and thereby radiative emission will be blocked. If any process which arrests the −C=N isomerization of Schiff base, it displays interesting fluorescence behavior. Here the stable chelation to Al^{3+} through the imine bond arrests the isomerization process leading to intense radiative emission. The proposed mechanism is depicted in Fig. 9.
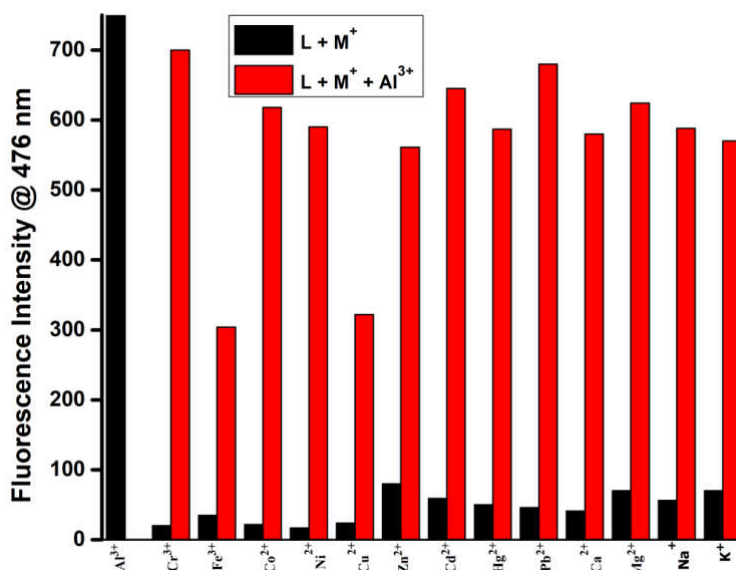
Fig 11. Competition study of L (20 μM) with Al^{3+} (1 equivalent) in the presence of other cations (1 equivalents) at an excitation wavelength of 320 nm (560 pmt voltage)

The limit of detection (LOD) was calculated from the slope of the calibration curve [Fig. 10 (a)] using the equation, $3\sigma/\text{slope}$ (σ is standard deviation and K is the slope of the calibration curve). It was found to be 0.79 µM [Fig. 10 (a)] and it was far below LOD proposed by the WHO. The extent of interaction between L and Al^{3+} was obtained from the association constant which was calculated by Benesi-Hilderbrand method and it was found to be 3.22×10^5 M^{-1} [Fig 10(b)].
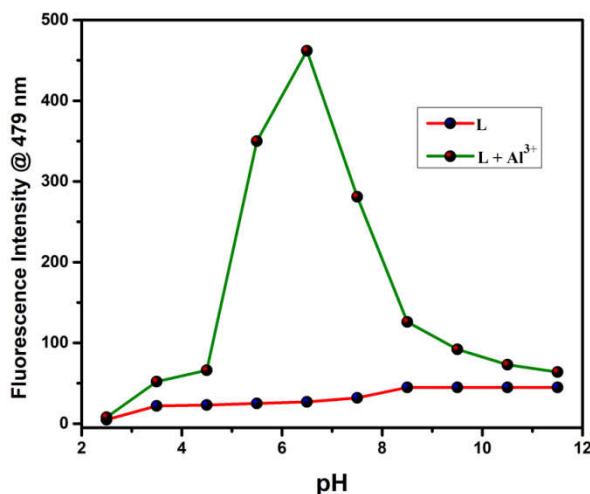
Fig. 12. Variation of fluorescent emission of L and L + Al^{3+} at different pH

To explore the practical applicability of the probe, competition experiment was carried out, i.e., the ability of L to detect Al^{3+} in the presence of other metal ions under same experimental condition. For this, 1 equivalent of Al^{3+} and 1 equivalent of other metal ions having same concentration were treated with 3 ml 10 µM solution of L in DMF. As depicted in Fig 11, except Fe^{3+} and Cu^{2+}, the other metal ions

did not have significant interference towards the detection of Al^{3+} by L. Fe^{3+} and Cu^{2+} have a little interference in the detection of Al^{3+} by L because of the paramagnetic nature of these metal ions[18, 26]. In most of the fluorescence sensors, these metal ions interfere in the sensing of various analytes.

Table No. 1: Comparison of sensing of L with the previously reported sensors

Probes	LOD	Association Constant	Medium (v/v)	Sensing response
Ref[27]	3.28×10^{-6}	8.32×10^{6} M^{-1}	Ethanol-water (95 : 5)	Turn-on
Ref[28]	4.8×10^{-7}	2.1×10^{4} M^{-1}	Methanol-water (80:20)	Turn-on
Ref[29]	1.5×10^{-6}	5.1×10^{4} M^{-1}	DMF-water (70:30)	Turn-on
Ref[30]	3×10^{-6}	9.91×10^{3} M^{-1}	THF-water (90:30)	Turn-on
Ref[31]	0.77×10^{-6}	1×10^{4} M^{-1}	Methanol-water (50:50)	Turn-on
Ref[32]	8.87×10^{-7}	5.23×10^{5} M^{-1}	Ethanol-water (95 : 5)	Turn-on
Ref[33]	5×10^{-7}	8.84×10^{3} M^{-1}	Ethanol-water (50 : 50)	Turn-on
Ref[34]	2×10^{-6}	4.63×10^{6} M^{-1}	Ethanol-water (90 : 10)	Turn-on
L	**0.79×10^{-6}**	**3.22×10^{5} M^{-1}**	**DMF-water (50 : 50)**	**Turn-on**

The effect of pH on the fluorescence intensity of L before and after the addition of Al^{3+} was studied using HEPES buffer and the fluorescence responses are depicted in Fig. 12. L exhibited almost same fluorescence response at a pH range of 2-11.5. In the case of L

with Al^{3+}, the fluorescence intensity increased with increasing the pH of the solution up to pH 6.5 and after that it decreased. From the Fig 12, it can be seen that L exhibited good response towards Al^{3+} in physiologically- and biologically important pH ranges. On comparing with the previously reported Al^{3+} probes functioning in organic/ aqueous medium, L exhibited comparatively good sensing response. The comparison was made based on the association constant, limit of detection and the solvent used. The details are shown in the Table 1.
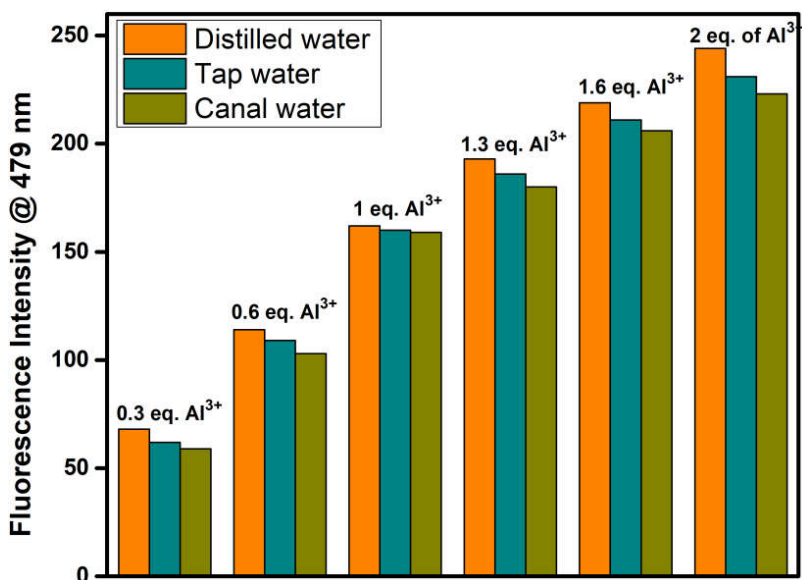
Fig 13. Fluorescence response of L towards Al^{3+} in various water samples

To explore the practical applicability of the probe, we carried out the detection of Al^{3+} in two different water samples. For this, 1 mM solution of Al^{3+} was prepared in tap water and canal water and fluorescence titrations were carried out. As depicted in Fig. 13, L

exhibited good turn–on fluorescence response towards Al^{3+} in both tap water and canal water.

4. Conclusions

Synthesized a coumarine based Schiff base *via* condensation of 8-formyl-7-hydroxy-4-methylcoumarine with isonicotinylhydrazide in ethanol solution. It exhibited turn-on fluorescence response with Al^{3+} in DMF and the other metal ions did not show this type of behavior under the same experimental conditions. The observed detection limit of Al^{3+} by the probe L was 0.79 μM and calculated association constant was 3.22 x 10^5 M^{-1} indicating the stable interaction between L and Al^{3+}. The effect of pH on the sensing ability of L suggested that Al^{3+} detection was possible in physiologically- and environmentally important pH ranges. Further, the applicability of the probe to detect Al^{3+} in two different water samples was established successfully.

References

1. S. Sen, T. Mukherjee, B. Chattopadhyay, A. Moirangthem, A. Basu, J. Marek and P. Chattopadhyay, *Analyst*, 2012, **137**, 3975-3981.

2. N. E. Alstad, B. M. Kjelsberg, L. A. Vøllestad, E. Lydersen and A. B. Poléo, *Environmental pollution*, 2005, **133**, 333-342.

3. V. Hornung, F. Bauernfeind, A. Halle, E. O. Samstad, H. Kono, K. L. Rock, K. A. Fitzgerald and E. Latz, *Nature immunology*, 2008, **9**, 847.

4. S. V. Verstraeten, L. Aimo and P. I. Oteiza, *Archives of toxicology*, 2008, **82**, 789-802.

5. G.-q. Wang, J.-c. Qin, C.-R. Li and Z.-y. Yang, *Spectrochimica Acta Part A: Molecular and Biomolecular Spectroscopy*, 2015, **150**, 21-25.

6. N. R. Chereddy, P. Nagaraju, M. N. Raju, V. R. Krishnaswamy, P. S. Korrapati, P. R. Bangal and V. J. Rao, *Biosensors and Bioelectronics*, 2015, **68**, 749-756.

7. S. Das, M. Dutta and D. Das, *Analytical Methods*, 2013, **5**, 6262-6285.

8. X. Lou, D. Ou, Q. Li and Z. Li, *Chemical Communications*, 2012, **48**, 8462-8477.

9. T. Gunnlaugsson, M. Glynn, G. M. Tocci, P. E. Kruger and F. M. Pfeffer, *Coordination chemistry reviews*, 2006, **250**, 3094-3117.

10. J. Zhang, B. Xing, J. Song, F. Zhang, C. Nie, L. Jiao, L. Liu, F. Lv and S. Wang, *Analytical chemistry*, 2013, **86**, 346-350.

11. M. H. Mashhadizadeh, M. Pesteh, M. Talakesh, I. Sheikhshoaie, M. M. Ardakani and M. A. Karimi, *Spectrochimica Acta Part B: Atomic Spectroscopy*, 2008, **63**, 885-888.

12. J. Di, S. Bi, T. Yang and M. Zhang, *Sensors and Actuators B: Chemical*, 2004, **99**, 468-473.

13. D. Harvey, *Modern analytical chemistry*, Boston: McGraw-Hill Companies, Inc., 2000.

14.   Z. M. Memon, E. Yilmaz and M. Soylak, *Journal of the Iranian Chemical Society*, 2017, **14**, 2521-2528.

15.   K. Soroka, R. S. Vithanage, D. A. Phillips, B. Walker and P. K. Dasgupta, *Analytical Chemistry*, 1987, **59**, 629-636.

16.   N. Yadav and A. K. Singh, *Materials Science and Engineering: C*, 2018, **90**, 468-475.

17.   S. M. Hossain, A. Lakma, R. N. Pradhan, A. Chakraborty, A. Biswas and A. K. Singh, *RSC Advances*, 2015, **5**, 63338-63344.

18.   P. Soufeena and K. Aravindakshan, *Journal of Luminescence*, 2019, **205**, 400-405.

19.   Y.-J. Chang, S.-S. Wu, C.-H. Hu, C. Cho, M. X. Kao and A.-T. Wu, *Inorganica Chimica Acta*, 2015, **432**, 25-31.

20.   C.-r. Li, J.-c. Qin, G.-q. Wang, B.-d. Wang, A.-k. Fu and Z.-y. Yang, *Inorganica Chimica Acta*, 2015, **430**, 91-95.

21.   W.-H. Ding, W. Cao, X.-J. Zheng, D.-C. Fang, W.-T. Wong and L.-P. Jin, *Inorganic chemistry*, 2013, **52**, 7320-7322.

22.   A. Kulkarni, S. A. Patil and P. S. Badami, *European journal of medicinal chemistry*, 2009, **44**, 2904-2912.

23.   Y. Dong, X. Mao, X. Jiang, J. Hou, Y. Cheng and C. Zhu, *Chemical Communications*, 2011, **47**, 9450-9452.

24.   Y. W. Choi, G. J. Park, Y. J. Na, H. Y. Jo, S. A. Lee, G. R. You and C. Kim, *Sensors and Actuators B: Chemical*, 2014, **194**, 343-352.

25.   J.-S. Wu, W.-M. Liu, X.-Q. Zhuang, F. Wang, P.-F. Wang, S.-L. Tao, X.-H. Zhang, S.-K. Wu and S.-T. Lee, *Organic letters*, 2007, **9**, 33-36.

26.   K. P. Carter, A. M. Young and A. E. Palmer, *Chemical reviews*, 2014, **114**, 4564-4601.

27.   Y.-W. Liu, C.-H. Chen and A.-T. Wu, *Analyst*, 2012, **137**, 5201-5203.

28. S. Das, D. Karak, S. Lohar, A. Banerjee, A. Sahana and D. Das, *Analytical Methods*, 2012, **4**, 3620-3624.

29. K. Kaur, V. K. Bhardwaj, N. Kaur and N. Singh, *Inorganic Chemistry Communications*, 2012, **18**, 79-82.

30. K. Kaur, V. K. Bhardwaj, N. Kaur and N. Singh, *Inorganic Chemistry Communications*, 2012, **26**, 31-36.

31. S. Goswami, A. Manna, S. Paul, K. Aich, A. K. Das and S. Chakraborty, *Dalton Transactions*, 2013, **42**, 8078-8085.

32. C.-H. Chen, D.-J. Liao, C.-F. Wan and A.-T. Wu, *Analyst*, 2013, **138**, 2527-2530.

33. Y. Lu, S. Huang, Y. Liu, S. He, L. Zhao and X. Zeng, *Organic letters*, 2011, **13**, 5274-5277.

34. J.-Q. Wang, L. Huang, L. Gao, J. H. Zhu, Y. Wang, X. Fan and Z. Zou, *Inorganic Chemistry Communications*, 2008, **11**, 203-206.

A FLUORESCENCE "TURN-ON" SENSOR FOR CYANIDE ION IN WATER AND ITS APPLICATION IN NATURAL SAMPLES
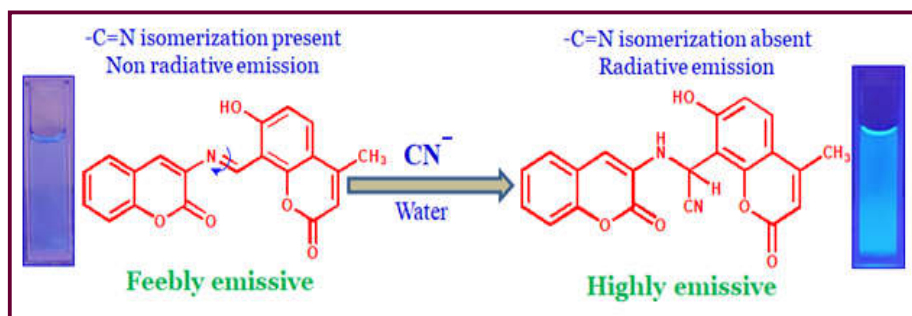
Work in Brief……

- *Synthesized and characterized a coumarin based Schiff's base.*

- *The probe exhibited a fluorescence "turn-on" response of towards cyanide ion in water via chemodosimetric signaling mechanism.*

- *The observed limit of detection was below to WHO permissible limit.*

- *Effect of pH on cyanide sensing by this probe was well established.*

- *The study was extended to natural samples for cyanide ion detection*

1. Introduction

Cyanide ions are extremely toxic to living organisms. Their wide release to environment is a major threat to life on earth [1, 2]. Compounds of cyanide have inevitable role in the production and purification of gold, plastic, fiber, resins, pharmaceuticals, etc, and this turn up the level of cyanide content in environment [3-5]. Many natural substances have a little contribution to the total cyanide release [6, 7]. Previous reports suggest that about 1,40,000 tons of CN⁻ ions are released per year [8, 9]. Because of the strong nucleophilicity of cyanide ion, it inhibits the active functions of metallo- and nonmetallo enzymes through binding with them. Binding of CN⁻ with the heme unit of cytochrome-C-oxidase produces difficulties in respiratory process, which eventually leads to death[10-14]. According to WHO, the acceptable limit of CN⁻ in drinking water is 1.9 μM[7, 15]. Under this circumstance, it is highly essential to detect this ion in water in a cost effective manner.

Among various methods, the development of molecular systems capable of producing a fluorescence response with CN⁻ has considerable attention because of the high sensitivity and selectivity observed in this detection[16-18]. The simplicity of detection, low cost and rapid response are the other attractions of this method. Molecular systems sense cyanide ion mainly through different sensing mechanisms. The interplay of secondary interaction between the receptor and cyanide ion, coordination complex based displacement

approach and chemodosimetric approach are the most reported mechanisms[6, 19-23]. The unique nucleophilicity of cyanide ion is the basis of chemodosimetric approach. Chemodosimtric sensors are highly selective because they form stable chemical bonds with the receptors and hence the binding is irreversible in nature. This will avoid the interference of other anions[24-26]. Coumarin based optical probes find considerable attention because of their interesting photophysical properties[27-30].

Most of the reported cyanide chemodosimeters function well only in organic solvents or organic/aqueous mixtures which limit their practical applicability. The poor response of the chemodosimeter in aqueous medium is due to the competition of the hydroxyl group with cyanide ion to bind with the electrophilic site of the sensor. The anion detection in aqueous solution is a challenge because water molecules compete with the anions for the analyte binding sites. Well established chemodosimeters in aqueous medium are scarce[16, 17, 31-33].

Kim *et al*[19] introduced a Schiff base derived from 3,5-Diamino-1,2,4-triazole and 2-hydroxy-1- naphthalehyde, which exhibited a colourimetric response toward cyanide in aqueous medium. A coumarin based Schiff base was reported by Wei *et al*[24]. It functioned as a colourimetric chemodosimeter for cyanide ion in DMSO/Water.

Here, we have synthesized a new chemosensor, 8-(3-methyleneamino-2H-chromen-2-one)-7-hydroxy-4-methyl-2H-chromen-2-one, L in a one step procedure by condensing 8-formyl-7-

hydroxy-4-methylcoumarine and 3-aminocoumarine. In aqueous solution L displayed a turn-on fluorescence response with CN⁻ without any interference with other common anions. Most of the reported cyanide sensors are effectively used in organic solvents or organic/aqueous solvent mixtures having higher organic solvent fraction[24, 34-38]. A few of them[13, 39, 40] operate well in aqueous medium too. Here, L showed fluorescence response in aqueous medium having only 2% of DMF (volume percentage), which is beneficial for practical applications. The binding affinity of CN⁻ with L was quantified and the limit of detection was found to be below that proposed by WHO. The sensing knack of L towards CN⁻ was studied at different pH. The practical applicability of the probe was studied by detecting cyanide contents in natural samples such as apple seeds and cassava leaves.

2. Experimental

2.1. Materials and methods

All the chemicals used for the study were purchased from Sigma Aldrich or Alfa Aesar. The solvents were received from the chemical suppliers and were used without further purification. Tertiary butyl ammonium salts of different anions were used for the sensing studies.

Elemental analyses were carried out on VarioEL III CHNS analyzer. A Jasco FTIR 4100 spectrometer was used to record FTIR spectrum (4000-400 cm⁻¹) of the compound. ^{1}H NMR- and ^{13}C NMR

spectra were recorded on a 400 MHz Bruker Avance III spectrometer using DMSO-d6. Electron-Spray Ionization Mass Spectrum (ESI-MS) was recorded on Waters (UPLC- TQD) mass spectrometer. Fluorescence spectrum was recorded on an Agilent Technologies model Cary Eclipse fluorescence spectrophotometer.

2.2. Synthesis of Schiff base

8-Formyl-7-hydroxy-4-methylcoumarine (1) and 3-amino coumarine (2) were synthesized according to the procedures in the literature [41-43] and scheme of the reaction is depicted as Scheme 1.

3-Aminocoumarine (1 mmol, 0.161 g) was dissolved in hot ethanol in a round bottom flask. To the hot solution, ethanol solution of 8-formyl-7-hydroxy-4-methylcoumarine (1 mmol, 0.204 g) was added in drops with constant stirring. The resulting reaction mixture was refluxed for about 4h. The above mixture was concentrated to half its volume. The orange coloured compound obtained was filtered, washed with ethanol and dried. Yield: 88%. Anal. Calcd for $C_{20}H_{13}NO_5$: C, 69.16; H, 3.77%; N, 4.03%; Found: C, 68.72%; H, 3.52%; N, 3.94 %. IR (cm^{-1}, KBr): ν (O-H) 3429 cm^{-1}, ν (C=O) 1730 cm^{-1}, ν(C=N) 1611 cm^{-1}. ^{1}H NMR (400 MHz, DMSO d$_6$, δ (ppm)) δ: 10.44 (1H, s), 5.67 (1H, s), 2.41(s, 3H); 6.30-7.95 (aromatic protons), ^{13}C NMR (400 MHz, DMSO d$_6$, δ (ppm)) δ 191.37, 158.90, 155.15, 153.70, 147.86, 133.35, 125.36, 124.99, 124.77, 124.49, 121.73, 115.39, 113.55, 112.09, 111.09, 107.70, 18.33.; ESI MS (m/z): [M + H]$^+$: Calculated: 348.08, Found: 348.3

2.3. Sample preparation for fluorescence sensing studies

A 1 mM stocks solution of L was prepared in DMF. From the above solution, 20 µM solution (50 ml) was prepared in water and was used for the sensing studies. Using tertiary butyl ammonium salts, stocks solutions of different anions were prepared in DMSO. Sensing studies were carried out by adding 0.5 equivalent salt solutions of different anions to different test tubes containing 3ml 20 µM solution of L. Shaken of well and the fluorescence responses were recorded at room temperature.

Fluorescence titration was carried out by using 10 µM solution of L in water. 0 to 1.2 equivalent of cyanide ion solution was gradually added. Fluorescence response was recorded after each addition. Based on the titration profile, association constant was calculated using Benesi-Hildebrand equation. For the construction of calibration curve, a 50 µM solution of cyanide was gradually added to 10 µM solution of L. LOD was calculated from the slope of the calibration curve using the equation, $3\sigma/\text{slope}$, where σ is standard deviation. Competition studies were conducted by adding appropriate amount of solution of CN^- and other competing anion (0.5 equivalents) to 3 ml of 20 µM solution of L. Fluorescence spectra of the samples were recorded at room temperature. The effect of pH was also checked using HEPES buffer. The quantum yield, ϕ was calculated before and after the addition of CN^- to L using quinine sulphate as standard.

$$\frac{1}{(F - F_0)} = \frac{1}{K_a(F_{max} - F_0)} \; x \; \frac{1}{[M]^n} + \frac{1}{(F_{max} - F_0)}$$

where, F_0 and F are the fluorescence intensities of probe molecule in the absence- and presence of the analyte, F_{max} is fluorescence intensity at maximum concentration of analyte, $[M]$ is concentration of analyte and K_a is the association constant.

2.4. Preparation of natural samples

Cyanide ion was extracted from two natural samples, apple seeds and cassava leaves. The well dried apple seeds were powdered and the powder was sonicated with methanol. The methanol extract was used for the sensing studies. For extraction of cyanide from cassava leaves, well chopped leaves were boiled in water and the sensing studies were conducted with the aqueous extract.

3. Results and discussion

3.1. Structural characterization
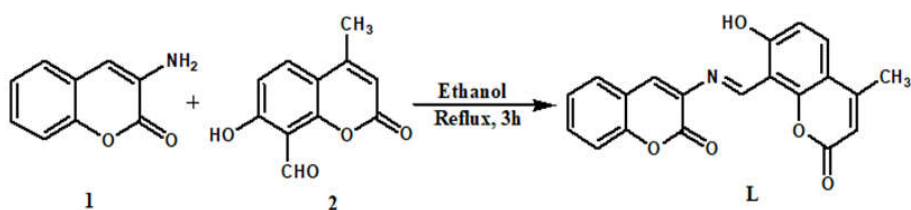
Scheme 1. Synthetic route of 8-(3-methyleneamino-2H-chromen-2-one)-7-hydroxy-4-methyl-2H-chromen-2-one (L)

8-(3-methyleneamino-2H-chromen-2-one)-7-hydroxy-4-methyl-2H-chromen-2-one, L was obtained by the condensation

reaction between 8-formyl-7-hydroxy-4-methylcoumarine and 3-aminocoumarine in ethanol. The synthetic route is given in the Scheme1. L was soluble in DMF, DMSO and acetonitrile. It was characterized by elemental analysis, IR- (Fig. 1), ^{1}H- NMR (Fig. 2) and ^{13}C NMR (Fig. 3) spectroscopic- and ESI-MS analysis (Fig. 4).

The elemental analysis data were close to the theoretically calculated ones. In the IR spectrum of L, the characteristic stretching frequency of–O-H appeared at 3429 cm^{-1} and that of –C=O appeared at 1730 cm^{-1}. The formation of imine bond was confirmed by the characteristic band appeared at 1611 cm^{-1}. In the mass spectrum, peak at (m/z) 348.3 (Calculated: 339.3) confirmed the formation of L. The formation L was again confirmed by ^{1}H NMR and ^{13}C NMR spectra.

Fig. 1. FTIR spectrum of L

Fig. 2. ^{1}H NMR spectrum of L in DMSO d$_6$

Fig. 3. ^{13}C NMR spectrum of L in DMSO d$_6$
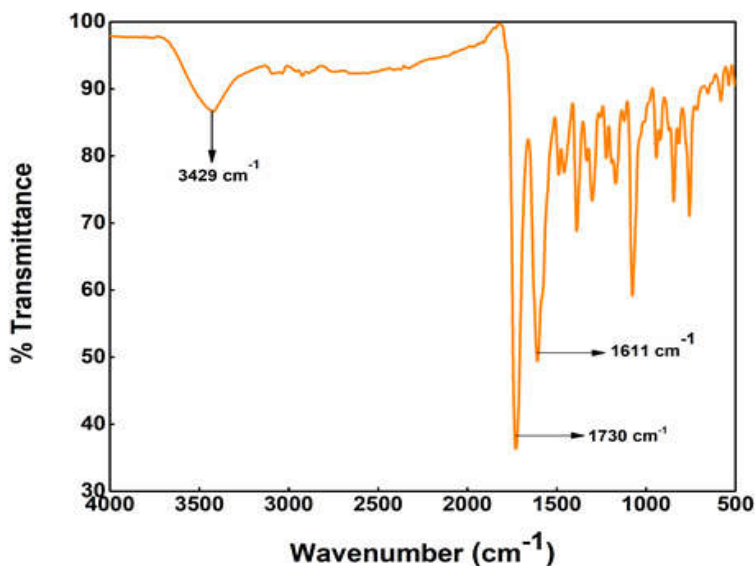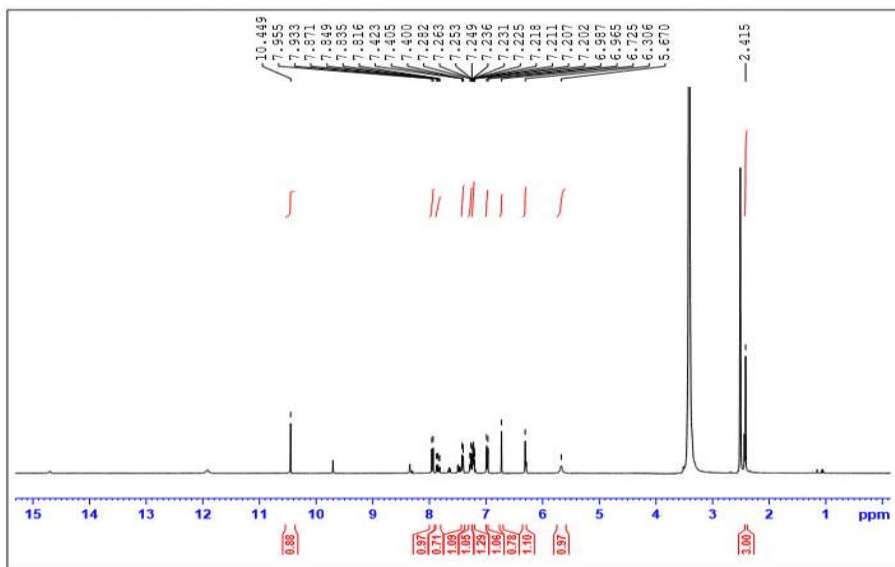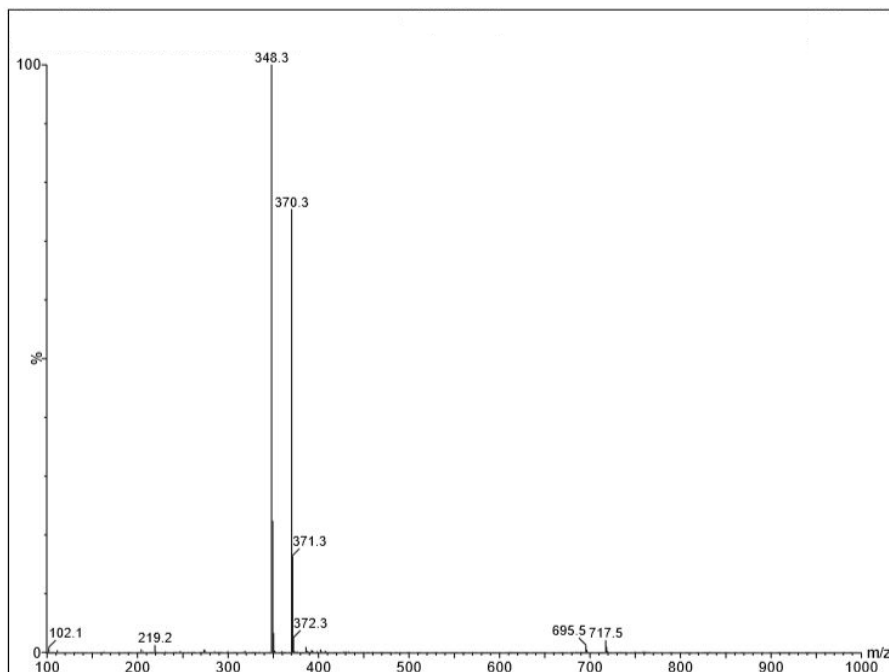
Fig. 4. ESI-MS (Positive mode) of L

3.2. Photophysical investigations

The fluorescence sensing ability of L was checked using a fluorescence spectrometer by adding tetrabutyl ammonium salt solution of anions like F^-, Cl^-, Br^-, I^-, CN^-, OH^-, OAc^-, NO_3^-, HSO_4^- and $H_2PO_4^-$ to the solution of L in water (2 % DMF). On exciting the solution of L at 360 nm, displayed a weak emission at 453 nm ($\phi = 0.003$). Imine based compounds are generally feebly emissive because of –C=N isomerization. The unbridged imine bonds exhaust a part of the excited state energy. Upon the addition of 0.5 equivalents of aforementioned solutions of anions to 20 μM solution of L, there were

no observable changes in the emission profile of L except with CN^- on exciting at 360 nm. The presence of CN^- induced a drastic fluorescence enhancement ($\phi = 0.011$) accompanied by a 10 nm blue shift in the emission spectral profile (Fig. 5). In consistent with the spectral change, the intensity of fluorescent emission enhanced in UV light.
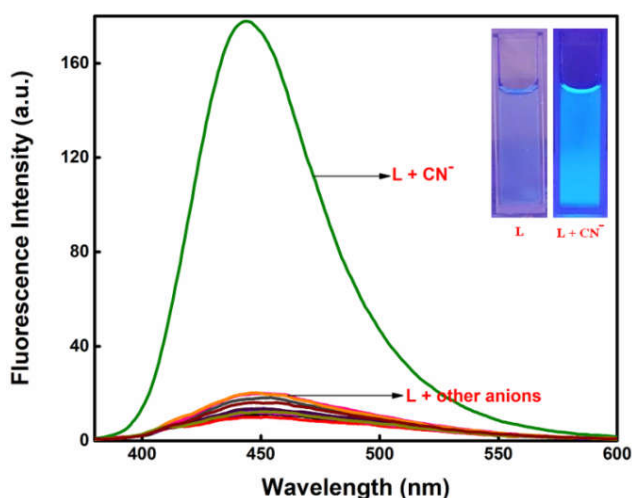
Fig 5. Fluorescent spectral changes of L (20 μM) in the presence of 1 equivalent various anions (F^-, Cl^-, Br^-, I^-, CN^-, OH^-, OAc^-, NO_3^-, HSO_4^- and $H_2PO_4^-$) in water, $\lambda_{ex} = 360$ nm (Inset : The colour of L and L+CN^- under UV lamp)

To get a quantitative information about the interaction between L and CN^-, fluorescence titration experiment was carried out. As depicted in Fig. 6, upon the addition of CN^- from 0 to 1.2 equivalents, the fluorescence intensity increased gradually accompanied by a blue shift in the emission maxima. On increasing the concentration of CN^-,

the emission intensity increased linearly up to 1.2 equivalents and thereafter it became constant.

To find out the binding stoichiometry between L and CN⁻, Job's plot analysis was carried out. Job's plot between the mole fractions of CN⁻ against the emission intensity pointed out that emission intensity reached its maximum at a mole fraction of 0.5 (Fig. 7). This observation is a clear indication of 1:1 binding stoichiometry between L and CN⁻. 1:1 binding stoichiometry was again conformed from ESI-MS analysis (Fig. 8). The observed peak at m/z = 520 (calculated m/z = 520) may be due to the formation of an adduct [L + CN⁻ + 2DMF + H] indicating the 1: 1 binding stoichiometry between L and CN⁻.
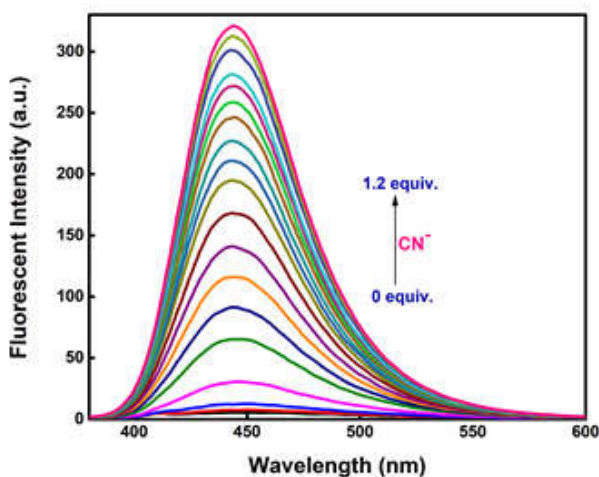
Fig 6. Fluorescence titration profile of L (10 μM) with CN⁻ (0 to 1.2 equivalents) in water (2 % DMF) on exciting at 360 nm.

To calculate LOD, a 50 µM cyanide ion solution was gradually added to 3 ml 10 µM solution of L in water. The emission intensity changed with concentration as shown in Fig. 9 (a) and was almost linear. From this linear plot, the LOD was calculated based on the equation, $3\sigma/K$, where, σ is standard deviation and K is the slope of the calibration curve. It was found to be 1.5 µM, which was below the WHO permissible cyanide content in drinking water (1.9 µM) [Fig. 9(a)]. By the use of Benesi-Hildbrand equation, the association constant of the complex formed was calculated as 3.31×10^4 M^{-1} [Fig. 9(b)].
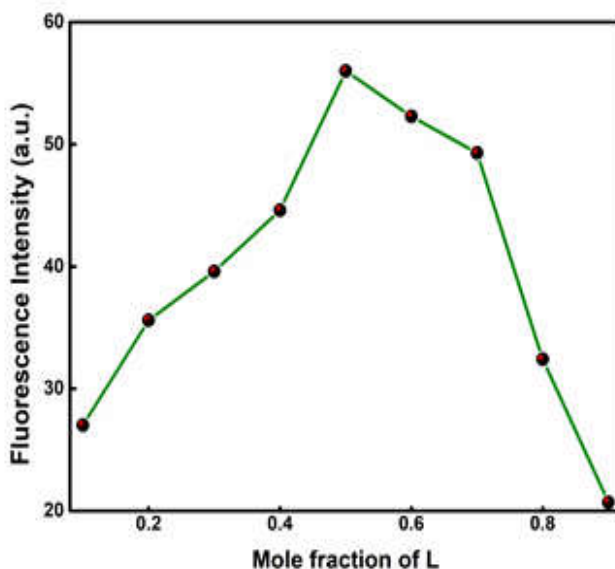
Fig 7. Jobs plot of L with CN$^-$
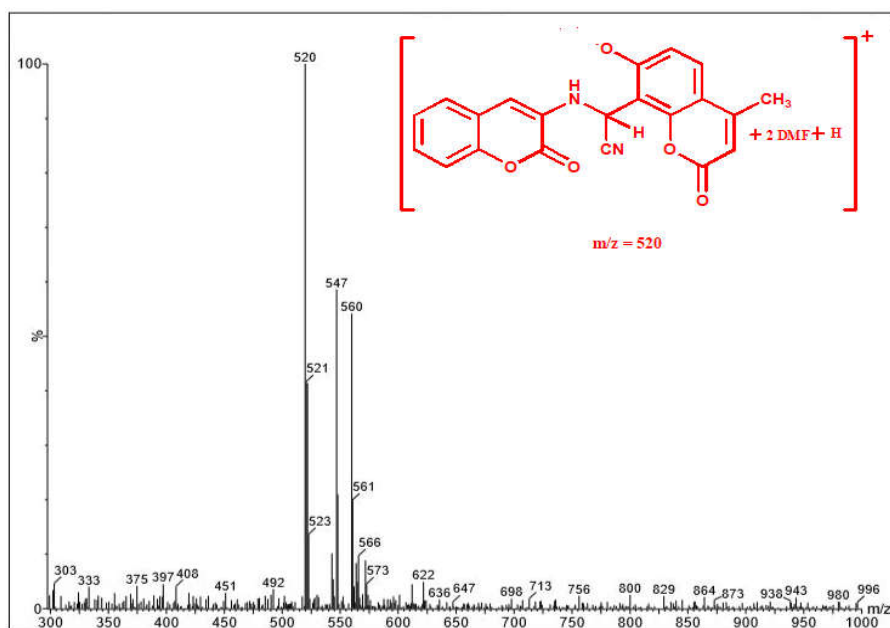
Fig. 8. ESI-MS spectrum of L with CN⁻
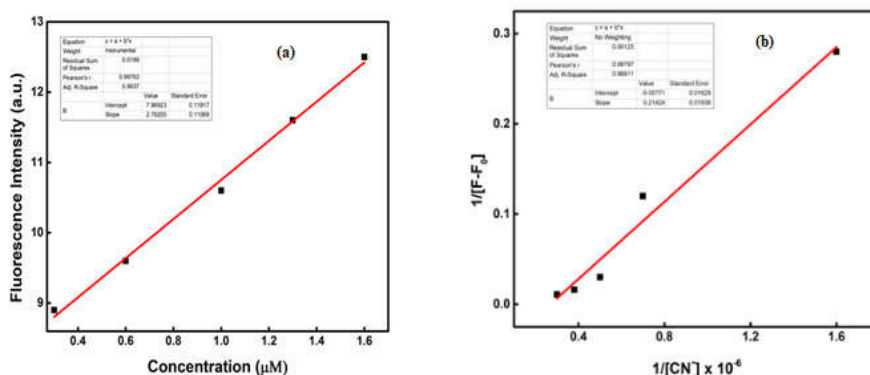
Fig. 9. (a) Calibration curve of L with CN⁻ for LOD calculation,
(b) Benesi-Hildebrand plot of L with CN⁻

To get an idea about the mechanism of cyanide ion sensing, conducted ^{1}H NMR titration in DMSO-d6 and the titration profile is shown in Fig 10. Cyanide ion solution was sequentially added as 0.1,

0.5 and 1 equivalents to a solution of L in 0.5 ml DMSO-d6. In free L, H_a proton (-O-H proton) appeared at 5.35 ppm. Upon the addition of different equivalents of CN⁻, there was no observable shift of -OH signal, indicating non-participation of –OH proton in cyanide ion binding. At the same time, two new peaks appeared at 3.15 and 5.51 ppm due to the H_d and H_c protons, respectively. This observation was attributed the nucleophilic addition of CN⁻ to the imine bond of the probe, L forming an adduct with strong fluorescent emission.
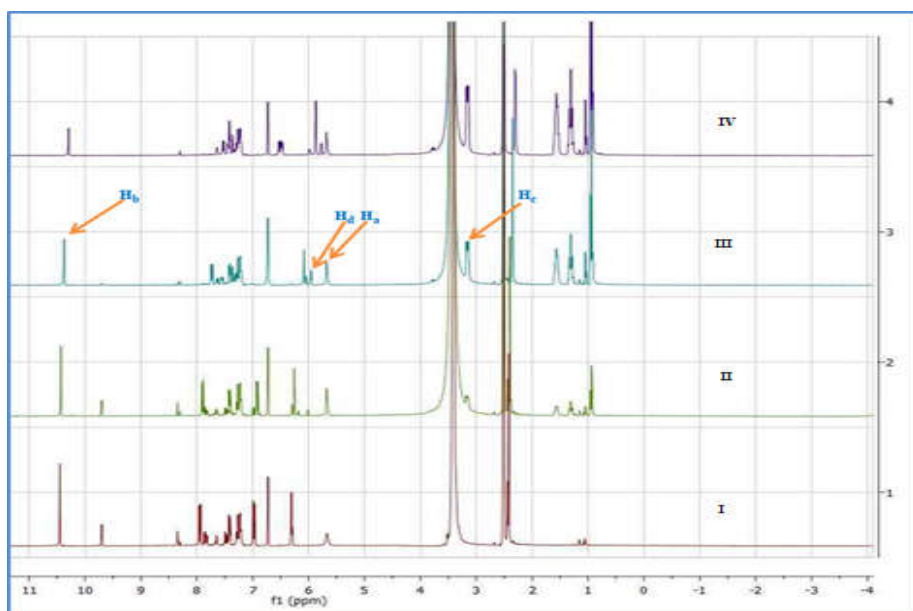
Fig. 10. ¹H NMR titration of L (I) with 0.1 (II), 0.5 (III) and 1(IV) equivalents of CN⁻

For getting more insight to the nucleophilic addition of CN⁻ to L, we compared the FTIR spectra of L before and after the addition of cyanide ion and are depicted in Fig. 11. The ν (O-H) appeared at 3429

cm^{-1} before and after the interaction with CN⁻. It divulged that -O-H proton remained unaffected by the cyanide addition. The ν –C=N, which appeared at 1611 cm^{-1} in free L, completely disappeared after the addition of CN⁻ indicating the cleavage of the imine bond. The presence of nitrile group was confirmed by the appearance of a new band at 2356 cm^{-1}. These spectral data together with the mass spectrum and ¹H NMR titration data supported the addition of cyanide ion to the imine carbon of L. The addition of CN⁻ to L is depicted in Scheme 2.
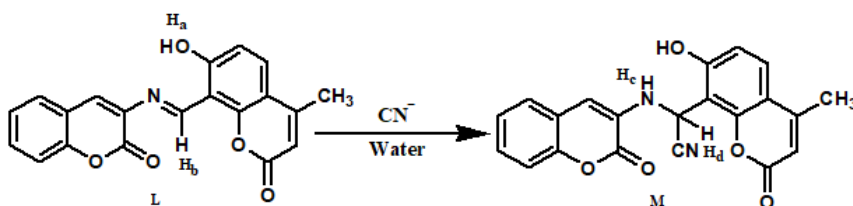
Scheme 2. Addition of CN⁻ to L
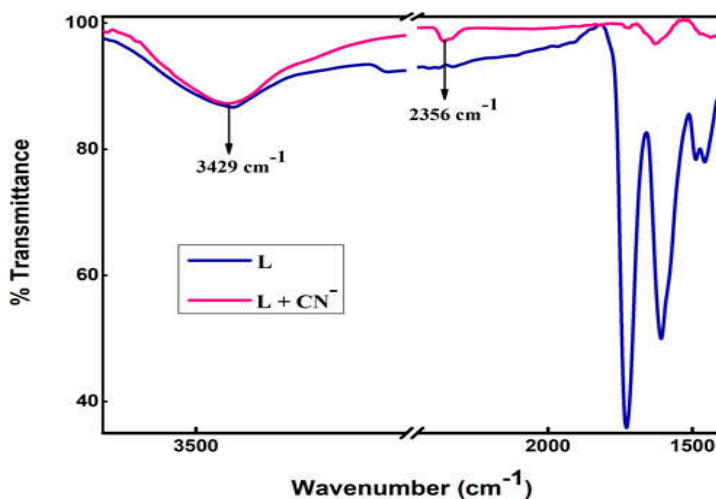
Fig 11. IR spectra of L and L with CN⁻

To explore the practical applicability of the probe, competition experiments were conducted. The observations are depicted in Fig. 12 and suggested that the other anions did not interfere in the detection of CN^- by the probe, L. The result divulged that L is good sensor for cyanide ion even in the presence other competing anions.
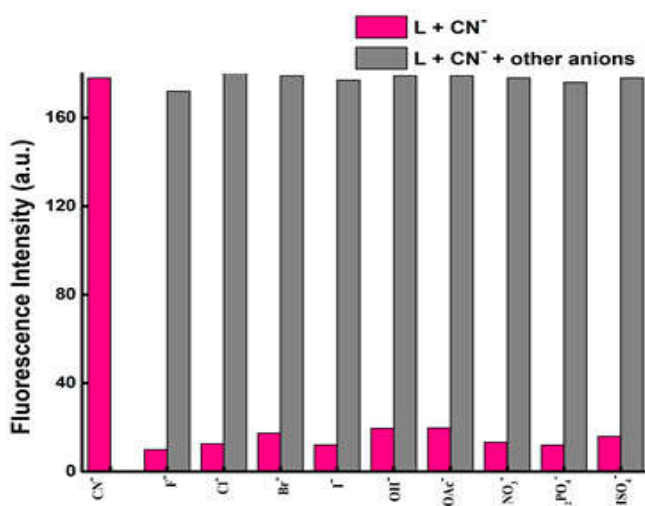
Fig. 12. Competition study of L (20 μM) with CN^- (0.5 equivalent) in the presence of other competing anions (0.5 equivalents) at an excitation wavelength of 360 nm.

The effect of pH on fluorescent emission of L before and after the addition of cyanide was checked using HEPES buffer and the responses are depicted in Fig 13. In acidic pH, both L and L+CN^- (M) did not exhibit any significant fluorescent emission because of the protonation of hydroxyl group. In basic pH, L and M formed phenoxide ions which are highly emissive entities. From the Fig. 13 it is clear that L is feebly emissive in basic pH. This is because in L, the deactivation channel, -C=N isomerization, diminishes the fluorescent

emission. At the same time, –C=N isomerization is absent in M. Formation of phenoxide ion is responsible for strong fluorescent emission in basic pH. In comparison with the previously reported CN⁻ probes which functioned in organic/aqueous medium, L exhibited comparatively good sensing response. The comparison was made based on the association constant, limit of detection and solvent used. The details are given in the Table 1.
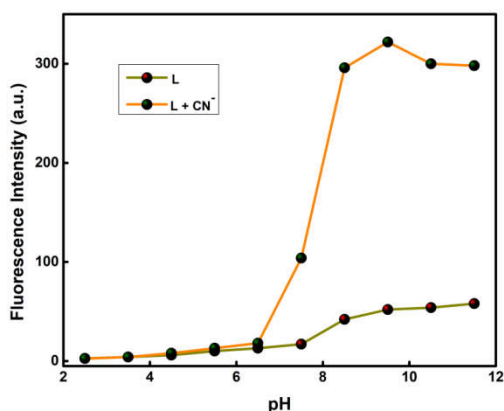
Fig. 13. Variation of fluorescent emission of L and L + CN⁻ (M) at different pH

Table No. 1: Comparison of sensing of L with the previously reported sensors

Probes	LOD	Medium (v/v)	Sensing response
Ref[18]	5.14×10^{-8}	DMSO/water (9:1)	Turn-on
Ref[13]	1.65×10^{-6}	DMSO:water (1:1)	Turn-on
Ref[44]	5.12×10^{-8}	DMSO:water (7:3)	Turn-on
Ref[24]	7.72×10^{-8}	DMSO:water (8:2)	Colourimetric
Ref[45]	8.32×10^{-7}	DMSO:water (9:1)	Turn-on
L	$\mathbf{1.5 \times 10^{-6}}$	**water (2 % DMF)**	**Turn-on**

3.3. Application of the probe on natural samples

We have examined the sensitivity of the probe on natural samples which contains cyanide ion and noticed an observable response. Two natural samples, apple seeds and cassava leaves were used for the study. An aqueous solution of L in 15 μM concentration was used for the study. As depicted in Fig. 14 (a), on increasing the concentration of the methanol extract of the apple seeds, the intensity of emission increased. We have also extended the applicability of the probe to detect cyanide content in cassava leaves. The aqueous extract of the cassava leaves was used for the sensing studies. As represented in Fig. 14 (b), the probe was responsive to the cyanide content in cassava leaves. The experiment was repeated with pure methanol and water and observed that these solvents have no significant effect on emission intensity. From the above observation it can concluded that the probe is useful for the detection cyanide ion in natural samples too.
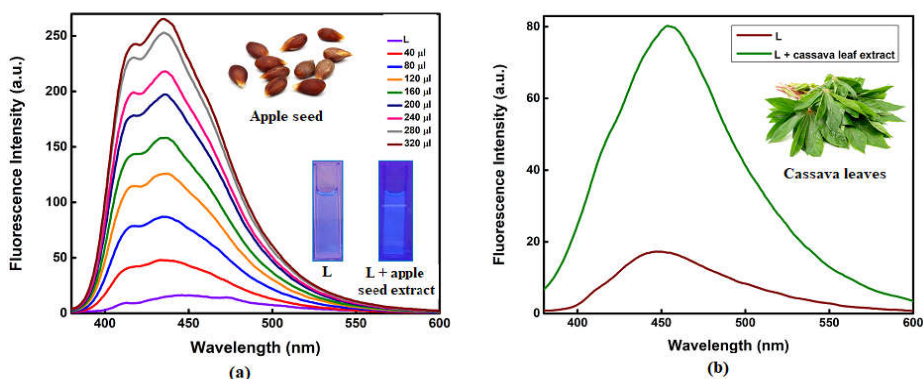
Fig. 14. Fluorescent response of L with cyanide content of natural samples (a) apple seeds and (b) cassava leaves

4. Conclusions

Synthesized and characterized a coumarin based Schiff base, 8-(3-methyleneamino-2H-chromen-2-one)-7-hydroxy-4-methyl-2H-chromen-2-one, L, which exhibited a selective fluorescent turn-on response towards cyanide ion. The mechanism studies divulged that the chemodosimetry is behind the cyanide ion selectivity. The unique nucleophilicity of cyanide ion leads its addition to the electrophilic imine bond. FTIR spectrum and mass spectrometric analysis together with ^{1}H NMR titration confirmed the operation of the nucleophilic addition reaction. Other anion didn't exhibit this kind of chemistry under the same experimental conditions. The competition studies indicated that other the anions didn't interfere in cyanide detection with the probe, L. The observed limit of detection was lower than that proposed by WHO. 1:1 binding stoichiometry was confirmed from Job's plot and mass spectrometric analysis. The cyanide detection was more pronounced in basic pH because of the formation of phenoxide ion. In acidic pH, protonation of the hydroxyl group diminishes the emission intensity. Further, the applicability of the probe for the detection of cyanide ions in natural samples was also exploited. The probe exhibited an observable response with the cyanide ion extracted from apple seeds and cassava leaves.

References

1. L. Shang, L. Jin and S. Dong, *Chemical Communications*, 2009, 3077-3079.

2. S.-Y. Chung, S.-W. Nam, J. Lim, S. Park and J. Yoon, *Chemical Communications*, 2009, 2866-2868.

3. C. R. Nicoleti, L. G. Nandi and V. G. Machado, *Analytical chemistry*, 2014, **87**, 362-366.

4. X. Cheng, Y. Zhou, J. Qin and Z. Li, *ACS applied materials & interfaces*, 2012, **4**, 2133-2138.

5. S. Vallejos, P. Estévez, F. C. García, F. Serna, L. José and J. M. García, *Chemical Communications*, 2010, **46**, 7951-7953.

6. Z. Xu, X. Chen, H. N. Kim and J. Yoon, *Chemical Society Reviews*, 2010, **39**, 127-137.

7. G. WHO, *ISBN*, **924**, 154460.

8. X. Chen, S.-W. Nam, G.-H. Kim, N. Song, Y. Jeong, I. Shin, S. K. Kim, J. Kim, S. Park and J. Yoon, *Chemical Communications*, 2010, **46**, 8953-8955.

9. Y. Shiraishi, S. Sumiya, K. Manabe and T. Hirai, *ACS applied materials & interfaces*, 2011, **3**, 4649-4656.

10. R. Badugu, J. R. Lakowicz and C. D. Geddes, *Journal of the American Chemical Society*, 2005, **127**, 3635-3641.

11. S. Kumar, P. Singh, G. Hundal, M. S. Hundal and S. Kumar, *Chemical Communications*, 2013, **49**, 2667-2669.

12. F. J. Baud, P. Barriot, V. Toffis, B. Riou, E. Vicaut, Y. Lecarpentier, R. Bourdon, A. Astier and C. Bismuth, *New England Journal of Medicine*, 1991, **325**, 1761-1766.

13. K. Rezaeian, H. Khanmohammadi and S. G. Dogaheh, *New Journal of Chemistry*, 2018, **42**, 2158-2166.

14. S. Sarveswari, A. J. Beneto and A. Siva, *Sensors and Actuators B: Chemical*, 2017, **245**, 428-434.

15. S. Goswami, S. Paul and A. Manna, *Dalton Transactions*, 2013, **42**, 10682-10686.

16. X. Huang, X. Gu, G. Zhang and D. Zhang, *Chemical Communications*, 2012, **48**, 12195-12197.

17. B. Shi, P. Zhang, T. Wei, H. Yao, Q. Lin and Y. Zhang, *Chemical Communications*, 2013, **49**, 7812-7814.

18. T.-B. Wei, J.-D. Ding, J.-F. Chen, B.-B. Han, X.-M. Jiang, H. Yao, Y.-M. Zhang and Q. Lin, *New Journal of Chemistry*, 2018, **42**, 1271-1275.

19. F. Wang, L. Wang, X. Chen and J. Yoon, *Chemical Society Reviews*, 2014, **43**, 4312-4324.

20. Y. Hao, K. H. Nguyen, Y. Zhang, G. Zhang, S. Fan, F. Li, C. Guo, Y. Lu, X. Song and P. Qu, *Talanta*, 2018, **176**, 234-241.

21. S. Saha, A. Ghosh, P. Mahato, S. Mishra, S. K. Mishra, E. Suresh, S. Das and A. Das, *Organic Letters*, 2010, **12**, 3406-3409.

22. K. H. Jung and K.-H. Lee, *Analytical chemistry*, 2015, **87**, 9308-9314.

23. G. J. Park, D. Y. Park, K.-M. Park, Y. Kim, S.-J. Kim, P.-S. Chang and C. Kim, *Tetrahedron*, 2014, **70**, 7429-7438.

24. Y.-L. Leng, J.-H. Zhang, Q. Li, Y.-M. Zhang, Q. Lin, H. Yao and T.-B. Wei, *New Journal of Chemistry*, 2016, **40**, 8607-8613.

25. L. Yang, X. Li, J. Yang, Y. Qu and J. Hua, *ACS applied materials & interfaces*, 2013, **5**, 1317-1326.

26. Z. Yang, Z. Liu, Y. Chen, X. Wang, W. He and Y. Lu, *Organic & biomolecular chemistry*, 2012, **10**, 5073-5076.

27. B. Sen, S. K. Sheet, R. Thounaojam, R. Jamatia, A. K. Pal, K. Aguan and S. Khatua, *Spectrochimica Acta Part A: Molecular and Biomolecular Spectroscopy*, 2017, **173**, 537-543.

28. J. Li, C.-F. Zhang, S.-H. Yang, W.-C. Yang and G.-F. Yang, *Analytical chemistry*, 2014, **86**, 3037-3042.

29. D. Ray and P. Bharadwaj, *Inorganic chemistry*, 2008, **47**, 2252-2254.

30. S. R. Trenor, A. R. Shultz, B. J. Love and T. E. Long, *Chemical reviews*, 2004, **104**, 3059-3078.

31. C. R. Nicoleti, L. G. Nandi and V. G. Machado, *Analytical chemistry*, 2015, **87**, 362-366.

32. F. Zelder and L. Tivana, *Organic & biomolecular chemistry*, 2015, **13**, 14-17.

33. W. Chen, Z. Zhang, X. Li, H. Ågren and J. Su, *RSC Advances*, 2015, **5**, 12191-12201.

34. K. Wang, L. Ma, G. Liu, D. Cao, R. Guan and Z. Liu, *Dyes and Pigments*, 2016, **126**, 104-109.

35. T. Wei, H. Li, Q. Wang, G. Yan, Y. Zhu, T. Lu, B. Shi, Q. Lin and Y. Zhang, *Supramolecular Chemistry*, 2016, **28**, 314-320.

36. B. Yu, C.-Y. Li, Y.-X. Sun, H.-R. Jia, J.-Q. Guo and J. Li, *Spectrochimica Acta Part A: Molecular and Biomolecular Spectroscopy*, 2017, **184**, 249-254.

37. X. Zhou, X. Lv, J. Hao, D. Liu and W. Guo, *Dyes and Pigments*, 2012, **95**, 168-173.

38. S. Madhu, S. K. Basu, S. Jadhav and M. Ravikanth, *Analyst*, 2013, **138**, 299-306.

39. Y. Zhang, D. Li, Y. Li and J. Yu, *Chemical Science*, 2014, **5**, 2710-2716.

40. F. Huo, J. Kang, C. Yin, J. Chao and Y. Zhang, *Sensors and Actuators B: Chemical*, 2015, **215**, 93-98.

41. H. Von Pechmann and C. Duisberg, *Berichte der deutschen chemischen Gesellschaft*, 1883, **16**, 2119-2128.

42. V. K. Gupta, N. Mergu, L. K. Kumawat and A. K. Singh, *Sensors and Actuators B: Chemical*, 2015, **207**, 216-223.

43. A. A. Kudale, J. Kendall, C. C. Warford, N. D. Wilkins and G. J. Bodwell, *Tetrahedron letters*, 2007, **48**, 5077-5080.

44. J.-H. Hu, Y. Sun, J. Qi, P.-X. Pei, Q. Lin and Y.-M. Zhang, *RSC advances*, 2016, **6**, 100401-100406.

45. Q. Lin, L. Liu, F. Zheng, P.-P. Mao, J. Liu, Y.-M. Zhang, H. Yao and T.-B. Wei, *RSC advances*, 2017, **7**, 38458-38462.

PART II

AGGREGATION INDUCED EMISSIVE ORGANIC

LUMINOGEN FOR PICRIC ACID SENSING

CHAPTER 7

INTRODUCTION

The study of light emitting behavior of an organic luminophore in the solid- or aggregated state has wide attention among the research community[1, 2]. Most of the luminophores exhibit high fluorescence efficiency in dilute solutions (here the molecule is in an isolated state) and their efficiencies either completely quench or diminish in the aggregated or solid state, which hinder their practical application in organic light emitting diodes (OLEDs), photovoltaic cells and optical sensors[3, 4]. Molecules have an intrinsic tendency to aggregate in concentrated solution or in solid state and formation of excimers and exciplexes lower their fluorescence efficiency. This type of quenching due to high concentration, discovered by Froster in 1954, commonly referred to as aggregation caused quenching (ACQ) is a major threat of luminescent materials. According to Brick, mentioned in his classic book *Photophysics of Aromatic Molecules*, molecules are very close in the aggregated state and result an intermolecular π-π stacking interaction between the adjacent aromatic rings[5]. The excited states of these aggregates non-radiatively return back to the ground states, resulting a decrease in fluorescence efficiency in the aggregated state. ACQ is very common in luminescent material and to tackle this effect of luminophores, numerous chemical, physical and engineering approaches have been put forward by various groups, but they have limited successes[6-8]. The discovery of inorganic quantum dots overcame the difficulties of luminescent materials to some extent, but they are associated with tedious synthetic route, cytotoxicity and limited variety[9, 10].

1. Aggregation induced emission/ aggregation induced emission enhancement – an outline

In 2001, Tang and coworkers[11] noticed an interesting photophysical property in an organosilicon compound (Hexaphenylsilole). They observed that this compound was non-emissive in good solvent but started to emit bright green fluorescence upon aggregation and this unique phenomenon was termed as Aggregation Induced Emission (AIE), which was just reverse of the common ACQ effect. The luminoges which exhibit AIE property are termed as AIEges. Another feature of aggregated luminogens, Aggregation Induced Emission Enhancement (AIEE), similar to the AIE, was reported in 2002 by Park *et al*[12]. AIEE active luminogens are feebly emissive in the isolated state and their emission enhance in the aggregated state. The beauty is that, the destructive molecular aggregation of conventional luminophore becomes a constructive effect in AIEgens. Tang *et al.*[13] very meaningfully quoted that *aggregation induced emission: The whole is more brilliant than the parts*. Attracted by this fascinating property of AIE/AIEE active luminogens, a variety of AIE/AIEE luminogens have been reported from various parts of the world[14-17]. Later, the detailed theoretical and experimental studies proved that the restriction of intramolecular motion (RIM) is the main mechanism behind the enhanced emission of the organic luminogens in their aggregated- or in solid state. The clear understanding of structure - property relationships helps to construct new structural motif with fascinating properties. The discovery of the novel AIE/AIEE phenomenon was a breakthrough in technological

innovations and intensive efforts have been made by various groups to develop functional materials with excellent emission behavior.

The introduction of the AIE property bright up the technological application of luminescent materials in optical and optoelectronic devices such as OLEDs, organic field effect transistor, photovoltaic cell and organic lasers, since in most cases luminescent material used are in thin film form. The AIEgens plays an inevitable role in biological field including bioimaging, therapy and diagnosis. The chemosensing response of this class of compounds has been explored to detect various environmentally and biologically important analytes such as cations, anions, explosives, amino acids and so forth. Now the research community is trying to apply this esteemed behaviour of organic luminogen into fingerprint and forensic investigations. A few reports are available in literature[18-20]. Because of these fundamental and technological applications, a large number of papers have been published from various parts of the world[21-25].

The AIE/AIEE behaviour of luminogens can be investigated by various analytical tools, of which the most common one is fluorescence spectroscopy. UV-Visible spectroscopy, Time resolved fluorescence spectroscopy, scanning electron microscopy contribute valuable information to support the fluorescence spectral data of AIEgens. Generally, molecular aggregates are prepared by reprecipitation method[26]. In this method, the luminogen in a good solvent is rapidly injected to a mixture of good solvent and poor solvent under sonication and immediately recorded the fluorescence

emission profile. In most cases, water is used as poor solvent. By varying the volume ratio of good solvent to poor solvent, the emission behavior is studied. The higher fraction of the poor solvent induces aggregation of the luminogen forming two type of nanoparticles. The crystalline particles enhance the fluorescence efficiency and amorphous particles diminish the emission intensity. Fluorescence life time is an important parameter to estimate AIE/AIEE behavior. It is the time spend by a fluorophore in the excited state before returning back to the ground state. The increasing life time of a fluorophore in the aggregated state divulges its AIE/AIEE behavior.

2. Premiere of AIE/AIEE

The abnormal emission behavior of hexaphenylsilole (HPS) (Fig. 1) observed by Tang and coworkers[11] in 2001 was a breakthrough in luminescent material research. In the routine thin layer chromatographic (TLC) test during the synthesis of HPS by silylation they observed interesting properties. The HPS was non-luminescent in the wet condition and upon evaporation of the solvent, a green spot appeared on the TLC plate under UV light. Later, detailed study of this unusual phenomenon was conducted. HPS was non-emissive in a good solvent, acetonitrile and upon the addition of a poor solvent, water into its solution in acetonitrile, intense emission was observed. In poor solvent, organic molecules tend to aggregate and form suspension of nanoparticles. This means, HPS is emissive in the aggregated state and Tang *et al*. termed this phenomenon as aggregation induced emission. This investigation excited researchers and large number of AIEgens

with various fluorophores have been reported. The mechanism behind the intense emission of AIE/AIEEgens. Their applications in optoelectronic devices, as chemical sensors etc. are dynamic research areas of today.
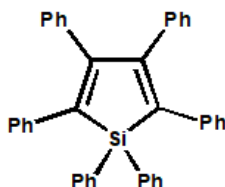
Fig. 1. Hexaphenylsilole (HPS)

Later, Park *et al.*[12] reported a compound, 1-cyano-1-trans-1,2-bis-(4'-methylbiphenyl)-ethylene (CN-MBE) (Fig. 2.) which was feebly emissive in dilute solution. They prepared fluorescent nanoparticle by reprecipitation method which exhibited intense emission. The emission intensity was about 700 times higher than the emission in solution state. They concluded that the emission enhancement was due to the synergetic effect of intramolecular planarization and J-type aggregation of nanoparticles. The fluorescence switching behavior of CN-MBE nanoparticles towards organic vapours was also tested.
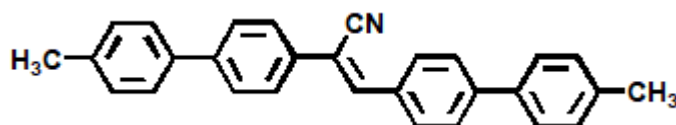
Fig. 2. 1-Cyano-1-trans-1,2-bis-(4'-methylbiphenyl)-ethylene (CN-MBE)

3. Progress of AIE/AIEE research

The identification of luminescent behaviour of HPS encouraged the scientific community to study the properties of the other group 14 metalloles. They are substituted metallacyclopenta-2,4-dienes, they are analogous of furan, pyrrole and thiophenes. The groups of Braye's and Leavitt's[27, 28] in 1959 reported the synthesis of Group 14 metalloles. They were given only a little attention at that time. However, later the reports of their electronic and spectroscopic properties made them inevitable candidates for a variety of applications[29-31]. Among them, siloles are the most studied one. By virtue of high electron mobility, siloles are used to make electron transport layer or emissive layer in the construction OLEDs. The high hole mobility efficacy of siloles prompted their application in solar cells and organic field effect transistors (OFETs)[32-34]. Nevertheless, this class of compound acquired much attention after the report of AIE property of HPS. Many siloles, germoles and stannoles showed remarkable AIE characteristic. Siloles, especially the aryl substituted siloles are the most attractive candidate[35-37]. Various groups reported the use of siloles as chemical sensors for the detection of analytes like organic vapours, explosives and DNA[38-40]. Silole containing polymers exhibit interesting emission behavior in their aggregated state and are used for OLEDs and for other thin layer device applications. Sohn *et al*[41] reported the AIE behavior of polytetraphenylsilole and they observed a 17.8 time's fluorescence emission enhancement in 99:1 water/THF system when compared with the polymer in a good solvent, THF. Tang[42] reported a number of silole incorporated polymers prepared by copolymerization

under Sonnogashira condition but their enhancement stopped at 60-70% water. Later, large number of silole embedded polymers was prepared and their utility in various areas were investigated.

Exciting progress has been made in AIE/AIEE research and various classes of AIEgens, including different types of hydrocarbons[43, 44], heteroatom containing hydrocarbons[45, 46], organic ion pairs[47], π-gelators[48], dendimers[49], metal organic frameworks[50], metal complexes[51], and a variety of polymers[52] having promising applications were reported. A large number of AIE/AIEE active linear, branched and cross linked polymers with outstanding applications in electronic devices such as polymer light emitting diodes and as fluorescent chemosensors for explosives, organic vapours, metal ions and biomolecules have been reported[53-55]. Red emitting AIE materials have been explored by various research groups. They emit from red to near infra red (NIR) region, so the excitation is possible with radiation in the visible region. The excitations in the visible region avoid the harmful effect of the frequently used UV radiation on biological samples. Dendrimers are another class of AIEgen widely explored by various groups. Organic-inorganic hybrid frameworks termed as metal organic frameworks (MOFs) received great research attention because of their versatile functions. MOFs have indispensible role in luminescent material research like OLEDs, luminescent sensors, etc. It is an emerging class of AIEgen and few reports are available in literature. Metal complexes are another fast growing variety of AIEgen, which contribute tremendous variety of fluorescent and phosphorescent materials in the aggregated and solid state. Combing

with the AIE behavior, this category of compounds can emit radiations covering in the entire visible- and NIR region. Boron complexes of π-conjugated chelates are another important class of luminescent materials, which display AIE/AIEE property. The active research efforts contributed large variety of AIEgens with exciting applications as biological probes, chemical sensor, optoelectronic systems and as stimuli responsive materials. AIEgens are generally considered as organic version of inorganic semiconductor quantum dots. The molecular diversity, structural tunability and biological compatibility are the superior features of AIEgens over the inorganic semiconductor quatum dots.

4. Common mechanism of AIE/AIEE

Fundamental science tells that any movement, both macroscopic and microscopic, consumes energy. In molecules, molecular rotation and molecular vibrations dissipate energy. Many conventional planar aromatic luminogens are highly emissive in dilute solutions and upon aggregation their fluorescence efficiency either quenches or completely vanishes. In planar aromatic molecule, due to π-electron conjugation, bonds have a partial double bond character, hence restriction of molecular motion have a slight role for ACQ effect in the aggregated or in solid state. However, upon aggregation the molecules are packed well resulting a π-π stacking interaction between the adjacent aromatic rings. This π-π stacking interaction prompts the formation of excimers and results in a fluorescence quenching effect. In molecules with a twisted geometry with a dihedral angle greater

than zero, there is no π-electron delocalization and hence intramolecular motions are very active in dilute solution. On absorbing radiation of particular wavelength by the electrons, the molecular motion (both rotation and vibration) dissipates the excited state energy and electrons non radiatively return back to the ground state. In the aggregated or solid state, due physical constraints, molecular motions are arrested and the molecule radiatively decays to the ground state. Hence, together with restriction of intramolecular motion (RIM), molecular rigidity and conformational flexibility have a decisive role on enhanced emission of luminogens in the aggregatged- or in solid state[56].

The restriction of molecular motions including restriction of intramolecular rotation (RIR) and restriction of intramolecular vibration (RIV) are the main mechanism behind the intensified emission of luminogens in their aggregated- or in solid state[57]. The other most common mechanisms, such as J-aggregation[58], twisted intramolecular charge transfer (TICT)[59, 60], excited state intramolecular proton transfer (ESIPT)[1, 61], etc., are also reported. However, there is no common mechanism applicable to all systems and each mechanism is applicable only to a specific system.

The role of RIM on AIE/AIEE can be verified by various experimental methods. The RIM process greatly depends on the viscosity of the medium, experimental temperature and pressure and thus, the effect molecular motions on fluorescent emission of AIEgens can be studied by varying the viscosity, temperature and pressure[62]. On

increasing viscosity of the medium, the molecular motions get arrested to some extent resulting in a strong fluorescence emission. Generally, glycerol, a highly viscous solvent (934 cP at 25˚C) is used to study the viscosity effect. Lowering of temperature, especially cryogenic cooling, enhances the fluorescence efficiency since molecular motions will be arrested at low temperature. The dynamic NMR spectrum recorded at various temperatures also provide valuable information about AIE/AIEE behavior. Pressure also has a significant effect on molecular motions. At higher pressure, molecules are in close proximity and hence the molecular motions are hindered leading to intense radiative emission. However, in some cases at higher pressure, an antagostic behavior is observed, i.e., on increasing pressure, emission intensity is reduced. When pressure is high, there is large chance for the formation of excimers through π-π stacking interaction, reducing the emission intensity. Thus, the effect of molecular motion on fluorescent emission can be predicted by increasing solvent viscosity and lowering experimental temperature. In some systems, the effect of pressure also supports the above experimental fact[63].

5. ESIPT active Schiff bases as AIE/AIEEgen

AIE/AIEE active Schiff bases are an important class of luminogens and have considerable attention because of their simplicity in synthesis. It is possible to design suitable structural motif by introducing rotatable moieties in their structural frameworks. Generally, organic molecules, including Schiff bases bearing an intramolecular hydrogen bonding between an electron donor

(-OH or –NH$_2$) in ortho position to the electron acceptors (–C=N or –C=O), exhibit the interesting phophysical process, ESIPT. They considerably enhance the fluorescence efficiency of organic luminogen in the solid- or in the aggregated state[64-66]. The ESIPT phenomenon was first coined in 1950 by Waller[67] in salicylic acid. ESIPT is an ultrafast reversible four level photophysical process (E→E*→K*→K), which occurs in femtosecond to picosecond (10^{-15} – 10^{-12}) time scale and mediated by intramolecular H-bonding[68]. Generally, in the ground state, the enol form (E) of an ESIPT compound is more stable and the keto form (K) is stable in the excited state. Both forms are stabilized by intramolecular H-bonding. The photoexcitation alters the electron distribution of enol form leading to an increase the acidity of the hydrogen bond donor and basicity of the hydrogen bond acceptor in the excited state of the ESIPT fluorophore. Subsequently, the ultrafast enol to keto tautomerization ($K_{ESIPT} > 10^{12}$ S^{-1}) occurs, i.e. the excited enol form (E*) rapidly gets converted to excited keto form (K*)[69]. Radiative deactivation happens from the excited keto form to the ground state, resulting ESIPT emission[70-72]. The reverse proton transfer from the ground keto form (K) generates the original enol form (E). The diagrammatic representation of four levels of ESIPT process is shown in Fig. 3.

The transient four level phototautomerization processes alter the electronic properties, such as electron distribution, energies of the electronic state and dipole moment of the fluorophre. Because of this transient change in the electronic properties, ESIPT emission is more sensitive to the environmental conditions, like nature of solvent.

Generally, in ESIPT fluorophores, emission can arise either from E*/K* or from both states depending upon the substituents, nature of solvent polarity and viscosity. The emission from E* with normal stocks shift is known as enol emission and a large Stocks shifted emission that occurs from K* is known as ESIPT emission. In protic or polar solvents, the intermolecular H-bonding between the fluorophore and the solvent molecules interrupts the ESIPT process and exhibits only the enol emission. The ESIPT emission is observed in hydrocarbon or non-polar solvents[72-75]. The unique feature of ESIPT luminogens is their large Stock's shift (~200 nm) without self-absorption as compared with other fluorophores. The striking feature is that the emission can be tuned by proper structural design of the fluorophore[76-79].

Fig. 3. Diagramatic representation of four level ESIPT process

The ultrafast photophysical ESIPT process along with the large stocks shift of ESIPT compounds can be applied in various fields including, UV photostabilizers, laser dyes, OLEDs, chemical sensors, fluorescent imaging, solar concentrators, optical and luminescent material, molecular probes and molecular logic gates, etc[80-84]. The unusual white light emission capability in the entire visible region is a prime attraction of the ESIPT fluorophore because white light production is a challenging task using conventional fluorophores. Usually, white light emission is achieved by mixing two or more organic fluorophores. However, with ESIPT fluorophores it can be acquired by a single molecule with better colour selectivity and reproducibility[79, 85, 86]. The innovative optoelectronic applications of ESIPT fluorophore have been limited mainly because of the concentration quenching and sensitivity of ESIPT fluorophores to the surrounding environment. The invention of AIE/AIEE luminogens helped to overcome these challenging issues and opend a new avenue to apply organic luminogens in optoelectronic devices like OLEDs, solar concentrators and molecular logic gates in the thin film or solid forms. The intensive research of various groups have proved the applicability of ESIPT process in the enhancement of luminescence behaviour and thereby established its practical application in the form of solid or as thin film[77, 87-89].

6. Contribution of AIE/AIEE active Schiff bases – A brief

Yang and coworkers[90] reported three new heterocyclic Schiff's bases derived from triphenylamine and benzimidazole scaffolds. Based

on the crystal structure, SEM and DLS analysis, the homogeneous particles formed in the aggregated state responsible for the AIE characteristic in THF-Water mixture. One of them able to sense Cr^{3+} and Al^{3+} through fluorescence turn-on signalling mechanism in HEPES buffer solution. The chelation enhanced fluorescence (CHEF) is mechanism behind the selective sensing. Kathiravan *et al.*[91] reported AIE of a pyrene Schiff base, 4-[(pyren-1ylmethylene)amino]phenol (Fig. 4) and its antimicrobial property. Hydrogen bonding of the imine bond with water suppressed the photoinduced electron transfer (PET) and thereby molecular motions are arrested, which has led to a radiative emission. This was proved by nanosecond transient absorption studies. In addition, antimicrobial- and bioimaging studies were also conducted.

A pyrene appended Schiff's base, 1,3-bis-((E)-pyrene-1-ylmethyleneamino)propane-2-ol (Fig. 5), was synthesized by Sinha *et al*[92]. The AIEE property of the compound was studied in DMF/water mixture. Its quantum yield varied from 0.034 to 0.450 from solution to the aggregated state. The photovoltaic effect of the luminescent molecule was checked by preparing a thin film of the compound. The solar cell using this generated a current of 4.4 mA/6.29V under illumination.
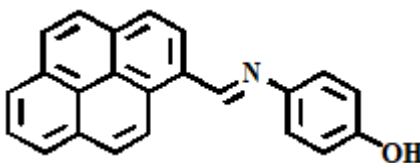
Fig. 4. 4-[(pyren-1ylmethylene)amino]phenol
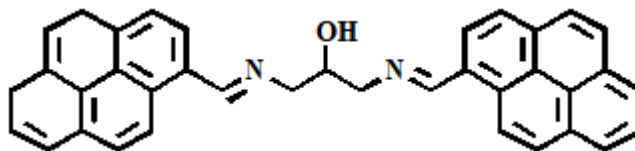
Fig. 5. 1,3-bis-((E)-pyrene-1-ylmethyleneamino)propane-2-ol

Zhou *et al.*[93] reported three Schiff's bases containing phenylbenzoxazole, which exhibited AIEE in THF-water mixture. The report concluded that in THF-water mixture with low water fraction, the molecular particles were slowly aggregated in to a crystalline fashion and became feebly emissive. In THF-water mixture having higher water fraction, the particles abruptly agglomerated in an amorphous fashion and strong emission occurred because of the absence of π-π stacking. Yang *et al.*[90] reported a Schiff base, which exhibited AIE phenomenon. The non-emissive Schiff base in THF started to emit on the addition of water and a 37 fold emission enhancement was recorded when the water fraction reached to 80% (volume percentage).

Moon *et al.*[94] reported two ESIPT compounds, which displayed AIEE in solid state. The metastable nanoparticles emitted white light. One of them produced a yellow fluorescence (λ_{max} = 535 nm) and other one emitted greenish-yellow colour (λ_{max} = 525 nm) in solid state. The white light emitting nanoparticles of these Schiff bases got converted to that the bulk material with time. Morphological studies of these aggregated particles of the Schiff base revealed that the spherical soft nanoparticles got converted to the hard nanoparticles with time.

These nanoparticles, displayed blue and yellow or greenish yellow fluorescence, respectively, with phenoxybenzonitrile and salicylidene units. In the presence of Cu^{2+}/Co^{2+} metal ions, the fluorescence of the salicylidene unit of the metastable nanoparticles was quenched. Thus, these two compounds displayed solid state fluorescence and form white fluorescent metastable nanoparticles in water.
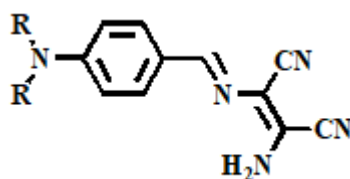
Fig. 6. Basic skeleton of diaminomaolnonitrile based Schiff

Two diaminomaolnonitrile based Schiff bases (Fig. 6) having donor-acceptor structure exhibiting AIE property were reported by Dong e*t al.*[95]. The AIE properties of these compounds were studied in THF-water mixture. On increasing the water fraction, their emission intensity enhanced with a red shift and reached a maximum value at higher water fraction. Similarly, the fluorescence quantum yield also increased at higher water fraction. Restriction of molecular motion is the reason for the emission enhancement. On increasing the water fraction, solvent polarity will be increased, which induced ICT process and thereby a red shift in the emission maxima was observed. By controlling the aggregate formation, their emission can be tuned from yellow to red region. Mechanochromic properties of the AIEgens were also explored. The applicability of the probe for bioimaging was also studied.

Zhou *et al.*[96] synthesized six D-π-A model carbazole Schiff base derivatives having basic skeleton as depicted in Fig. 7 with various terminal functionalities and investigated their emission properties. The structure - property relationship was investigated based on the UV-Visible and fluorescence spectra and theoretical calculations. The results revealed that all the six compounds showed intramolecular charge transfer responsible for the optical properties. The non-emissive or weekly emissive luminogen in pure acetonitrile solution, displayed strong emission in acetonitrile/water system. SEM analysis revealed the morphology of the aggregated particles. Cytotoxic tests and bioimaging studies of these compounds were also explored.
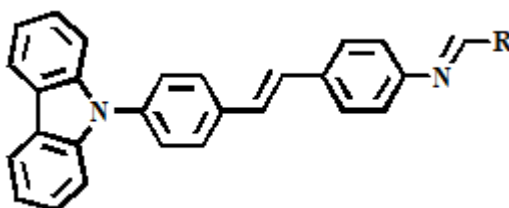
Fig. 7. . Basic skeleton of carbazole Schiff basederivatives

An AIE active photochromic compound, 4-(1,2,2-triphenylvinyl)aniline salicylaladehyde hydrazine was reported by Li *et al*[25]. This compound displayed AIE property in ethanol/water mixture. The enhanced emission was mechanistically explained with the help of RIR and ESIPT. The reversible photochromic behaviour, i.e., the colour and fluorescence change of the molecule upon UV irradiation were revealed and observed a good fatigue resistance. The

photochromic features made this compound a promising material for erasable photo-patterning application.
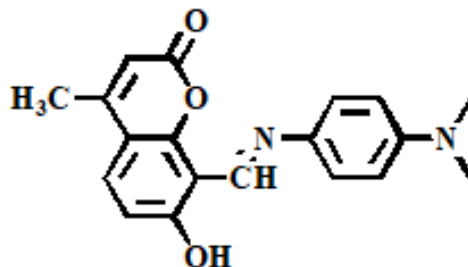
Fig. 8, 8-((4-diethylamino-2-ylimino)methyl)-7-hydroxy-4-methyl-2H-chromen-2-one

A coumarin based red fluorogen (Fig. 8) with AIE property was reported by Qi *et al*[97]. The solvatochromic property of the compound was also studied. In pure DMF solution, it was weakly emissive. In a mixture of water/DMF system (from 10% to 40% of water fraction), the emission intensity decreased slightly with a red shift of the emission maximum. When water fraction was higher than 40%, the emission maximum red shifted from 540 nm to 640 nm together with an enhancement in the emission intensity. This observation was explained on the basis of twisted intramolecular charge transfer (TICT) and ESIPT. The observed stokes shift, 245 nm was very high.

Zhou *et al.*[98] reported eight triphenylamine substituted styrene Schiff's bases having basic skeleton as shown in Fig. 9. They had various terminal functionalities and all of them displayed different AIE or ACQ behaviors in THF/water mixture. The crystallographic studies

of these compounds revealed that the formation of excimers and π-π interactions were thorny obstacles for fluorescent emission, while J-aggrgation and secondary interactions like, C-H…π, C-H…N, C-H…O, C…O and N…O between adjacent and same molecules blocked the molecular rotations and thereby induced fluorescence emission. The combinations of these two opposite interactions were responsible for the AIE characteristics of a few of these compounds and ACQ behavior of the remaining. These observations revealed that structural variations (molecular packing and molecular interactions) have a vital role in the photophysical properties of the organic luminogens.
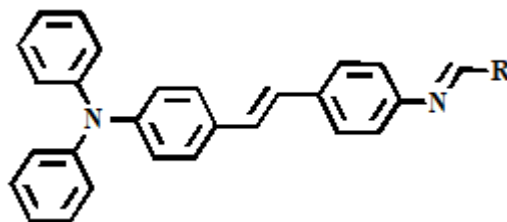
Fig. 9. Basic skeleton of triphenylamine based Schiff bases
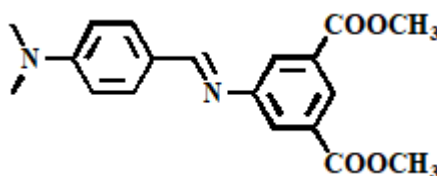
Fig. 10. (E)-Dimethyl-5-((4-(diethylamino)-2-hydroxybenzylidene)amino)isophthalate

Photoluminescent behavior of dimethylaminophenol functionalized Schiff base (Fig. 10) was reported by Han *et al.*[99] based on the mechanism of crystallization induced emission enhancement (CIEE). Certain AIEgens exhibit enhanced emission intensity in their crystalline state when compared with the amorphous state. It was feebly emissive in amorphous phase but showed strong emission upon crystallization, which was confirmed by spectroscopic and fluorescence microscopic methods. The fluorescence emission was sensitive to molecular packing. In strong alkaline medium, the fluorescence of the amorphous form got switched on and in acetic acid vapors it got switched off. The protonation and deprotonation were further confirmed by ^{1}H NMR and UV-Visible spectroscopy. This stimuli responsive fluorescence is applied for security printing and data storage technologies.

7. AIE/AIEE active chemosensor

Aggregation induced emissive fluorothores displayed promising advancement in the detection of various analytes including ions, carbohydrates, aminoacids, DNA, proteins, gases, explosives etc[100-102]. Tang and coworkers[54] developed hexaphenylsilole based AIE active CO_2 sensor. It worked based on the formation of carbamate ionic liquid. The introduction of two amino functionalities to the above compound enabled it to detect nitroaromatics *via* fluorescence quenching of the aggregated particles. Upon structural modification, the above sensor displayed a turn on fluorescence response toward cyanide ions in aqueous solution. Thus, by proper structural

modification, it is possible to tune the selectivity of the probes towards various analytes.

Molecular rotors dissipate the excited state energy of AIE active fluorophores. On suppressing the rotation through molecular rotors, strong emission can be achieved. Schiff bases, the imine functionalized compounds, function as fluorescence sensors for various guest molecules by suppressing the –C=N isomerization *via* complexing through the imine bond in solution state. This strategy for the detection of analytes is also applicable to Schiff bases in their aggregated state. Together with this complexing behavior, restriction of molecular motion in the aggregated state makes the Schiff bases promising AIEgens for the detection of various analytes.

Das *et al.*[103] developed an AIE active fluorophore that displayed a turn-on fluorescence response toward Al^{3+} in methanol-aqueous HEPES buffer (5 mM, pH 7.3, 9:1, v/v). Naked eye detection was possible with the compound due to its bright yellow green fluorescence under UV light. The other metal ions did not interfere with the turn-on response of compound with Al^{3+}. The applicability of the probe for fluorescence cell imaging using HeLa cells was also investigated. The L-Al^{3+} bound complex facilitates the tracking of interactions of DNA in solution. Das and coworkers[104] reported another AIEgen, which exhibited fluorescence sensing toward Zn^{2+} and Al^{3+} and a colourimetric response towards Cu^{2+} and F^-. The AIE behavior of the probe was studied in methanol-water mixture and an emission was observed at 525 nm on exciting at 390 nm. The

observed turn-on fluorescence response of the probe towards Zn^{2+} and Al^{3+} in 9:1 methanol-HEPES buffer (5 mM, pH 7.3) was due to the triggered AIE activity. A colourimetric response of the compound with Cu^{2+} was observed in buffer medium and with F^- was observed in acetonitrile solution. Theoretical explanations for the interactions between the reported compound and analytes were also explored.
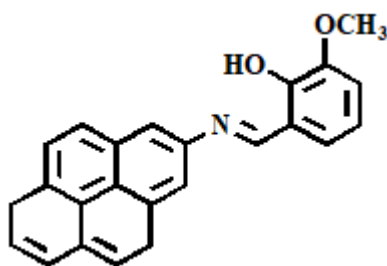
Fig. 11. 3-Methoxy-2-((pyren-2ylimino) methyl)phenol

Misra and coworkers[105] reported a pyrene based Schiff's base, 3-methoxy-2-((pyrene-2-yl-imino)methyl)phenol (Fig.11) and explored its AIEE property. This compound showed a turn-on response towards Al^{3+} with a 200 fold enhancement in acetonitrile solution. Chelation enhanced fluorescence was responsible for this emission enhancement. With excess of Al^{3+}, probe displayed a dramatic enhancement in emission intensity due to the aggregate formation. The binding stoichiometry, LOD, reversibility of the probe and effect of pH were well established. The AIEE property of the compound was studied in acetonitrile/water system by varying the percentage of water. The compound formed a well defined rod-shaped one

dimensional microcrystals in aggregated state and exhibited optical waveguide effect.

Tong *et al.*[106] reported a fluorescence probe for thiols. It worked by selective cleavage of a bond of the probe, generating salicylaldehyde azine. Upon the addition of cysteine to an aqueous solution (10 mM PBS buffer at pH 7.4 containing 30% DMSO) of the probe, a turn-on fluorescence response was observed at 558 nm. For practical application of the probe, fluorescence test paper strip was developed. The study was also extended to detect thiols in serum samples.
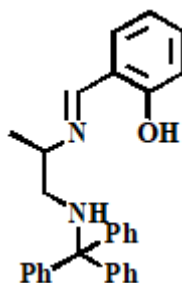
Fig. 12. Structure of [2-(2-(Tritylamino)ethylideneamino)methylphenol]

A multifunctional AIE active molecule, 2-((-tritylamino)ethylideamino)methyl)phenol (Fig. 12) was prepared by Laskar *et al.*[107] by reacting N-tritylethane-1,2-diamine and salicylaldehyde. The mechanoluminescence and the selectivity of the probe towards Zn^{2+} were also studied. The AIE property was examined in methanol/water mixture. The emission intensity was found to increase with increasing the water fraction from 0% to 50% with small

red shift in the emission profile. As the water fraction increased above 50%, the emission intensity decreased. The mechanism of AIE was explained with RIR and also with J-aggregation. The compound exhibited an irreversible mechanoluminescence property by changing its colour from blue to green (λ_{max} 445 nm to 512 nm) upon grinding. On applying pressure on this compound the same colour change occurred (blue to green) in a reversible manner. The reversible colour change was again possible by lowering the temperature to that of liquid N_2. The probe exhibited a turn-on blue fluorescence response with Zn^{2+} upon exciting at 365 nm. The detection limit was observed in the parts per million level.

Sensitive and selective detection of fluoride ion was achieved by Laskar *et al.*[108] by the use of an AIE active salicylaldehyde based Schiff's base. The AIE activities in the aggregated state (methanol/water mixture) as well as in the solid state were due to the J-aggrgation of the particles. Together with this, ESIPT played an active role. The compound also exhibited mechanofluorochromic property, i.e. its color changed from yellow to greenish-yellow upon grinding. The compound exhibited selective fluorescence response toward F^- without the interference of the other anions. The binding stoichiometry, detection limit, mechanism of selectivity and the effect of pH were also studied. A theoretical support was also given to the experimental facts.

Hui *et al.*[109] reported a thiosemicarbazone based Schiff base having AIEE property and its application in Hg^{2+} detection. The AIEE

characteristic of the compound was studied in DMSO/water system and an intense emission was observed at a water fraction of 70%. On the addition of Hg^{2+}, this compound exhibited a selective fluorescence quenching response in DMSO/water (9:1, v/v) buffered with tris-HCl (pH 7). The limit of detection was observed as 0.97 µM. It revealed the applicability of the compound for Hg^{2+} detection at very low concentration. The mechanism of selectivity and stoichiometry of binding were studied. The competition experiments were also conducted. The applicability of the probe for the detection of Hg^{2+} in real samples was also accounted.
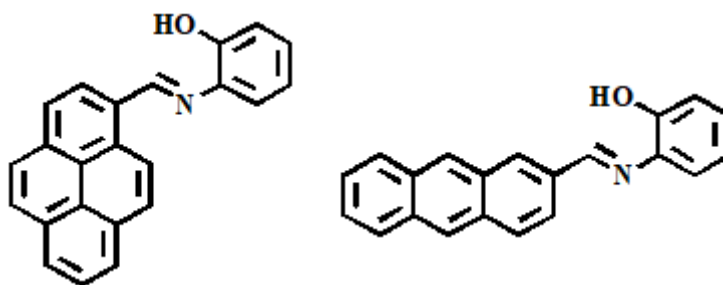
Fig. 13. Structure of pyrene and anthracene derived Schiff bases

Two Schiff bases, one based on pyrene moiety, and the other based on anthracene moiety, (Fig. 13) were reported by Lin *et al.*[110]. The fluorescence sensing ability of these probes towards various metal ions and their AIE properties were examined. The pyrene based Schiff base exhibited a turn-on response towards Cu^{2+} in acetonitrile. The anthracene based Schiff base displayed a turn-on response towards Fe^{3+} in THF. These turn-on responses are due to the chelation enhanced fluorescence. These compounds can be used to detect respective metal ions (Cu^{2+} and Fe^{3+}) in a wide range of pH (1-14 and

2-14). The binding stoichiometry, association constant and mechanism of binding were also well established. The AIE study was conducted using water as a poor solvent. Pyrene based Schiff's base showed intense emission at a water fraction of 80% and anthracene based Schiff's base exhibited maximum fluorescence at a water fraction of 60%. In both cases, high quantum yields further confirmed AIE behaviors of these compounds. The main mechanism behind the emission enhancement was RIR. The H-bond formation, suppression of PET, charge transfer and intramolecular charge transfer are the other mechanisms responsible for the AIE characteristic. The shift in the emission maxima (either blue or red shift) was originated due to the suppression of twisted intramolecular charge transfer.

Yang *et al.*[23] reported a bis-schiff base, having an AIE activity. Its selectivity towards Hg^{2+} was also well established. AIE property was investigated in THF/water mixtures having different water fraction. The compound was non-emissive compound in THF. It displayed maximum intense emission in THF/water mixture having 40 % water content. On further increasing the percentage of water, the emission intensity decreased due to the presence of insoluble particles. Restriction of molecular motion in the aggregated state was responsible for the radiative emission. The optical response of the compound with Hg^{2+} was investigated in THF, THF-water mixture and in living cells also. The visual colour changes both under day light and UV light together with UV-Visible and fluorescence spectral responses revealed the selectivity of the probe for the detection of Hg^{2+}. The limit of detection and competition studies also supported the applicability of

the probe for the detection of trace amount of Hg^{2+}. The good biocompatibility and low toxicity of the compound contributed to its use for detecting Hg^{2+} in living cells.

8. AIE/AIEE of salicylaldehyde azines

The activation of restriction of molecular motion (RIM) process is the main strategy in the development of new AIEgens. Organic fluorophores having rotatable C-C, C-N and N-N single bonds are subjected to various kinds of molecular motions, like, rotational and vibrational motions, which consume their excited state energy. In the aggregated- or solid state, these molecular motions are arrested and thereby radiative emission occurs. Thus, fluorophores having rotatable single bonds are utilized to develop AIEgens with intriguing properties. The design and synthesis of these types of molecules acquired more research interest. Salicylaldehyde azines display ESIPT together with intriguing AIE/AIEE characteristic which empower the efficacy of this class of compounds and attest their indispensable role as solid state luminescent materials. In the molecular state of this type of luminogens, the molecular motions (rotations or vibrations) impede the ESIPT process and thus, they are weak in emission. Molecular motions are restricted by forming aggregates or in solid state and this open a door for ESIPT process, resulting an enhancement in emission intensity. However, the ESIPT process does not fully support the enhanced emission in the aggregated state. The large stokes shifts of ESIPT compounds improve the quantum efficiency of the AIEgens

without any self absorption. This is the prime attraction of this class of compounds which makes them promising fluorescent materials.
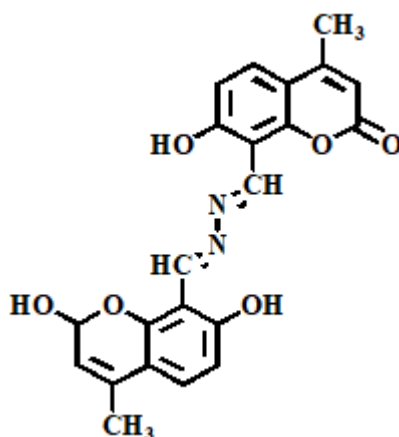
Fig. 14 (a) 8,8′-((1E,10E)-Hydrazine-1,2-diylidenebis(methanylylidene))bis-
(7-hydroxy-4-methyl-2H-chromen-2-one)
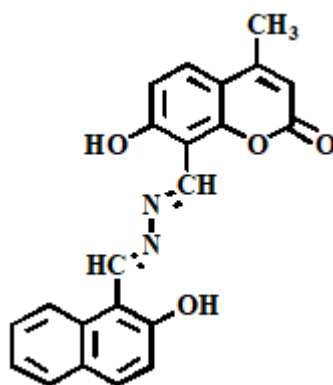
Fig. 14 (b) 7-Hydroxy-8-((E)-((E)-((2-hydroxynaphthalen-1-yl)-
methylene)hydrazono)methyl)-4-methyl-2H-chromen-2-one

Wang *et al.*[111] reported two novel AIE active coumarine Schiff bases [Fig. 14 (a) & (b)] and their fluorescence imaging studies. Both

of these compounds form nanoparticles in a mixture of good- and poor solvent. The former displayed a reddish orange fluorescence and the later emitted saffron yellow fluorescence in their aggregated states. The compounds showed larger Stokes shifts. The applicability of these compounds to fluorescence cell imaging was also explored

Ouyang *et al.*[112] reported 4 different donor substituted paraphenylene derived AIEgens with basic skeleton depicted in Fig. 15. They were prepared by condensing paraphenylene diamine with substituted- and unsubstituted salicylaldehydes. These 4 reported derivatives, depending on the terminal electron donor groups, emitted different colours (green, yellow and orange) by assuming four different morphologies in THF/water mixture. Upon altering the water fraction, 4-hydroxy substituted AIEgens emitted various colours ranging from green → yellow → orange. This report highlights one of the strategies to tune of emission colours of ESIPT compounds and is valuable in luminescent material research.
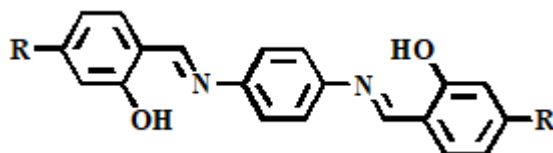
Fig. 15. Basic skeleton of paraphenylene derived Schiff base
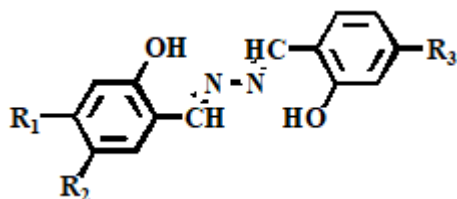
Fig. 16. Basic skeleton of salicylaldehyde azine

Tong *et al.*[113] reported a series of AIEE active salicylaldehyde azines having basic skeleton depicted in Fig. 16. Their colours varied from green to red depending on the substituents on the backbone. Azine without any substitution led to a yellow emission (λ_{max} = 542 nm). A green emission (λ_{max} = 513 nm) was observed with electron donating –OH group at the fourth position of azine. Chlorine substitution led to long wavelength red emission (λ_{max} = 570 nm) in ethanol/water system. The AIEE active probe was explored for the detection of hydrazine in water. Benzophenone azine (Fig. 17) was reported by Tong *et al.*[89], exhibiting AIE characteristic. It exhibited polymorph-dependent ESIPT fluorescence. The discussions showed that restriction of molecular motion together with ESIPT were the main mechanism responsible for the AIE behavior. This compound displayed solid state emission which was tuned with annealing or melting treatments. It showed good stability and reproducibility. This report conveyed a new strategy for the synthesis of stimuli responsive materials and their importances in real world applications.
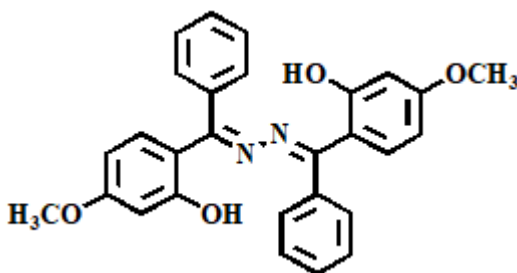
Fig. 17. (2-Hydroxy-4-methoxyphenyl)(phenyl)-methanone azine

Fan *et al.*[114] reported a simple Schiff base, by condensing N,N-bis(salicylidene)-p-4,4-diaminobiphenyl with salicylaldehyde (Fig. 18) moiety. It exhibited AIE property. Its applicability for the selective detection of Al^{3+} in the aggregated state was studied. It was also used to detect Al^{3+} in living cells. The detection limit was found to be 0.4 μM with minimum interference from other common competitive metal ions. The Job's plot analysis, ^{1}H NMR and FT-IR spectral analysis supported the selective response of the probe, which was due to the restriction of molecular rotation and also due to the rigidity of molecular assembly. The compound exhibited good biocompatibility and therefore, can be used to detect Al^{3+} in living cells.
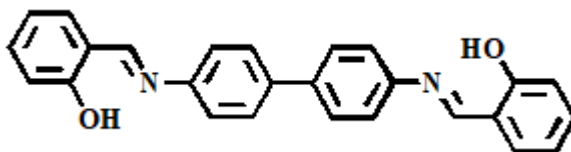
Fig.18. N,N-bis(salicylidene)-p-4,40-diaminobiphenyl

Misra *et al*[115]. reported a salicylaldehyde azine Schiff's base, 1-(2-hydroxynapthylmethylene)-2-3-(3-methoxy-2-hydroxybenzylidene) hydrazine, (Fig. 19). It exhibited turn-on fluorescence response towards Zn^{2+} in DMF/Water system. The selective response was found to be based3 on its CHEF/AIEE features. But at higher water fraction, the probe work based on AIEE effect. Zn^{2+} ions triggered AIEE activity of the probe through individual emission signals. The aggregated particles arranged in one dimensional rod shaped microcrystals and showed pronounced optical waveguide effect. The binding stoichiometry and interference studies on Zn^{2+} sensing were

evaluated and the intensity of emission was almost stable in the pH range of 6 - 9. The AIEE mechanism were well established from fluorescence anisotropy, DLS, SEM, optical fluorescence microscope, time resolved photoluminescence and fluorescence reversibility studies.
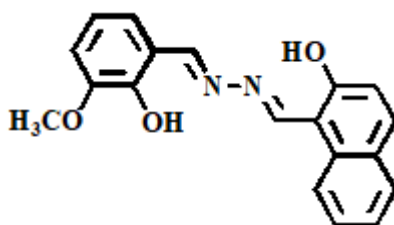
Fig.19.1-(2-Hydroxynapthylmethylene)-2-3-(3-methoxy-

2-hydroxybenzylidene)hydrazine

9. AIE/AIEEgens as optical probes for nitroaromatics

Explosives are major threat to environment and human life in terms of their destructive nature and toxicity. For national security issues and environmental concern, it is highly desirable to develop suitable methods for the detection of explosives. Common methods adopted for the detection of explosives include gas chromatography, mass spectrometry, surface enhanced raman spectroscopy, ion mobility spectrometry, etc. They require expensive instrumental facilities[116-118]. The fluorescence based sensing methods offer high sensitivity and selectivity. Moreover, such methods have other merits such as simplicity, rapid response, cost effectiveness and naked eye detection[119, 120].
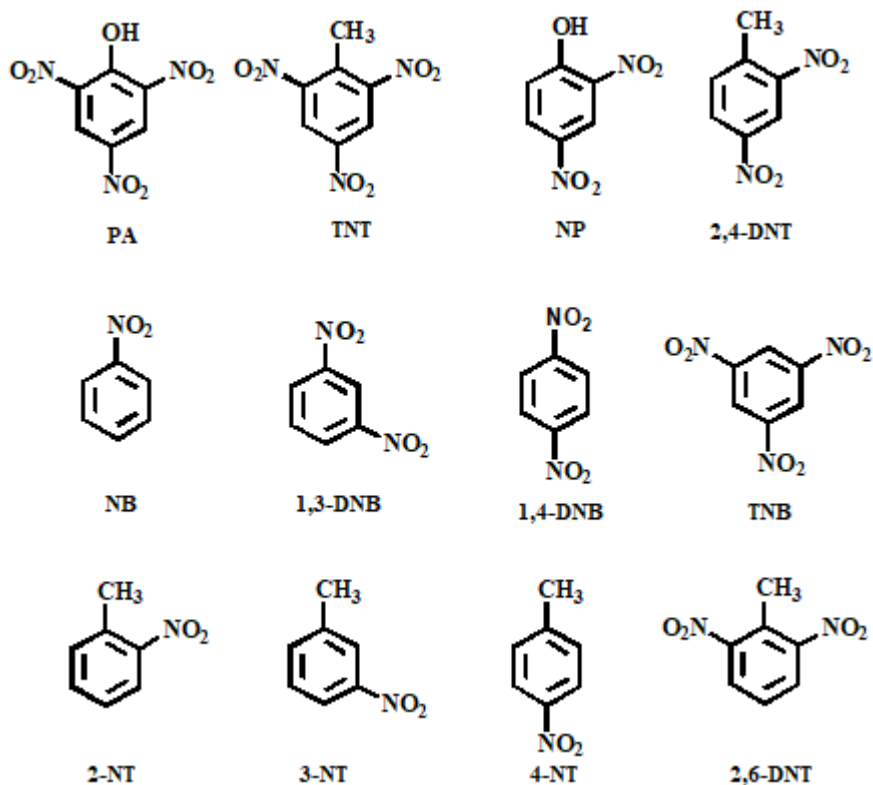
Fig 20. Chemical structures of various nitroaromatic explosives

Nitroaromatics, commonly used explosives, are a benzene ring functionalized compounds having various numbers of nitro groups. The chemical structures of various nitroaromatics are shown in Fig 20. Because of their moderate vapour pressures and low reactivity, it is difficult to detect them. Among the various nitroaromatics, 2,4,6-trinitrophenol (TNP) or picric acid (PA) is a superior explosive and a main constituent of industrial explosives and landmines[121]. PA has crucial roles in chemical, pharmaceutical, dye and leather industries. Compared to other nitroaromatics, the high solubility of PA

results in its contamination in soil and ground water. Its exposure causes several health problems such as skin irritation, anemia, headache and various respiratory issues[122-124]. Therefore, it is highly desirable to detect the PA using conventional fluorophores with remarkable photophysical response[125-127].

The neutral nitroaromatic species are electron deficient in nature and thereby quench the fluorescence of the luminogens. This quenching response can be quantified with the help of fluorescence spectroscopy. The fluorescence based detection is not only possible *via* fluorescence quenching but also through fluorescence enhancement, spectral shift and in terms of life time measurement. The nitroaromatic acceptor forms complex with donor fluorophore. Photoinduced electron transfer from the donor to the acceptor is responsible for the change in the photphysical properties of the fluorophore. These changes can be monitored with the help of UV-Visible or fluorescence spectroscopy[128-130].

Among the various types fluorephores, AIE/AIEE active ones are having considerable attention as sensory materials for the selective detection of nitroaromatics. Aggregation induced emission endue the majority of organic fluorophore with an amazing emission behaviour in aqueous solution. This makes these molecules are efficient fluorescence sensors to detect various analyte, including nitroaromatics in aqueous medium. AIE/AIEE active simple organic fluorophores as well as conjugated polymeric materials are widely employed as

sensing materials for nitroaromatics detection[131-133]. However, simple molecule based nitroaromatic sensors are scarce in literature.

Bhalla and coworkers[134] reported petacenequinone derivative which formed fluorescent nanoaggregate in THF/water mixture. Its working mechanism was aggregation induced emission enhancement. The detection of various nitroaromatics was carried out in THF/water mixture having a water fraction of 90% and it was found that the fluorophore was more sensitive to PA. The detection was possible *via* fluorescence quenching. The quenching response was studied using Stern-Volmer plot. Detection of PA in solid state was also possible using TLC plate and test paper strip coated with the fluorophore.

Hang *et al.*[135] reported two traizine derivatives which exhibited fluorescence emission in the aggregated and in solid state because of their aggregation induced emission behavior. The AIE behavior in THF/water mixture was used for the detection of picric acid. These triazine based compounds exhibited excellent performance for the detection of PA with a quenching constant of 10^7 M^{-1} and very low detection limit of 15 ppb, and therefore, these are good fluorophores for the detection of PA.

Shanmuggam and coworkers[136] designed and synthesized a novel tetraphenylethene-2-pyrone conjugate. It exhibited aggregation induced emission enhancement in THF/Water mixture. The fluorescent nanoaggregate was used to detect nitroaromatics. The fluorescence titration with nitroaromatics was achieved using nanoaggregates of the probe in THF/water mixture having a water fraction of 90%. The

incremental addition of PA to the nanoaggregate led the quenching of fluorescence of the aggregate. The quenching efficiency was studied using Stern-Volmer equation. In addition, fluorescent test paper strip was also developed for the detection of PA in solid state.

Patil *et al.*[137] reported a fluoranthene-tetraphenylethene conjugated luminogen which displayed aggregation induced blue shifted emission. The nanoaggregate of the compound in water/THF medium exhibited promising fluorescence response towards various nitroaromatics, especially PA. The quenching response of the nanoaggregate of luminogen with PA was studied by Stern-Volmer equation and observed favourable limit of detection. The fluorescence quenching took place *via* photoinduced electron transfer through static quenching mechanism. The detection was also possible with solid state test paper strip method.

Misra and coworkers[138] explored the selective sensing ability of a pyrene based Schiff base (Fig. 21). By controlling the ratio of water, this compound exhibited AIE activity by emitting intense cyan fluorescence with well defined morphologies. The detection of nitroaromatics was studied using fluorescent hydrosol of the compound in higher water content. Together with the low detection limit and high Stern-Volmer constant, naked eye detection of trace amount of PA was successfully achieved *via* fluorescence quenching of the hydrosol of the compound. Solid state detection was also accomplished by developing fluorescent test paper strip.
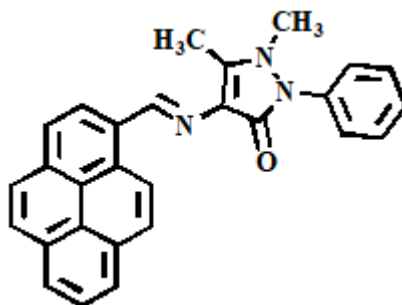
Fig. 21. 4-((Pyren-1-yl)methyleneamino)-1,2- dihydro-

2,3-dimethyl-1-phenylpyrazol-5-one

10. Conclusions

The discovery of aggregation induced emission behaviour of organic luminogens was utilized in many technological areas, especially in optical- and optoelectronic fields. Because in most of the optoelectronic devices such as OLEDs, organic field effect transistor, photovoltaic cell and organic lasers, luminescent materials are used in the form of thin film form. The AIEgens play an inevitable role in biological fields including bioimging, therapy and diagnosis. The chemosensing response of this class of compounds has been explored to detect various environmentally- and biologically important analytes such as cations, anions, explosives, amino acids and so forth. The promising features of AIEgens attracted various research groups and the active research in this area leads to many technological innovations. Application AIE/AIEE active polymers for the detection of nitroaromatics including picric acid are available in literature.

However, nitroaromatic sensors based on simple organic molecules are scanty in literature.

11. Significance and scope of the present investigation

Aggregation induced emission or aggregation induced emission enhancement of organic luminogens helped to overcome the difficulties associated with the conventional fluorophores. These types of compounds are used in many technological areas. Their high fluorescence efficiency in the solid state is highly beneficial in optoelectronic devices, where the fluorescent material is used in the form of thin film. Chemosensors based on the AIE/AIEE behaviour received much attention because most of them exhibit high emission in environmental friendly solvent water.

Motivated from the extensive applications of AIE/AIEE active materials, we have accepted a challenge to develop and study the behaviour of AIEgens. Here, we have designed and developed an AIEE active luminogen and the mechanism of its intense emission in the aggregated state was studied. The applicability of this lumonogen for the detection of nitroaromatic explosive, picric acid was also examined. Our findings in this regard are discussed in the coming chapters.

References

1. Z. Chi, X. Zhang, B. Xu, X. Zhou, C. Ma, Y. Zhang, S. Liu and J. Xu, *Chemical Society Reviews*, 2012, **41**, 3878-3896.

2. A. Montali, C. Bastiaansen, P. Smith and C. Weder, *Nature*, 1998, **392**, 261.

3. T. P. Saragi, T. Spehr, A. Siebert, T. Fuhrmann-Lieker and J. Salbeck, *Chemical reviews*, 2007, **107**, 1011-1065.

4. K. Y. Pu and B. Liu, *Advanced Functional Materials*, 2009, **19**, 277-284.

5. J. B. Birks, *Aromatic Molecules*, Wiley: New York, 1970.

6. J. Wang, Y. Zhao, C. Dou, H. Sun, P. Xu, K. Ye, J. Zhang, S. Jiang, F. Li and Y. Wang, *The Journal of Physical Chemistry B*, 2007, **111**, 5082-5089.

7. S. Hecht and J. M. Fréchet, *Angewandte Chemie International Edition*, 2001, **40**, 74-91.

8. L. Chen, S. Xu, D. McBranch and D. Whitten, *Journal of the American Chemical Society*, 2000, **122**, 9302-9303.

9. A. M. Derfus, W. C. Chan and S. N. Bhatia, *Nano letters*, 2004, **4**, 11-18.

10. A. L. Routzahn and P. K. Jain, *Nano letters*, 2015, **15**, 2504-2509.

11. J. Luo, Z. Xie, J. W. Lam, L. Cheng, H. Chen, C. Qiu, H. S. Kwok, X. Zhan, Y. Liu and D. Zhu, *Chemical communications*, 2001, 1740-1741.

12. B.-K. An, S.-K. Kwon, S.-D. Jung and S. Y. Park, *Journal of the American Chemical Society*, 2002, **124**, 14410-14415.

13. J. Mei, Y. Hong, J. W. Lam, A. Qin, Y. Tang and B. Z. Tang, *Advanced materials*, 2014, **26**, 5429-5479.

14. H. Li, X. Zhang, Z. Chi, B. Xu, W. Zhou, S. Liu, Y. Zhang and J. Xu, *Organic letters*, 2011, **13**, 556-559.

15.   R. Hu, N. L. Leung and B. Z. Tang, *Chemical Society Reviews*, 2014, **43**, 4494-4562.

16.   L. N. Neupane, E.-T. Oh, H. J. Park and K.-H. Lee, *Analytical chemistry*, 2016, **88**, 3333-3340.

17.   Z. Wang, J. Nie, W. Qin, Q. Hu and B. Z. Tang, *Nature communications*, 2016, **7**, 12033.

18.   Y. Li, L. Xu and B. Su, *Chemical Communications*, 2012, **48**, 4109-4111.

19.   A. H. Malik, A. Kalita and P. K. Iyer, *ACS applied materials & interfaces*, 2017, **9**, 37501-37508.

20.   P. Singh, H. Singh, R. Sharma, G. Bhargava and S. Kumar, *Journal of Materials Chemistry C*, 2016, **4**, 11180-11189.

21.   Y. Hong, *Methods and applications in fluorescence*, 2016, **4**, 022003.

22.   F. Bu, R. Duan, Y. Xie, Y. Yi, Q. Peng, R. Hu, A. Qin, Z. Zhao and B. Z. Tang, *Angewandte Chemie International Edition*, 2015, **54**, 14492-14497.

23.   W. Fang, G. Zhang, J. Chen, L. Kong, L. Yang, H. Bi and J. Yang, *Sensors and Actuators B: Chemical*, 2016, **229**, 338-346.

24.   K. Li, W. Qin, D. Ding, N. Tomczak, J. Geng, R. Liu, J. Liu, X. Zhang, H. Liu and B. Liu, *Scientific reports*, 2013, **3**, 1150.

25.   L. Wang, Y. Li, X. You, K. Xu, Q. Feng, J. Wang, Y. Liu, K. Li and H. Hou, *Journal of Materials Chemistry C*, 2017, **5**, 65-72.

26.   A. D. Peng, D. B. Xiao, Y. Ma, W. S. Yang and J. N. Yao, *Advanced Materials*, 2005, **17**, 2070-2073.

27.   E.-H. Braye, W. Hübel and I. Caplier, *Journal of the American Chemical Society*, 1961, **83**, 4406-4413.

28.   F. Leavitt, T. Manuel and F. Johnson, *Journal of the American Chemical Society*, 1959, **81**, 3163-3164.

29.   C. Booker, X. Wang, S. Haroun, J. Zhou, M. Jennings, B. L. Pagenkopf and Z. Ding, *Angewandte Chemie International Edition*, 2008, **47**, 7731-7735.

30.   C. P.-y. Chan, M. Haeussler, B. Z. Tang, Y. Dong, K.-k. Sin, W.-c. Mak, D. Trau, M. Seydack and R. Renneberg, *Journal of immunological methods*, 2004, **295**, 111-118.

31.   M. M. Sartin, A. J. Boydston, B. L. Pagenkopf and A. J. Bard, *Journal of the American Chemical Society*, 2006, **128**, 10163-10170.

32.   K. L. Chan, M. J. McKiernan, C. R. Towns and A. B. Holmes, *Journal of the American Chemical Society*, 2005, **127**, 7662-7663.

33.   K. Tamao, M. Uchida, T. Izumizawa, K. Furukawa and S. Yamaguchi, *Journal of the American Chemical Society*, 1996, **118**, 11974-11975.

34.   M. S. Liu, J. Luo and A. K. Jen, *Chemistry of materials*, 2003, **15**, 3496-3500.

35.   T. L. Bandrowsky, J. B. Carroll and J. Braddock-Wilking, *Organometallics*, 2011, **30**, 3559-3569.

36.   H.-C. Su, O. Fadhel, C.-J. Yang, T.-Y. Cho, C. Fave, M. Hissler, C.-C. Wu and R. Réau, *Journal of the American Chemical Society*, 2006, **128**, 983-995.

37.   H. J. Tracy, J. L. Mullin, W. T. Klooster, J. A. Martin, J. Haug, S. Wallace, I. Rudloe and K. Watts, *Inorganic chemistry*, 2005, **44**, 2003-2011.

38.   Z. Li, Y. Q. Dong, J. W. Lam, J. Sun, A. Qin, M. Häußler, Y. P. Dong, H. H. Sung, I. D. Williams and H. S. Kwok, *Advanced Functional Materials*, 2009, **19**, 905-917.

39.   S. J. Toal, K. A. Jones, D. Magde and W. C. Trogler, *Journal of the American Chemical Society*, 2005, **127**, 11661-11665.

40.   S. J. Toal and W. C. Trogler, *Journal of Materials Chemistry*, 2006, **16**, 2871-2883.

41.   H. Sohn, R. R. Huddleston, D. R. Powell, R. West, K. Oka and X. Yonghua, *Journal of the American Chemical Society*, 1999, **121**, 2935-2936.

42.   C. K. Jim, J. W. Lam, A. Qin, Z. Zhao, J. Liu, Y. Hong and B. Z. Tang, *Macromolecular rapid communications*, 2012, **33**, 568-572.

43.	Y. T. Wu, M. Y. Kuo, Y. T. Chang, C. C. Shin, T. C. Wu, C. C. Tai, T. H. Cheng and W. S. Liu, *Angewandte Chemie International Edition*, 2008, **47**, 9891-9894.

44.	C. J. Bhongale, C.-W. Chang, C.-S. Lee, E. W.-G. Diau and C.-S. Hsu, *The Journal of Physical Chemistry B*, 2005, **109**, 13472-13482.

45.	Z. Yang, Z. Chi, T. Yu, X. Zhang, M. Chen, B. Xu, S. Liu, Y. Zhang and J. Xu, *Journal of Materials Chemistry*, 2009, **19**, 5541-5546.

46.	Z. Ning, Z. Chen, Q. Zhang, Y. Yan, S. Qian, Y. Cao and H. Tian, *Advanced Functional Materials*, 2007, **17**, 3799-3807.

47.	L. Peng, M. Wang, G. Zhang, D. Zhang and D. Zhu, *Organic letters*, 2009, **11**, 1943-1946.

48.	P. Xue, R. Lu, G. Chen, Y. Zhang, H. Nomoto, M. Takafuji and H. Ihara, *Chemistry–A European Journal*, 2007, **13**, 8231-8239.

49.	B. Xu, J. Zhang, H. Fang, S. Ma, Q. Chen, H. Sun, C. Im and W. Tian, *Polymer Chemistry*, 2014, **5**, 479-488.

50.	Z. Wei, Z.-Y. Gu, R. K. Arvapally, Y.-P. Chen, R. N. McDougald Jr, J. F. Ivy, A. A. Yakovenko, D. Feng, M. A. Omary and H.-C. Zhou, *Journal of the American Chemical Society*, 2014, **136**, 8269-8276.

51.	Y.-Z. Xie, G.-G. Shan, P. Li, Z.-Y. Zhou and Z.-M. Su, *Dyes and Pigments*, 2013, **96**, 467-474.

52.	R.-H. Chien, C.-T. Lai and J.-L. Hong, *The Journal of Physical Chemistry C*, 2011, **115**, 5958-5965.

53.	X. Huang, X. Gu, G. Zhang and D. Zhang, *Chemical Communications*, 2012, **48**, 12195-12197.

54.	Y. Liu, Y. Tang, N. N. Barashkov, I. S. Irgibaeva, J. W. Lam, R. Hu, D. Birimzhanova, Y. Yu and B. Z. Tang, *Journal of the American Chemical Society*, 2010, **132**, 13951-13953.

55.	J. Liu, Y. Zhong, P. Lu, Y. Hong, J. W. Lam, M. Faisal, Y. Yu, K. S. Wong and B. Z. Tang, *Polymer Chemistry*, 2010, **1**, 426-429.

56.	J. Mei, N. L. Leung, R. T. Kwok, J. W. Lam and B. Z. Tang, *Chemical reviews*, 2015, **115**, 11718-11940.

57.   J. Chen, C. Law, J. Lam, Y. Dong and S. Lo, *Chem. Mater*, 2003, **15**, 1535-1546.

58.   J. B. Birks, *New York*, 1970.

59.   Z. Zhao, P. Lu, J. W. Lam, Z. Wang, C. Y. Chan, H. H. Sung, I. D. Williams, Y. Ma and B. Z. Tang, *Chemical Science*, 2011, **2**, 672-675.

60.   Y. Hong, J. W. Lam and B. Z. Tang, *Chemical Society Reviews*, 2011, **40**, 5361-5388.

61.   Z. Zhao, J. W. Lam and B. Z. Tang, *Journal of Materials Chemistry*, 2012, **22**, 23726-23740.

62.   S. Li, Q. Wang, Y. Qian, S. Wang, Y. Li and G. Yang, *The Journal of Physical Chemistry A*, 2007, **111**, 11793-11800.

63.   B. Z. Tang and A. Qin, *Aggregation-induced emission: fundamentals*, John Wiley & Sons, 2013.

64.   A. P. Demchenko, K.-C. Tang and P.-T. Chou, *Chemical Society Reviews*, 2013, **42**, 1379-1408.

65.   G.-J. Zhao and K.-L. Han, *Accounts of chemical research*, 2012, **45**, 404-413.

66.   F. Laquai, Y. S. Park, J. J. Kim and T. Basché, *Macromolecular rapid communications*, 2009, **30**, 1203-1231.

67.   A. Weller, *Naturwissenschaften*, 1955, **42**, 175-176.

68.   J. Goodman and L. Brus, *Journal of the American Chemical Society*, 1978, **100**, 7472-7474.

69.   B. Dick and N. P. Ernsting, *Journal of Physical Chemistry*, 1987, **91**, 4261-4265.

70.   J. Wu, W. Liu, J. Ge, H. Zhang and P. Wang, *Chemical Society Reviews*, 2011, **40**, 3483-3495.

71.   A. S. Klymchenko and A. P. Demchenko, *Physical Chemistry Chemical Physics*, 2003, **5**, 461-468.

72. F. S. Rodembusch, F. P. Leusin, L. F. Campo and V. Stefani, *Journal of luminescence*, 2007, **126**, 728-734.

73. J. Cheng, D. Liu, W. Li, L. Bao and K. Han, *The Journal of Physical Chemistry C*, 2015, **119**, 4242-4251.

74. J. Zhao, S. Ji, Y. Chen, H. Guo and P. Yang, *Physical Chemistry Chemical Physics*, 2012, **14**, 8803-8817.

75. C.-C. Hsieh, C.-M. Jiang and P.-T. Chou, *Accounts of chemical research*, 2010, **43**, 1364-1374.

76. V. S. Padalkar and S. Seki, *Chemical Society Reviews*, 2016, **45**, 169-202.

77. J. E. Kwon and S. Y. Park, *Advanced Materials*, 2011, **23**, 3615-3642.

78. J. Cheng, D. Liu, L. Bao, K. Xu, Y. Yang and K. Han, *Chemistry–An Asian Journal*, 2014, **9**, 3215-3220.

79. K.-C. Tang, M.-J. Chang, T.-Y. Lin, H.-A. Pan, T.-C. Fang, K.-Y. Chen, W.-Y. Hung, Y.-H. Hsu and P.-T. Chou, *Journal of the American Chemical Society*, 2011, **133**, 17738-17745.

80. S. Park, J. Seo, S. H. Kim and S. Y. Park, *Advanced Functional Materials*, 2008, **18**, 726-731.

81. T. Mutai, H. Tomoda, T. Ohkawa, Y. Yabe and K. Araki, *Angewandte Chemie International Edition*, 2008, **47**, 9522-9524.

82. K.-Y. Chen, C.-C. Hsieh, Y.-M. Cheng, C.-H. Lai and P.-T. Chou, *Chemical communications*, 2006, 4395-4397.

83. J. Catalán, J. Del Valle, R. Claramunt, D. Sanz and J. Dotor, *Journal of luminescence*, 1996, **68**, 165-170.

84. P. S. Sherin, J. Grilj, Y. P. Tsentalovich and E. Vauthey, *The Journal of Physical Chemistry B*, 2009, **113**, 4953-4962.

85. S. Park, J. E. Kwon, S. H. Kim, J. Seo, K. Chung, S.-Y. Park, D.-J. Jang, B. M. Medina, J. Gierschner and S. Y. Park, *Journal of the American Chemical Society*, 2009, **131**, 14043-14049.

86. H. Shono, T. Ohkawa, H. Tomoda, T. Mutai and K. Araki, *ACS applied materials & interfaces*, 2011, **3**, 654-657.

87. R. Hu, S. Li, Y. Zeng, J. Chen, S. Wang, Y. Li and G. Yang, *Physical Chemistry Chemical Physics*, 2011, **13**, 2044-2051.

88. Z. Tu, M. Liu, Y. Qian, G. Yang, M. Cai, L. Wang and W. Huang, *RSC Advances*, 2015, **5**, 7789-7793.

89. R. Wei, P. Song and A. Tong, *The Journal of Physical Chemistry C*, 2013, **117**, 3467-3474.

90. G. Liu, M. Yang, L. Wang, J. Zheng, H. Zhou, J. Wu and Y. Tian, *Journal of Materials Chemistry C*, 2014, **2**, 2684-2691.

91. A. Kathiravan, K. Sundaravel, M. Jaccob, G. Dhinagaran, A. Rameshkumar, D. Arul Ananth and T. Sivasudha, *The Journal of Physical Chemistry B*, 2014, **118**, 13573-13581.

92. U. Panda, S. Roy, D. Mallick, P. Dalapati, S. Biswas, N. B. Manik, A. Bhattacharyya and C. Sinha, *Journal of Luminescence*, 2016, **175**, 44-49.

93. L. Wang, Z. Zheng, Z. Yu, J. Zheng, M. Fang, J. Wu, Y. Tian and H. Zhou, *Journal of Materials Chemistry C*, 2013, **1**, 6952-6959.

94. A. Kundu, P. Hariharan, K. Prabakaran, D. Moon and S. P. Anthony, *Crystal Growth & Design*, 2016, **16**, 3400-3408.

95. T. Han, X. Gu, J. W. Lam, A. C. Leung, R. T. Kwok, T. Han, B. Tong, J. Shi, Y. Dong and B. Z. Tang, *Journal of Materials Chemistry C*, 2016, **4**, 10430-10434.

96. X. Gan, G. Liu, M. Chu, W. Xi, Z. Ren, X. Zhang, Y. Tian and H. Zhou, *Organic & biomolecular chemistry*, 2016, **15**, 256-264.

97. L. Q. Yan, Z. N. Kong, Y. Xia and Z. J. Qi, *New Journal of Chemistry*, 2016, **40**, 7061-7067.

98. M. Yang, D. Xu, W. Xi, L. Wang, J. Zheng, J. Huang, J. Zhang, H. Zhou, J. Wu and Y. Tian, *The Journal of organic chemistry*, 2013, **78**, 10344-10359.

99. T. Han, X. Feng, D. Chen and Y. Dong, *Journal of Materials Chemistry C*, 2015, **3**, 7446-7454.

100. M. M. Watt, J. M. Engle, K. C. Fairley, T. E. Robitshek, M. M. Haley and D. W. Johnson, *Organic & biomolecular chemistry*, 2015, **13**, 4266-4270.

101. S. Gui, Y. Huang, F. Hu, Y. Jin, G. Zhang, L. Yan, D. Zhang and R. Zhao, *Analytical chemistry*, 2015, **87**, 1470-1474.

102. X. Wang, J. Hu, G. Zhang and S. Liu, *Journal of the American Chemical Society*, 2014, **136**, 9890-9893.

103. S. Samanta, S. Goswami, M. N. Hoque, A. Ramesh and G. Das, *Chemical Communications*, 2014, **50**, 11833-11836.

104. S. Samanta, U. Manna, T. Raya and G. Dasa.

105. M. Shyamal, P. Mazumdar, S. Maity, G. P. Sahoo, G. Salgado-Morán and A. Misra, *The Journal of Physical Chemistry A*, 2016, **120**, 210-220.

106. L. Peng, Z. Zhou, R. Wei, K. Li, P. Song and A. Tong, *Dyes and Pigments*, 2014, **108**, 24-31.

107. S. S. Pasha, H. R. Yadav, A. R. Choudhury and I. R. Laskar, *Journal of materials chemistry C*, 2017, **5**, 9651-9658.

108. P. Alam, V. Kachwal and I. R. Laskar, *Sensors and Actuators B: Chemical*, 2016, **228**, 539-550.

109. L. Feng, W. Shi, J. Ma, Y. Chen, F. Kui, Y. Hui and Z. Xie, *Sensors and Actuators B: Chemical*, 2016, **237**, 563-569.

110. M. Shellaiah, Y.-H. Wu, A. Singh, M. V. R. Raju and H.-C. Lin, *Journal of Materials Chemistry A*, 2013, **1**, 1310-1318.

111. H. Xiao, K. Chen, D. Cui, N. Jiang, G. Yin, J. Wang and R. Wang, *New Journal of Chemistry*, 2014, **38**, 2386-2393.

112. C. Niu, L. Zhao, T. Fang, X. Deng, H. Ma, J. Zhang, N. Na, J. Han and J. Ouyang, *Langmuir*, 2014, **30**, 2351-2359.

113. W. Tang, Y. Xiang and A. Tong, *The Journal of organic chemistry*, 2009, **74**, 2163-2166.

114. X. Wen and Z. Fan, *Analytica chimica acta*, 2016, **945**, 75-84.

115.   M. Shyamal, P. Mazumdar, S. Maity, S. Samanta, G. P. Sahoo and A. Misra, *ACS Sensors*, 2016, **1**, 739-747.

116.   O. Pinrat, K. Boonkitpatarakul, W. Paisuwan, M. Sukwattanasinitt and A. Ajavakom, *Analyst*, 2015, **140**, 1886-1893.

117.   S. F. Hallowell, *Talanta*, 2001, **54**, 447-458.

118.   G. Vourvopoulos and P. Womble, *Talanta*, 2001, **54**, 459-468.

119.   H. Chen, B. Dong, Y. Tang and W. Lin, *Accounts of chemical research*, 2017, **50**, 1410-1422.

120.   Y. Tang, D. Lee, J. Wang, G. Li, J. Yu, W. Lin and J. Yoon, *Chemical Society Reviews*, 2015, **44**, 5003-5015.

121.   M. E. Germain and M. J. Knapp, *Chemical Society Reviews*, 2009, **38**, 2543-2555.

122.   S. Hussain, A. H. Malik, M. A. Afroz and P. K. Iyer, *Chemical Communications*, 2015, **51**, 7207-7210.

123.   A. J. Davidson, I. D. Oswald, D. J. Francis, A. R. Lennie, W. G. Marshall, D. I. Millar, C. R. Pulham, J. E. Warren and A. S. Cumming, *CrystEngComm*, 2008, **10**, 162-165.

124.   P. C. Ashbrook and T. A. Houts, *Chemical Health and Safety*, 2001, **6**, 27.

125.   N. Venkatramaiah, S. Kumar and S. Patil, *Chemical Communications*, 2012, **48**, 5007-5009.

126.   R. Sodkhomkhum, M. Masik, S. Watchasit, C. Suksai, J. Boonmak, S. Youngme, N. Wanichacheva and V. Ervithayasuporn, *Sensors and Actuators B: Chemical*, 2017, **245**, 665-673.

127.   Z.-H. Fu, Y.-W. Wang and Y. Peng, *Chemical Communications*, 2017, **53**, 10524-10527.

128.   S. Zahn and T. M. Swager, *Angewandte Chemie International Edition*, 2002, **41**, 4225-4230.

129.   S. Doose, H. Neuweiler and M. Sauer, *ChemPhysChem*, 2009, **10**, 1389-1398.

130.   S. Shanmugaraju, S. A. Joshi and P. S. Mukherjee, *Journal of Materials Chemistry*, 2011, **21**, 9130-9138.

131.   Y. Salinas, R. Martínez-Máñez, M. D. Marcos, F. Sancenón, A. M. Costero, M. Parra and S. Gil, *Chemical Society Reviews*, 2012, **41**, 1261-1296.

132.   S. W. Thomas, G. D. Joly and T. M. Swager, *Chemical reviews*, 2007, **107**, 1339-1386.

133.   P. Lu, J. W. Lam, J. Liu, C. K. Jim, W. Yuan, N. Xie, Y. Zhong, Q. Hu, K. S. Wong and K. K. Cheuk, *Macromolecular rapid communications*, 2010, **31**, 834-839.

134.   P. Vishnoi, M. G. Walawalkar, S. Sen, A. Datta, G. N. Patwari and R. Murugavel, *Physical Chemistry Chemical Physics*, 2014, **16**, 10651-10658.

135.   Z. F. An, C. Zheng, R. F. Chen, J. Yin, J. J. Xiao, H. F. Shi, Y. Tao, Y. Qian and W. Huang, *Chemistry–A European Journal*, 2012, **18**, 15655-15661.

136.   V. Mahendran, K. Pasumpon, S. Thimmarayaperumal, P. Thilagar and S. Shanmugam, *The Journal of organic chemistry*, 2016, **81**, 3597-3602.

137.   Y. Chandrasekaran, N. Venkatramaiah and S. Patil, *Chemistry–A European Journal*, 2016, **22**, 5288-5294.

138.   M. Shyamal, S. Maity, P. Mazumdar, G. P. Sahoo, R. Maity and A. Misra, *Journal of Photochemistry and Photobiology A: Chemistry*, 2017, **342**, 1-14.

CHAPTER 8

MATERIALS AND METHODS

This chapter deals with a brief description of the materials used, analytical methods and the instrumental technique adopted for the study.

1. Chemicals and reagents

The following chemicals were used for the studies discussed in Part II.

Resorcinol, 2,4-dihydroxysalicylaldehyde, hydrazine hydrate, picric acid, hexamine, ethylacetoacetate, quinine sulphate and glycerol.

The solvents, methanol, ethanol, acetonitrile, acetone and ethyl acetate were received from the chemical suppliers and were used without further purification. Conc. sulphuric acid and conc. hydrochloric acid were also used. Double distilled water was used to conduct the entire studies.

2. Synthesis of coumarin

Synthesis of coumarin was discussed in Chapter 2 of Part I.

3. Methods

3. 1. Reprecipitatation method

This pure chemical technique first reported by Nakanishi and coworkers[1, 2], is commonly used for the preparation organic nanoparticles. In this method, the solution of the target compound is

rapidly injected to a solvent/non solvent mixture, which induces the nucleation and growth of nanoparticles.

4. Instrumental techniques

Melting points of the probes were detected using standard melting point apparatus. CHN analyses were carried out on Vario EL III CHNS analyzer. The FTIR spectra (4000 – 400 cm^{-1}) were recorded as KBr pellets on a Jasco FTIR 4100 spectrometer. The ^{1}H NMR and ^{13}C NMR spectra were recorded on a 400MHz Bruker Avance III spectrometer using CDCl$_3$. The Electron-Spray Ionization Mass Spectrum (ESI-MS) was recorded on Waters **(**UPLC- TQD) mass spectrometer. The UV-Visible studies were carried out on a Jasco UV-Visible spectrophotometer, model V-550. Fluorescence measurements were carried out on an Agilent Technologies model Cary Eclipse Fluorescence spectrophotometer. SEM analysis was conducted on ZEISS GeminiSEM 300.
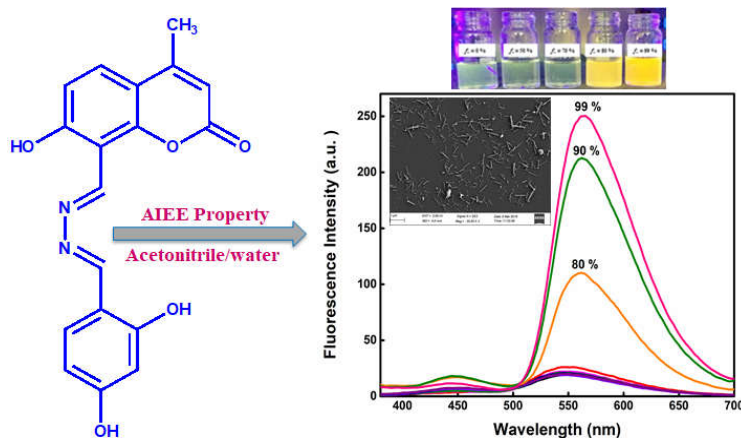
References

1.   H. Kasai, H. S. Nalwa, H. Oikawa, S. Okada, H. Matsuda, N. Minami, A. Kakuta, K. Ono, A. Mukoh and H. Nakanishi, *Japanese journal of applied physics*, 1992, **31**, L1132.

2.   H. S. Nalwa, A. Kakuta, A. Mukoh, H. Kasai, S. Okada, H. Oikawa, H. Nakanishi and H. Matsuda, *Advanced Materials*, 1993, **5**, 758-760.

AGGREGATION INDUCED EMISSION ENHANCEMENT (AIEE) BEHAVIOR OF COUMARIN DERIVED SCHIFF BASE

Work in Brief... ...

- *Synthesized and characterized a new Schiff base, 1-(8-methanylylidene-7-hydroxy-4-methyl-2H-chromen-2-one)-2-(2, 4-dihydroxybenzylidene) hydrazine.*

- *The synthesized compound exhibited a yellow emission at 562 nm in the aggregated state with relatively large Stock's shift of 205 nm.*

- *Discussed the effect of intramolecular motions and the interplay of ESIPT on aggregation induced emission enhancement (AIEE).*

- *The scanning electron microscopic study was carried out to investigate the morphology of the nanoaggregate.*

- *The aggregated luminogen displayed yellow emission in the pH range of 4-7 without affecting the intensity*

1. Introduction

Solid state luminescent organic materials find promising applications in organic light emitting diodes (OLED), fluorescent sensors, bioimaging and so forth [1-6]. The major problem of fluorescent materials is that they become highly emissive in isolated molecular state. Their emission either quenches or they will not be emissive in the solid- or aggregated state which limit their applications. This effect, the quenching of fluorescence with concentration, is commonly known as aggregation caused quenching (ACQ) [7, 8]. The intramolecular rotation in dilute solutions causes the dissipation of the excited state energy. The intermolecular π-π stacking interactions of aromatic skeleton of organic molecules result in the formation of excimers and exciplexes which also lead to the quenching of fluorescence [9]. In 2001, Tang and co-workers [10, 11] reported an interesting property in silole-based organic molecules, which was just reverse of the common ACQ effect. They observed that the non-emissive system in isolated state strongly emit bright green fluorescence upon aggregation and this unique phenomenon is termed as aggregation induced emission (AIE) [12]. Another feature of aggregated luminogens, aggregation induced emission enhancement (AIEE) was reported in 2002 by Park *et al* [6]. AIEE active luminogens are feebly emissive in the isolated state and their emission gets enhanced in the aggregated state. The main mechanism proposed for AIE/AIEE activity is the restriction of intramolecular motion (RIM) in the aggregated- or solid state [13]. The other mechanisms reported are intramolecular charge transfer (ICT) [14], J-aggregation [15], twisted intramolecular charge transfer (TICT) [12, 16], excited state intramolecular proton transfer (ESIPT) [17], and *cis-trans*

isomerization [17]. However, there is no common mechanism applicable to all systems and each mechanism is applicable only to a specific system.

The AIE/AIEE active ESIPT luminogens have much attraction in photochemistry and photophysics [18]. The attractive feature of ESIPT luminogens is their large Stock's shift without self-absorption. ESIPT active hydrazine Schiff bases are highly fluorescent in solid state or in aggregated state and have many practical applications [19, 20] and therefore, a number of ESIPT active hydrazine based Schiff bases are reported [21-24]. In the molecular state of this type of luminogens, the molecular motions (rotations or vibrations) impede the ESIPT process and therefore, they are weak in emission. Molecular motions are restricted by forming aggregates or in solid state and this opens a door for ESIPT, resulting an enhancement in emission intensity. However, the ESIPT process does not fully support the enhanced emission in the aggregated state [13].

Keeping the above facts in mind, we have designed and synthesized a new Schiff base, 1-(8-methanylylidene-7-hydroxy-4-methyl-2H-chromen-2-one)-2-(2,4-dihydroxybenzylidene) hydrazine, L by condensing 8-formyl-7-hydroxy-4-methylcoumarine and 2,4-dihydroxysalicylaldehyde with hydrazine. L was feebly emissive in pure acetonitrile solution and showed pronounced AIEE activity by forming an H-type aggregate in acetonitrile/water system. The emission was observed in yellow region with relatively large Stock's shift.

2. Experimental

2.1. Materials and methods

All the chemicals used for the study were purchased from Sigma Aldrich or Alfa Aesar. The solvents were received from the chemical suppliers and were used without further purification. The sensing study was carried out using nitrate salts of different metals.

Elemental analyses were carried out on VarioEL III CHNS analyzer. A Jasco FTIR 4100 spectrometer was used to record the FTIR spectrum (4000-400 cm^{-1}) of the compound. The ^{1}H NMR- and ^{13}C NMR spectra were recorded on a 400 MHz Bruker Avance III spectrometer using DMSO-d6. The electron-spray ionization mass spectrum (ESI-MS) was recorded on Waters (UPLC- TQD) mass spectrometer. The UV-Visible- and fluorescence spectra were recorded on a Jasco UV-Visible Spectrophotometer, model V-550 and Agilent Technologies model Cary Eclipse Fluorescence Spectrophotometer, respectively.

2.2. Synthesis of Schiff base

The procedures for the synthesis of 7-hydroxy-4-methylcomarine and 8-formyl-7-hydroxy-4-methylcoumarin were adopted from the literature [25, 26]

1 mmol of 8-formyl-7-hydroxy-4-methylcoumarin (0.204 g) was refluxed with excess of hydrazine hydrate (1.5 mmol, 75 µL) in 30 ml ethanol for about 6 h. On concentrating the above mixture, obtained a pale yellow solid product. It was filtered and washed with

acetone. 1 mmol of the product obtained was dissolved in 15 ml methanol by stirring. To this solution, 1 mmol of 2, 4-dihydroxybenzaldehyde dissolved in 15 ml methanol was added in drops and the mixture was refluxed for about 4 h. The bright yellow solid product obtained was filtered washed with ethanol, dried and kept in a desiccator. Yield: 78%. Anal. Calcd for $C_{18}H_{14}N_2O_5$:   C, 63.90; H, 4.17%; N, 8.28%; Found: C, 71.12%; H, 5.17%; N, 8.63%. IR (cm^{-1}, KBr): v(C=N) 1625 cm^{-1}. ^{1}H NMR (400 MHz, DMSO d$_6$, δ (ppm)) δ: 12.62 (1H, s), 11.11 (1H, s), 10.43 (1H, s), 9.20 (1H, s), 8.92 (s, 1H), 7.79 (d, 1H), 7.51 (d, 1H), 6.99(d, 1H), 6.43 (d, 1H), 6.41 (s,1H), 6.31 (s,1H), 2.41(s, 3H); ^{13}C NMR (400 MHz, DMSO d$_6$, δ (ppm)) δ 163.72,159.08, 156.36, 153.81, 153.23, 129.59, 113.33, 110.84, 105.31, 79.05, 18.29; ESI MS (m/z): [M + H]$^+$: Calculated: 339.3, Found: 339.2

2.3. Preparation of nanoaggregates

1 mM stock solution of L was prepared in acetonitrile. An aliquot of 200 μL of the stock solution was added to a 10 ml standard flask and diluted with acetonitrile/water system in appropriate ratio to get a final concentration of 20 μM. Sonicated the above solution for 15 minutes. Absorption- and emission spectra were recorded immediately.

3. Results and discussion

3.1. Structural characterization

The compound, 1(8-methanylylidene-7-hydroxy-4-methyl-2H-chromen-2-one)-2-(2, 4-dihydroxybenzylidene) hydrazine, L was synthesized in a two-step procedure (Scheme 1). L was readily soluble

in acetonitrile, DMF and DMSO. The formation of the target compound was confirmed by elemental analyses, IR, ^{1}H NMR, ^{13}C NMR spectroscopic and mass spectrometric studies. The details of characterizations are incoroerated in Chapter 3 of Part I.
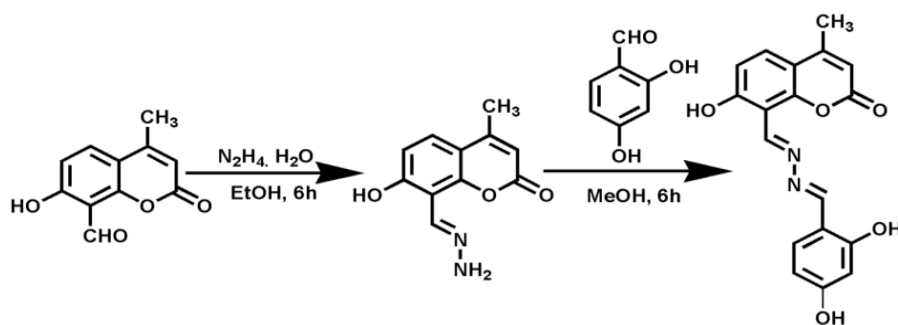
Scheme 1. Synthetic route of 1(8-methanylylidene-7-hydroxy-4-methyl-2H-chromen-2-one)-2-(2, 4-dihydroxybenzylidene) hydrazine, L

3.2. Photophysical investigations

To investigate the aggregation induced emission enhancement (AIEE) feature of the probe, its fluorescence spectrum was recorded by adding different amounts of a poor solvent (deionized water) to a solution of L in acetonitrile. The water fraction (f_w) was varied from 0 to 99 % and the emission behavior was monitored with an excitation wavelength of 356 nm. In dilute acetonitrile solution (20 μM) L was feebly emissive at 448 and 549 nm with an excitation of 356 nm. The former short wavelength emission was due to the excited state enol form, E* (normal emission) and the later one at higher wavelength was the ESIPT emission (excited state keto form, K*)[27]. The emission spectra and the fluorescence image revealed that as the water fraction (f_w) increased from 0 up to 70% there was no significant change in the

emission behavior. Interestingly, at the f_w >80, the emission intensity increased and a yellow emission was observed at 562 nm. The intensity of emission increased continuously from f_w >80%. As f_w increased to 80%, 90% and 99 %, a dramatic enhancement of fluorescence intensity to 5.5, 10.5 and 12.5 fold, respectively, was observed, which indicated an obvious AIEE effect. The fluorescence quantum yield gave a quantitative measurement of AIEE. It increased from 0.05 to 0.1 as f_w increased from   80 to 99 %. Along with the emission enhancement, as the water fraction increased, there was a 12 nm red shift in the fluorescence spectral profile. The red shift of the emission maxima indicated the change of single molecule into aggregates *via* intermolecular interactions between molecules.
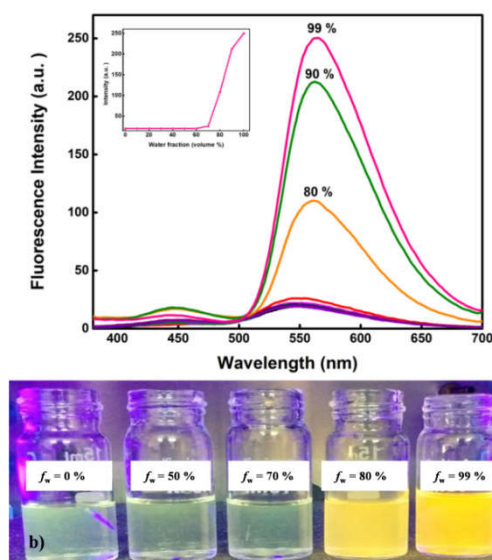

Fig. 4. a) The fluorescence spectra of L in acetonitrile-water mixture with different water fraction (f_w). b) Colour change of L (20 μM) at in acetonitrile/water mixture at different water fraction under UV light
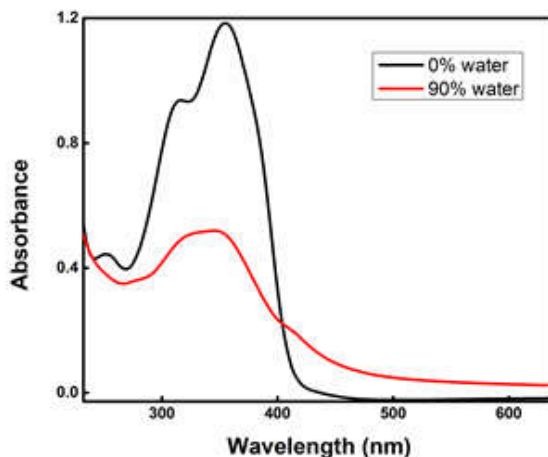
Fig. 5. UV-Visible spectra of L in solution state and in aggregated state

The absorption spectra of L (20 μM) in pure acetonitrile and in acetonitrile/water mixture of f_w 90% are shown in Fig 5. The absorption spectral profile significantly changed when water fraction increased. Water content of 90%, reduced the intensity of absorption of L centered at 356 nm followed by a slight hypsochromic shift. Meanwhile, new shoulder emerged at 419 nm and leveled-off the tails in the visible region, which was attributed to Mie scattering caused by nanoparticles [27, 28]. This indicated the formation of aggregates. Generally, blue shifts (hypsochromic shifts) in the absorption spectrum originate from H-type aggregates (head-head) and result a significant decrease in emission intensity. Red shifts (bathochromic shifts) in absorption spectra originate from J-type aggregates (head-tail) and result an enhancement in emission intensity. In the present case, a blue shift was observed in absorption spectrum of L in acetonitrile/water mixture of f_w 90%, which indicated the formation of H-type aggregates. At the same time, upon aggregation, the intensity of

emission increased, which is in contradiction to common behavior of H-aggregates. The enhanced emission of H-aggregates is not common but a few reports are available in literature. Wurthner *et al* [29] reported that a merocyanine dye formed H-aggregate and showed abnormal emission. According to them, the non-vanishing of transition probability between the ground state and lower excited state is responsible for the operation of a weak fluorescence. A compound 1,4-di[(E)-2-phenyl-1-propenyl]-benzene (PPB), reported by Diau *et al* [30], showed enhanced emission, contradictory to the blue shifted absorption maxima. The herringbone type aggregation together with edge-to-face arrangement are responsible for this abnormal emission enhancement. The H-aggregated luminogens with ultrafast strong ESIPT property also exhibited abnormal fluorescence behavior as reported by another group [30]. In the present case, the abnormal luminescence enhancement of L in the aggregated state may be due to the interplay of strong intramolecular proton transfer in the excited state.

The scanning electron microscopic study was carried out to examine the morphology and average diameter of the fluorescent nanoparticles formed. Fig. 6 depicts the SEM images of L in the isolated (a) - and aggregated (b) states. In the isolated state, particles have no specific morphology and they are in the micrometer range. Upon aggregation (from the figure it is clearly visible), the particles form well defined nanorods with an average diameter of 349 nm (Fig. 6). The formation of these organic nanoparticles in the aggregated state with a well defined morphology supported the fluorescence behavior.
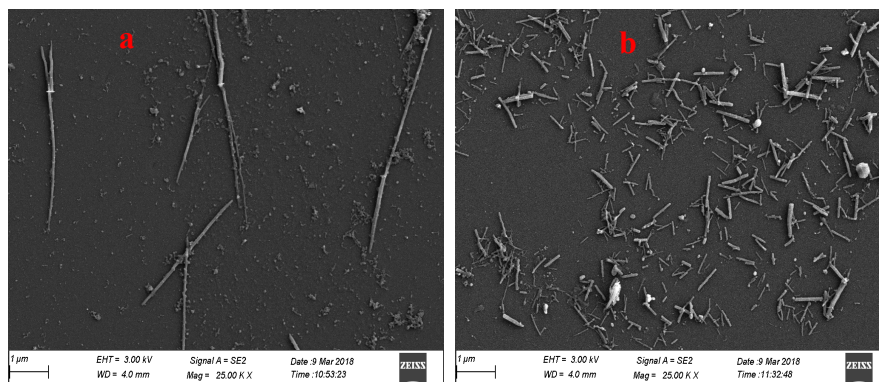
Fig. 6. SEM images of L a) In isolated state, b) In aggregated
state (water/acetonitrile in 90/10 v/v) having a concentration of 10 x 10^{-6} M

To get more insight of the AIEE property, the life time of the fluorophore in the excited state was checked both in pure acetonitrile solution and in acetonitrile/water mixture. The measurement of excited state life time is more informative than the fluorescence intensity measurement because it is an intrinsic property, which does not depend on the concentration of the fluorophore and excitation wavelength intensity. The fluorescence decay profile of L in pure acetonitrile and acetonitrile/water mixture are depicted in Fig.7. In pure acetonitrile, L showed a biexponential decay with an average life time of 0.58 ns and in acetonitrile/water mixture the fluorophore existed in the excited state with an average life time of 4.3 ns, followed by a single exponential decay. The increase in the life time in acetonitrile/water mixture with higher water fraction indicated the lowering of radiationless decays in the aggregated state.
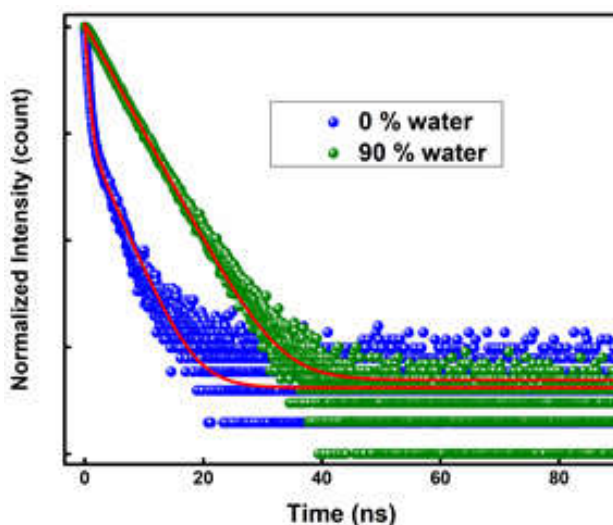
Fig. 7. Fluorescence decay of L in pure acetonitrile and in acetonitrile/water
mixture (1 : 9)

The intramolecular rotations around the freely rotatable rotors like C-C, C-N and N-N, have significant role to activate the non-radiative decay process by consuming the excited state energy. To determine the mechanism of fluorescence enhancement on aggregation, the effect of viscosity on the emission was studied by blending methanol with glycerol. The viscosity of the solvent was varied by varying the ratio of glycerol to methanol in the mixture. As the glycerol fraction increased, the intensity of emission centered at 562 nm increased without any significant change in the emission maxima (Fig. 8). This emission enhancement was mainly due to the viscosity effect, which divulged that the restriction of intramolecular rotation has a significant effect on the AIEE property of L. From the Fig 4 (a), it can be seen that as the water fraction increased, the nature of the emission spectral profile changed. Up to 70 % water fraction,

the active involvement of intramolecular rotation around the N-N and C-N rotors dissipate the excited state energy, which weakens the ESIPT emission. When the water fraction reaches 80%, L starts to exhibit strong ESIPT emission with a Stokes shift of 205 nm. This observation indicated that up to 70% water fraction, the intramolecular motions inhibited the ESIPT process, thus L was feebly emissive. From 80% water fraction, due to physical constraints the intramolecular motions were blocked, which endued the ESIPT process by maintaining suitable geometry and resulted a strong radiative ESIPT emission. Thus, restriction of intramolecular rotation enriched the ESIPT process and led to a radiative emission. In addition to the large Stokes shift, a 12 nm red shift was observed. The energy gap between the excited keto state and ground state was smaller than that of the non-ESIPT state, thus a red shifted emission was observed in ESIPT luminogens[31].
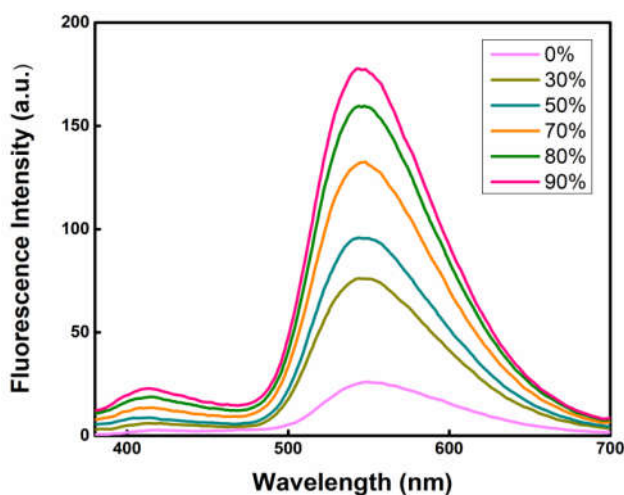

Fig. 8. The fluorescence spectra of L in methanol-glycerol mixture with different glycerol fraction

The effect of pH on the emission is an important factor for the practical application of the luminogens. We have checked the effect of pH on the emission intensity of aggregate of L in acetonitrile/water mixture with f_w 90% using HEPES as buffer. The pH of the buffer was adjusted using 1N HCl and 1N NaOH. From the Fig 9, it can be seen that on increasing pH from 2 to 6, the intensity of ESIPT emission increased and above pH 6 it decreased. There was no noticeable change in the emission intensity in the pH range of 4-7. Above pH 7, the intensity of ESIPT emission decreased and favored the emission from enol form. At pH 10, the ESIPT emission quenched completely. The protonation and deprotonation of hydroxyl group in acidic and basic medium, respectively, impede the ESIPT process, there by quenching the emission centered at 562 nm. The results indicated that in the luminogen, L the ESIPT process is successfully operated at physiologically and environmentally important pH range of 4-7. Therefore, it can be used for practical applications in this pH range.
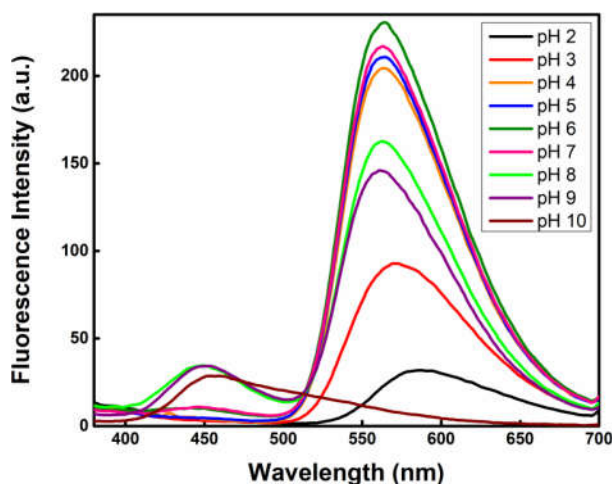

Fig. 9. Emission spectra of L in acetonitrile/water mixture (1:9 v/v) at different pH

4. Conclusions

A new hydrazine based ESIPT active Schiff base, 1-(8-methanylylidene-7-hydroxy-4-methyl-2H-chromen-2-one)-2-(2,4-dihydroxybenzylidene)hydrazine, L has been synthesized and characterized. It exhibited a normal emission at 448 nm and an ESIPT emission at 549 nm in pure acetonitrile solution. The feebly emissive L started to exhibit yellow ESIPT emission at 562 nm in acetonitrile/water system having a water fraction of 80 % and above. The remarkable AIEE property with high stocks shift value was quantified by measuring the quantum yield using quinine sulfate as standard. The effect of viscosity on the emission intensity was checked and the result divulged that the restriction of molecular motion activated the ESIPT process and resulted an enhancement in emission intensity. The increased life time at higher water fraction again confirmed up the AIEE property of L. The formation of the well-defined nanorods observed in FESEM images supported the observed fluorescent property. In the pH range of 4-7 there was no remarkable change in the emission intensity, which indicated that the ESIPT process was active in this practically applicable pH range without any interference of H^+ and OH^- ions.

References

1.   C. W. Tang and S. A. VanSlyke, *Applied physics letters*, 1987, **51**, 913-915.

2.   M. Shyamal, P. Mazumdar, S. Maity, S. Samanta, G. P. Sahoo and A. Misra, *ACS Sensors*, 2016, **1**, 739-747.

3.   L. N. Neupane, E.-T. Oh, H. J. Park and K.-H. Lee, *Analytical chemistry*, 2016, **88**, 3333-3340.

4.   Y. Liu, S. Chen, J. W. Lam, P. Lu, R. T. Kwok, F. Mahtab, H. S. Kwok and B. Z. Tang, *Chemistry of Materials*, 2011, **23**, 2536-2544.

5.   L. Wang, L. Yang and D. Cao, *Current Organic Chemistry*, 2014, **18**, 1028-1049.

6.   B.-K. An, S.-K. Kwon, S.-D. Jung and S. Y. Park, *Journal of the American Chemical Society*, 2002, **124**, 14410-14415.

7.   Y. Hong, J. W. Lam and B. Z. Tang, *Chemical Society Reviews*, 2011, **40**, 5361-5388.

8.   S. A. Jenekhe and J. A. Osaheni, *Science*, 1994, **265**, 765-768.

9.   S. W. Thomas, G. D. Joly and T. M. Swager, *Chemical reviews*, 2007, **107**, 1339-1386.

10.   J. Luo, Z. Xie, J. W. Lam, L. Cheng, H. Chen, C. Qiu, H. S. Kwok, X. Zhan, Y. Liu and D. Zhu, *Chemical communications*, 2001, 1740-1741.

11.   B. Z. Tang, X. Zhan, G. Yu, P. P. S. Lee, Y. Liu and D. Zhu, *Journal of Materials Chemistry*, 2001, **11**, 2974-2978.

12.   Y. Hong, J. W. Lam and B. Z. Tang, *Chemical communications*, 2009, 4332-4353.

13.   J. Mei, Y. Hong, J. W. Lam, A. Qin, Y. Tang and B. Z. Tang, *Advanced materials*, 2014, **26**, 5429-5479.

14.   B.-R. Gao, H.-Y. Wang, Y.-W. Hao, L.-M. Fu, H.-H. Fang, Y. Jiang, L. Wang, Q.-D. Chen, H. Xia and L.-Y. Pan, *The Journal of Physical Chemistry B*, 2009, **114**, 128-134.

15. J. Wang, J. Mei, W. Yuan, P. Lu, A. Qin, J. Sun, Y. Ma and B. Z. Tang, *Journal of Materials Chemistry*, 2011, **21**, 4056-4059.

16. J. Zhang, B. Xu, J. Chen, L. Wang and W. Tian, *The Journal of Physical Chemistry C*, 2013, **117**, 23117-23125.

17. L. McDonald, J. Wang, N. Alexander, H. Li, T. Liu and Y. Pang, *The Journal of Physical Chemistry B*, 2016, **120**, 766-772.

18. Y. Shigemitsu, T. Mutai, H. Houjou and K. Araki, *The Journal of Physical Chemistry A*, 2012, **116**, 12041-12048.

19. V. S. Padalkar and S. Seki, *Chemical Society Reviews*, 2016, **45**, 169-202.

20. R. Hu, S. Li, Y. Zeng, J. Chen, S. Wang, Y. Li and G. Yang, *Physical Chemistry Chemical Physics*, 2011, **13**, 2044-2051.

21. R. Wei, P. Song and A. Tong, *The Journal of Physical Chemistry C*, 2013, **117**, 3467-3474.

22. H. Xiao, K. Chen, D. Cui, N. Jiang, G. Yin, J. Wang and R. Wang, *New Journal of Chemistry*, 2014, **38**, 2386-2393.

23. W. Tang, Y. Xiang and A. Tong, *The Journal of organic chemistry*, 2009, **74**, 2163-2166.

24. A. Kathiravan, K. Sundaravel, M. Jaccob, G. Dhinagaran, A. Rameshkumar, D. Arul Ananth and T. Sivasudha, *The Journal of Physical Chemistry B*, 2014, **118**, 13573-13581.

25. A. Kulkarni, S. A. Patil and P. S. Badami, *European journal of medicinal chemistry*, 2009, **44**, 2904-2912.

26. Y. Dong, X. Mao, X. Jiang, J. Hou, Y. Cheng and C. Zhu, *Chemical Communications*, 2011, **47**, 9450-9452.

27. J. Zhao, S. Ji, Y. Chen, H. Guo and P. Yang, *Physical Chemistry Chemical Physics*, 2012, **14**, 8803-8817.

28. H. Auweter, H. Haberkorn, W. Heckmann, D. Horn, E. Lüddecke, J. Rieger and H. Weiss, *Angewandte Chemie International Edition*, 1999, **38**, 2188-2191.
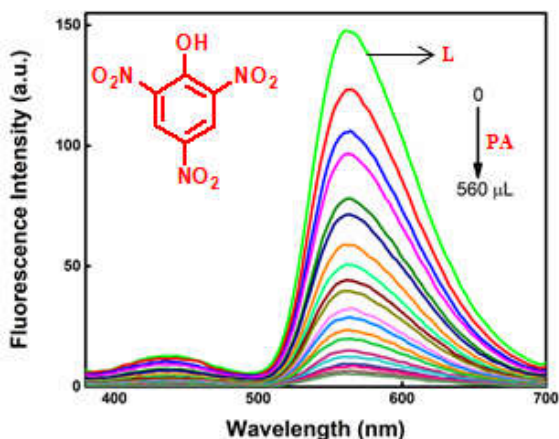
29. U. Rösch, S. Yao, R. Wortmann and F. Würthner, *Angewandte Chemie*, 2006, **118**, 7184-7188.

30. C. J. Bhongale, C.-W. Chang, C.-S. Lee, E. W.-G. Diau and C.-S. Hsu, *The Journal of Physical Chemistry B*, 2005, **109**, 13472-13482.

31. J. Mei, N. L. Leung, R. T. Kwok, J. W. Lam and B. Z. Tang, *Chemical reviews*, 2015, **115**, 11718-11940.

AIEE ACTIVE PROBE: A FLUORESCENCE SENSOR FOR PICRIC ACID

Work in brief………

- *The applicability of the aggregate of a new Schiff base, 1-(8-methanylylidene-7-hydroxy-4-methyl-2H-chromen-2-one)-2-(2, 4-dihydroxybenzylidene) hydrazine.L was explored for the detection of picric acid (PA).*

- *Aggregate of L gave "turn-off" fluorescence response with PA in water.*

- *Mechanism of quenching studied by applying Stern-Volmer equation.*

- *The limit of detection was calculated from the calibration curve of fluorescence titration.*

1. Introduction

For national security issues and environmental concern, it is highly desirable to develop suitable methods for the detection of explosives. Among the various nitroaromatic explosives, 2,4,6-trinitrophenol (TNP) or picric acid (PA), a superior explosive, is the main constituent of industrial explosives and landmines[1]. PA also has crucial roles in chemical, pharmaceutical, dye and leather industries. Compared to other nitroaromatics, the high solubility of PA results in its contamination in soil and groundwater. Its exposure causes several health problems such as skin irritation, anemia, headache and various respiratory issues[2-4]. Several methods are available to detect explosives which include X-ray imaging, thermal neutron analysis, gas chromatography, electrochemical and spectrometric methods, etc. Majority of these need expensive instrumental facilities[5-8]. Optical based methods, especially fluorescence based sensing methods have many attractions such as simplicity, high sensitivity and selectivity, rapid response and cost effectiveness[9-11]. Considering the practical applicability, it is highly desirable to develop efficient probes to detect PA in water.

The responses of fluorescence based chemical sensors with analytes are mainly either by fluorescence enhancement or by fluorescence quenching. Nitroaromatics, generally electron deficient species, diminishes the emission intensity of fluorophore. Fluorescence quenching occurs when the fluorophore interacts with the analyte. The quenching process usually follows two types of mechanisms, static

quenching or dynamic quenching. The static quenching occurs when the sensor interacts with the analyte and form a fluorophore-quencher complex. Collision of the quencher molecule with the excited fluorophore leads to dynamic quenching. It is also known as collision quenching. These two mechanisms can be distinguished using time-resolved fluorescence spectroscopy. For this, the fluorescence decay lifetime of the fluorophore is measured in the absence- and presence of the quencher. In the case of static quenching, the fluorescence life time remains unchanged on increasing the concentration of the quencher, but in the case of dynamic quenching, fluorescence lifetime decreases with increasing concentration of the quencher[11].

Most of the organic fluorophores for nitroaromatics function effectively in organic solvents. However, their sensing ability is not good in aqueous medium. Terrerism activities lead to the contamination of water and soil with nitroaromatics. Nitroaromatics exhibit comparatively good water solubilty and low volatility which again increase their contamination in the environment. Thus, it is always essential to develop a suitable method to detect this type of life threatening analytes in aqueous medium[12]. The AIE/AIEEgens exhibit intense fluorescence in their aggregated state and are environmental friendly sensing systems for various analytes, including nitroaromatics.

Here, we have studied the sensing ability of highly emissive aggregate of 1-(8-methanylylidene-7-hydroxy-4-methyl-2H-chromen-2-one)-2-(2, 4-dihydroxybenzylidene) hydrazine, L to detect most

potent nitroaromatic explosive, picric acid in water *via* fluorescence quenching. The mechanism of sensing was also explored.

2. Experimental

2.1. Materials and methods

Double distilled water was used for the entire study. Acetonitrile was received from the chemical suppliers and was used without further purification.

The UV-Visible- and Fluorescence spectra were recorded on a Jasco UV-Visible spectrophotometer, model V-550 and Agilent Technologies model Cary Eclipse Fluorescence Spectrophotometer, respectively. Theoretical studies of the complex was performed by DFT/B3LYP/3-21G method and TDDFT calculations.

2.2. Synthesis of Schiff base

Synthesis of the Schiff base is discussed in Chapter 3 of Part II.

2.3. Sample preparation for sensing studies

For sensing studies, 1 mM stock solution of L in acetonitrile and 2,4,6-trinitrophenol in double distilled water were prepared. An aggregate of L was prepared by adding an aliquot of 100 μL to acetonitrile/water mixture having a water fraction of 90 % and recorded its emission spectra on exciting at 356 nm.

The nature of quenching was studied using Stern-Volmer equation.

$$\frac{I_0}{I} = 1 + k_q \tau_0 [Q]$$

$$\frac{I_0}{I} = 1 + K_D [Q]$$

where, F_0 and F are the fluorescence intensities in the absence and presence of a quencher, respectively, τ_0 is lifetime of the fluorophore in the absence of a quencher, k_q the bimolecular quenching constant, K_D is Stern–Volmer quenching constant and $[Q]$ is the concentration of the quencher. In the case of static quenching, the equation becomes,

$$\frac{I_0}{I} = 1 + K_S [Q]$$

where K_S Stern-Volmer constant for static quenching

For combined static and dynamic quenching, the Stern – Volmer equation changes to -

$$\frac{I_0}{I} = (1 + K_S [Q])(1 + K_D [Q])$$

$$\frac{I_0}{I} = 1 + (K_S + K_D)[Q] + K_S K_D x [Q]^2$$

At very low concentration of the quencher, the term $[Q]^2$ is small and thereby a linear plot is obtained . On increasing the concentration of the quencher, the linearity of the plot changes and bends upward. This equation explains the upward bending of Stern – Volmer plot at higher concentration of the quencher is velar from the equation[13].

3. Results and discussion

3.1. Structural characterization

Details of the structural characterization of L are discussed in Chapter 4 of Part I.
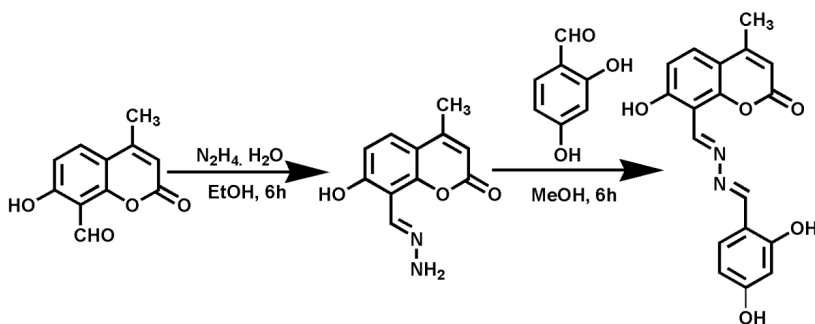
Scheme 1. Synthetic route of 1(8-Methanylylidene-7-hydroxy-4-methyl-2H-chromen-2-one)-2-(2, 4-dihydroxybenzylidene) hydrazine, L

3.2. Detection of nitroaromatics

The detection of nitroaromatics was performed using the aggregates of L formed in acetonitrile/water (1:9) mixture. The analysis was carried out using picric acid (PA) as model compound. The fluorescence intensity quenched gradually by the sequential addition of 1 mM PA (0-4 equivalents) in water (Fig. 1). Upon the addition of 1 equivalent of PA, observed fluorescence quenching efficiency ($(1-I/I_0)$ x 100 %) was 52% and the quenching efficiency reached 90% by the addition of 2.8 equivalents PA.
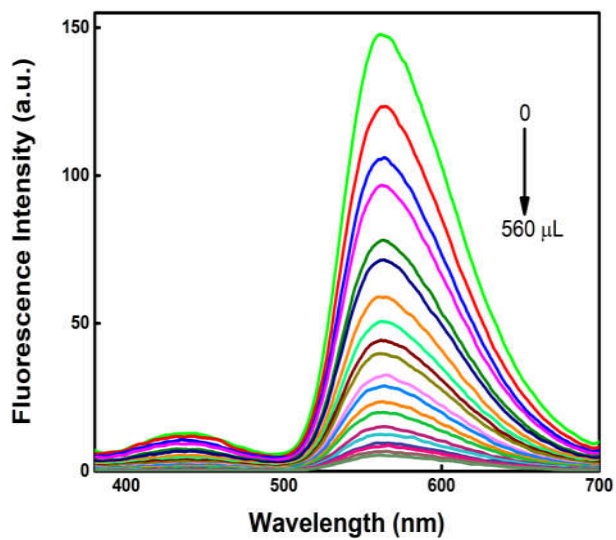
Fig 1. Fluorescence spectral change of aggregated L in
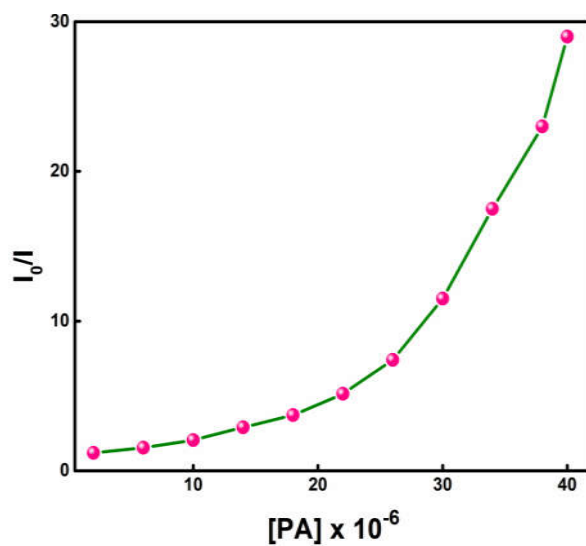acetonitrile/water mixture (1:9 v/v) as a function of PA in water

Fig. 2 Stern-Volmer plot of aggregated L in
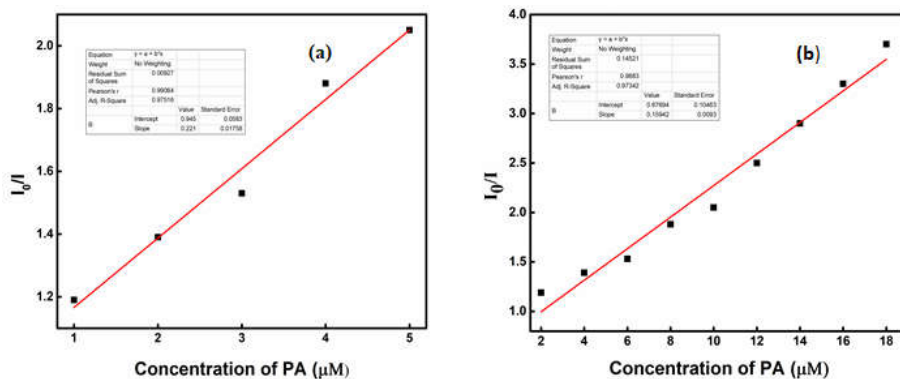acetonitrile/water (1:9) mixture with PA

Fig. 3. a)Stern-Volmer plot of upto 1 equivalent of PA.
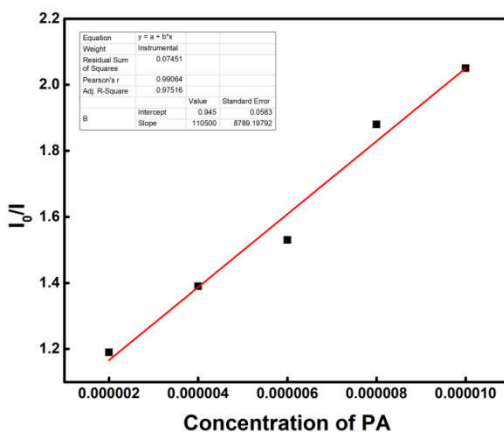b) Stern-Volmer plot of upto 2.8 equivalent of PA

Fig. 4. Calibration curve of L - PA for LOD calculation

The quenching behaviour was studied by fitting the data in Stern-Volmer equation, $I_0/I = 1 + K_{sv}[Q]$, where I_0- and I are the emission intensities of aggregate L in the absence- and presence of the quencher, respectively, Ksv is the Stern-Volmer- or quenching constant and [Q] quencher concentration. The plot of I_0/I *vs*

concentration of PA is shown in Fig 2. Up to 1 equivalents of PA the Stern-Volmer constant was found to be 2.21 x10^5 [Fig. 3. a)] and the plot remained linear up to 2.8 equivalents of PA. Above 2.8 equivalents of PA, the S-V constant was 1.59 x 10^5 [Fig. 3 b)]. On further increasing PA concentration, the plot showed an upward bend indicating the super amplified quenching effect. The detection limit was calculated from the slope of the calibration curve based on the equation, 3σ/slope, where σ is the standard deviation and it was found to be 9.5 μM (Fig. 4).
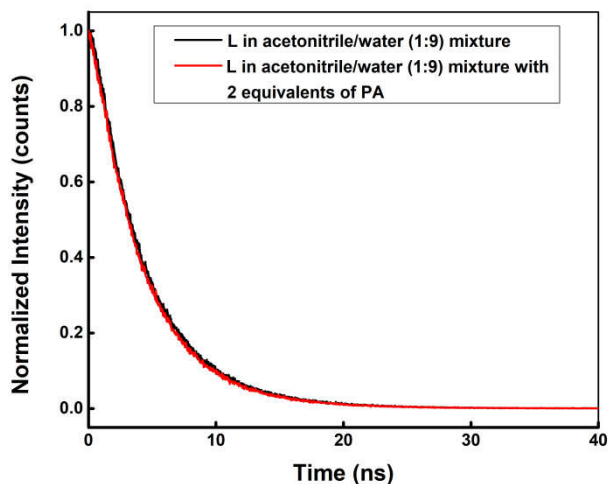

Fig. 5. Fluorescence decay profile of L before and after
the addition of PA (2 equivalents) Acetonitrile/water (1:9) mixture

Fluorescence quenching may occur either by static- or dynamic mechanism. Here, the non-linearity of the S-V plot demonstrated the combined effect of static- and dynamic quenching[14]. The linearity of the plot at the beginning indicates that the quenching follows static mechanism at lower concentration of PA. It was further confirmed

from the excited state fluorescence life time measurement. The nanoaggregate of L in acetonitrile/water (1:9) mixture exhibited a fluorescence life time of 4.3 ns. It remained as constant after the addition of 2 equivalents of PA (Fig 5). But at higher concentration of PA, the S–V plot bend upward indicating the involvement of dynamic quenching process. Thus, in the present case, fluorescence quenching followed both static- and dynamic mechanisms.
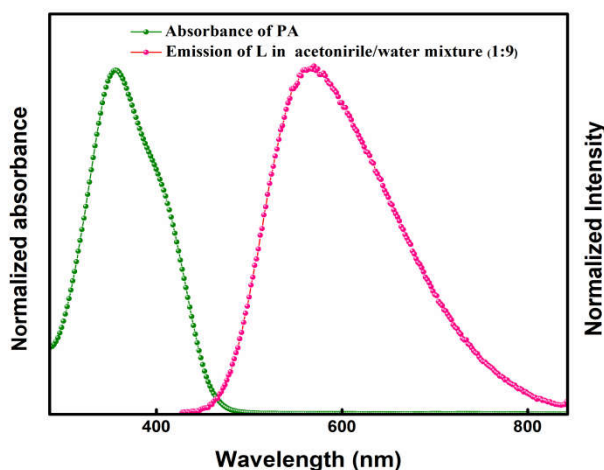

Fig. 6. Normalized UV-Visible spectra of picric acid in
water and aggregated L in acetonitrile/water (1:9, v/v) mixture

Generally, when an electron rich fluorophore interacts with an electron deficient species, there will be a good possibility of photoinduced electron transfer (PET) from the excited state of the fluorophore to the ground state of the quencher which leads to the annihilation of the emission intensity of the luminogen. In addition to PET, energy transfer also has a significant role in fluorescence quenching. In the present case, the overlap of absorption spectra of PA

and the emission spectra of the nanoaggregate of L in the range of 429-493 indicates the occurance of energy transfer from the fluorophore to the quencher (Fig. 6). This small overlapping region indicates that the energy transfer is responsible for the fluorescence quenching to some extent.

To get an idea about the PET process, quantum chemical calculations were carried out by DFT method. The optimized energy level diagram (Fig. 7) clearly indicates the involvement of PET process. The LUMO (-4.52 eV) of the PA is found to have lower energy than the LUMO (1.87 eV) of the aggregared L, indicating a strong feasibility of PET. From the above result, it is evident that photoinduced electron transfer together with energy transfer are responsible for the fluorescence quenching of the aggregated L in the presence of PA.
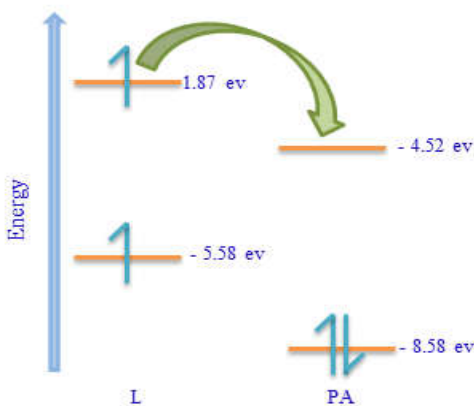

Fig. 7. Energy level diagram of L and PA

4. Conclusions

The aggregate of L was ued for the detection of nitroaromatic explosive, picric acid *via* fluorescence quenching in water and got a satisfactory result. At very low concentration, the quenching followed static mechanism and a combination of static and dynamic quenching mechanism took place at higher concentration of the quencher. The detection limit was found to be 9.5 µM in water. The photoinduced electron transfer together with energy transfer were responsible for the quenching of fluorescence of aggregate of L.

References

1.   M. E. Germain and M. J. Knapp, *Chemical Society Reviews*, 2009, **38**, 2543-2555.

2.   S. Hussain, A. H. Malik, M. A. Afroz and P. K. Iyer, *Chemical Communications*, 2015, **51**, 7207-7210.

3.   A. J. Davidson, I. D. Oswald, D. J. Francis, A. R. Lennie, W. G. Marshall, D. I. Millar, C. R. Pulham, J. E. Warren and A. S. Cumming, *CrystEngComm*, 2008, **10**, 162-165.

4.   P. C. Ashbrook and T. A. Houts, *Chemical Health and Safety*, 2001, **6**, 27.

5.   K. Håkansson, R. V. Coorey, R. A. Zubarev, V. L. Talrose and P. Håkansson, *Journal of mass spectrometry*, 2000, **35**, 337-346.

6.   M. E. Walsh, *Talanta*, 2001, **54**, 427-438.

7.   S. F. Hallowell, *Talanta*, 2001, **54**, 447-458.

8.   G. Vourvopoulos and P. Womble, *Talanta*, 2001, **54**, 459-468.

9.   Y. Peng, A.-J. Zhang, M. Dong and Y.-W. Wang, *Chemical Communications*, 2011, **47**, 4505-4507.

10.   D. Dinda, A. Gupta, B. K. Shaw, S. Sadhu and S. K. Saha, *ACS applied materials & interfaces*, 2014, **6**, 10722-10728.

11.   X. Sun, Y. Wang and Y. Lei, *Chemical Society Reviews*, 2015, **44**, 8019-8061.

12.   P. Vishnoi, M. G. Walawalkar, S. Sen, A. Datta, G. N. Patwari and R. Murugavel, *Physical Chemistry Chemical Physics*, 2014, **16**, 10651-10658.

13.   P. Lu, J. W. Lam, J. Liu, C. K. Jim, W. Yuan, N. Xie, Y. Zhong, Q. Hu, K. S. Wong and K. K. Cheuk, *Macromolecular rapid communications*, 2010, **31**, 834-839.

14.   D. Zhao and T. M. Swager, *Macromolecules*, 2005, **38**, 9377-9384.

RESEARCH PUBLICATIONS

Antipyrine derived Schiff base: A colurimetric sensor for Fe(III) and "turn-on" fluorescent sensor for Al(III)

P.P. Soufeena, K.K. Aravindakshan[*]

Department of Chemistry, University of Calicut, Malappuram, Kerala 673635, India

ARTICLE INFO

ABSTRACT

A new Schiff base, 1,5-dimethyl-4-(2-hydroxy-1,2-diphenylethylideneamino)-2-phenylpyrazol-3-one (L) was synthesized by the condensation of 4-amino-2,3-dimethyl-1-phenyl-3-pyrazolin-5-one (4-aminoantipyrine) with 2-hydroxy-1,2-di(phenyl)ethanone (benzoin). It was characterized by elemental analysis and spectroscopic techniques. The optical response of the compound, L towards various metal ions like Fe^{3+}, Co^{2+}, Ni^{2+}, Cu^{2+}, Zn^{2+}, Al^{3+}, Mg^{2+}, Ca^{2+}, Ba^{2+}, Pb^{2+}, Cd^{2+} and Hg^{2+} was monitored in methanol solution. L showed a remarkable colourimetric response towards Fe^{3+} and fluorescence "turn-on" behavior towards Al^{3+}. Binding with Fe^{3+} induced a "naked-eye" purple coloration under day light. The recognition of L with Al^{3+} was responsible for blue fluorescent emission at 463 nm. The UV–Visible and fluorescent spectral studies of L with different metal ions were consistent with the visual observation. Due to the transient nature of the complex formed between L and Fe^{3+} in methanol, the stability of the complex formed in an aprotic solvent, acetonitrile was also ascertained. The stoichiometry and association constant of the complex formed were calculated.

1. Introduction

Design and synthesis of simple organic molecules for selective detection of metal ions have considerable importance in the present scenario. This method of detection has several advantages such as simplicity, selectivity, low cost, rapid and real-time monitoring, visual detection, etc. [1–3]. Previously adopted techniques for the detection of metal ions like, atomic absorption spectrometry [4], chromatography [5], plasma emission spectrometry [6], ion sensitive electrodes [7], neutron activation analysis [8], etc., need expensive instrument facilities. The quantitative determination of metal ions by these methods will be tedious due to the interference of other metal ions [9]. Therefore, researchers are focusing to develop simple organic molecules with remarkable optical responses (colorimetric and fluorimetric) towards various analytes [10–13].

Among the organic molecules, Schiff bases have promising optical response towards metal ions because of their high chelating ability. The ease of synthesis and relatively high yield are the advantages of this class of compounds [14]. Many imine based optical probes have been reported in literature [15–20]. When the probe binds a metal ion, its photophysical properties will be changed and these changes can be monitored by optical methods. There are several mechanisms behind these changes, which include photoinduced electron/energy transfer

(PET), charge-transfer (LMCT and MLCT), intramolecular charge-transfer (ICT), excimer or exciple formation and excited-state intra-/intermolecular proton-transfer (ESPT) [21–23]. The –C=N isomerization in Schiff bases is another signaling mechanism, reported in 2007 to develop fluorogenic probes for metal ions [24]. This –C=N isomerization dissipates the excited state energy of the molecule and, therefore, non-radiative emission happens. Introduction of a guest molecule, especially a metal ion, endues the molecule with radiative emission via covalent binding with –C=N bond. Schiff bases also have a tendency to undergo hydrolytic cleavage in the presence of any electrophylic catalysts like, acids, metal ions, etc. This hydrolytic cleavage of imine bond by metal ions is another aspect in the development of metal based sensing systems and based on this strategy many optical probes were developed for the specific detection of Fe^{3+}, Cu^{2+} and Al^{3+} [25–27]. The selectivity of a probe towards a metal ion depends on many factors including the nature of the solvent used [2,28].

Among the transition metal ions, the selective detection of iron(III) has considerable importance because of its active involvement in various biological processes. Its excess intake as well as deficiency lead to several health problems [29,30]. In addition to the biological field, clinical, environmental and industrial areas require a selective optical probe for the qualitative and quantitative determination of iron [5]. Al^{3+}, the third most abundant element on the earth crust, finds a

---

[*] Corresponding author.
 E-mail address: aravindkuttamath@yahoo.com (K.K. Aravindakshan).

Coumarin based yellow emissive AIEE active probe: A colorimetric sensor for Cu^{2+} and fluorescent sensor for picric acid

P.P. Soufeena, T.A. Nibila, K.K. Aravindakshan *

Department of Chemistry, University of Calicut, Malappuram, Kerala 673 635, India

ARTICLE INFO

ABSTRACT

A hydrazine derived ESIPT active Schiff base, 1-(8-methanylylidene-7-hydroxy-4-methyl-2H-chromen-2-one)-2-(2, 4-dihydroxybenzylidene) hydrazine, L was synthesized and characterized by elemental analysis and by various spectroscopic techniques. L exhibited a colourimetric response towards Cu^{2+} ion by changing from colorless to yellow with relatively a little or no interference of other common metal ions. The probe also showed good response for the detection of Cu^{2+} in real water samples. The H-aggregated L displayed AIEE property in acetonitrile/water mixture. The restriction of molecular motions endued the luminogen with a yellow fluorescence through ESIPT emission at 562 nm having relatively large Stock's shift of 205 nm. The scanning electron microscopic study was carried out to investigate the morphology of the nanoaggregate. The aggregated luminogen displayed it yellow emission in the pH range of 4–7 without affecting the intensity. The applicability of the probe for the detection of picric acid was also checked.

© 2019 Elsevier B.V. All rights reserved.

1. Introduction

Monitoring of environmental pollutants and biological important metal ions is highly essential in present scenario. Among the transition metal ions, Cu^{2+}, an essential trace metal, is closely related to human life [1–4]. Because of the redox nature of Cu^{2+}, its enzymes involve in electron transfer, oxygen binding and oxidation catalysis [5–7]. It also has inevitable roles in bone and tissue formation, cellular respiration, immune and brain functions, and gene transcription [8–10]. Copper is also essential to the growth of plants and microorganisms [11]. Contrary to these active physiological roles of Cu^{2+}, its excessive intake adversely affect human health and leads to neurodegenerative diseases likes Menkes, Wilson's, Parkinson's, Alzheimer's and Prion disease [12–16]. The effluents from industries and the agricultural waste contribute copper contamination in water, air and soil. Therefore, on account of health and environmental issues, it is essential to monitor Cu^{2+} in a cost effective manner. For monitoring various metal ions, researchers are interested in methods based on chemical sensors. The simplicity in detection is the prime attraction of these methods. Their advantages are rapid response, high sensitivity and selectivity and inexpensive instrumental facility [17–19]. The changing photophysical properties of chemical sensors before and after the interaction with the metal ions can be monitored and quantified using UV–Visible- or fluorescence spectroscopic method. Among these optical sensing methods, colorimetric sensing is attractive because of the advantages of naked eye

detection. A challenge of this chemical sensor based method for copper ion is the interference of other metal ions like Fe^{3+}, Zn^{2+}, Hg^{2+} and Pb^{2+} [20]. Even though, a number of chemical probes are available for monitoring Cu^{2+} [21–26], the development of new one with better capability is still challenging.

Solid state luminescent organic materials find promising applications in organic light emitting diodes (OLED), fluorescent sensors, bioimaging and so forth [27–32]. The major problem of fluorescent materials is that they become highly emissive in isolated molecular state and their emission either quenches or they will not be emissive in the solid or aggregated states which limit their applications. This effect, the quenching of fluorescence with concentration is commonly known as Aggregation Caused Quenching (ACQ) [33,34]. The intermolecular π-π stacking interactions of aromatic skeleton of organic molecules result in the formation of excimers and exciplexes which lead to quenching of fluorescence [35]. In 2001, Tang and co-workers [36,37] reported an interesting property in silole-based organic molecules, which was just reverse of the common ACQ effect. They observed that the non-emissive system in isolated state strongly emit bright green fluorescence upon aggregation and this unique phenomenon is termed as Aggregation Induced Emission (AIE) [38]. Another feature of aggregated luminogens, Aggregation Induced Emission Enhancement (AIEE), similar to the AIE was reported in 2002 by Park *et al* [32]. AIEE active luminogens are feebly emissive in the isolated state and their emission enhance in the aggregated state. The main mechanism proposed for AIE/AIEE activity is the restriction of intramolecular motion (RIM) in the aggregated- or solid state [39]. The other mechanisms reported are intramolecular charge transfer (ICT) [40], J-aggregation

---

* Corresponding author.
E-mail address: aravindkuttamath@yahoo.com (K.K. Aravindakshan).